Journal of Crystal Growth 97 (1989) 497–501
North-Holland, Amsterdam

QUASI-EQUILIBRIUM CLUSTERING UPON SUPERSATURATION IN HOMOGENEOUS PHASE FORMATION

V.C. NONINSKI

Higher Institute of Chemical Technology, LEPGER, Sofia 1156, Bulgaria

Received 10 July 1988; manuscript received in final form 17 April 1989

The Gibbs–Thomson equation is observed while taking into account the size-dependence of the specific surface free energy, σ, derived in two different ways. It is shown that on supersaturation the most probable state of all atoms (molecules) in the parent phase in homogeneous phase formation is in the form of clusters and not of single atoms (molecules). Definition of critical supersaturation and barrierless condensation in the case of homogeneous phase formation is given.

1. Introduction

As is known in the theory of phase formation, the relation between the radius of the nucleus, r, and the supersaturation p_r/p_∞ is given by the Gibbs–Thomson isotherm:

$$RT \ln(p_r/p_\infty) = 2\sigma M/r\rho, \tag{1}$$

where R is the gas constant, T is the absolute temperature, M is the molecular weight of the substance, ρ is the density of the substance, p_r is the vapour pressure of the supersaturated system, p_∞ is the vapour pressure of the infinite drop (crystal) and σ is the specific surface free energy. Specific surface free energy of a cluster, σ, is the work for the formation of a unit of its surface. Usually, in eq. (1), σ is considered to be constant over the whole range of cluster dimensions. The constancy of σ is preserved for clusters of relatively high values of r. However, for clusters of smaller size the value of σ already becomes dependent on the radius of the drop. As shown by Gibbs [1], the dependence of σ on the surface curvature cannot be ignored when the problems of nucleation are treated, because the size of the nucleus is very small and the surface free energy begins to play a significant role in the work of formation of the cluster.

The first theoretical consideration of the effect of the droplet size on surface tension (specific surface free energy) is made by Tolman [2] on the basis of Gibbs's thermodynamic theory of capillarity and his own assessment of the sign and magnitude of the superficial density. Tolman derived the following equation for the said dependence:

$$\sigma = \sigma_\infty \exp\left[\int_\infty^{r_2} \frac{\frac{2\delta}{r_2^2}\left(1+\frac{\delta}{r_2}+\frac{\delta^2}{3r_2^2}\right)}{1+\frac{2\delta}{r_2}\left(1+\frac{\delta}{r_2}+\frac{\delta^2}{3r_2^2}\right)} \mathrm{d}r_2\right], \tag{2}$$

where r_2 is the cluster radius, δ is the half-interfacial thickness and σ_∞ is the specific surface free energy of the flat surface.

Later other authors also estimated the dependence of σ on the radius of the cluster [3–6]. The equations derived, however, contain empirical constants whose physical meaning is far from evident.

Noninski [7,8] derived an equation for the relation of σ upon r for convex and concave surface by calculating the energy of the Van der Waals interaction between a sphere and a medium of the same substance surrounding it:

$$\sigma = \frac{A}{d_0^2} + \frac{2A}{r^2}\ln\frac{d_0}{r+d_0}, \tag{3}$$

where

$$A = \tfrac{1}{15}\pi n^2 \beta,$$

0022-0248/89/$03.50

d_0 is the diameter of a molecule, n is the number of molecules in a unit volume, β is the constant from the expression for the energy of attraction between two molecules $E = -\beta/r_1^6$, r is the radius of the drop equal to the distance between the centre of the drop and the centres of the outmost, peripheral molecules, situated at the cluster/parent-phase interface.

As is seen, eq. (3) contains quantities which are known from the experiment or can be calculated with sufficient accuracy. Therefore, in the cases in which the experimental value of σ is known, eq. (3) can be checked. Proof for the validity of eq. (3) is the very good concordance between the calculated value of σ for flat surface of pure water (73.52 erg cm^{-2}) and the experimentally established value of σ for purified water (71.97 erg cm^{-2}). Other proof for the validity of the above can be found in ref. [8] where it is shown that r in (3) at $\sigma = 0$ should be equal to the distance between the centres of the molecules at the critical temperature (especially after considering the intermolecular Born repulsion forces). Indeed, the value of r calculated according to eq. (2) in ref. [8] at $\sigma = 0$ is confirmed by the literature experimental data for the distance between the molecules at the critical temperature of 52 substances given in table 1 of ref. [8].

In the present paper the Gibbs–Thomson equation is observed in which the dependence of σ upon the radius of the cluster is taken into account, according to an approximation of Tolman's formula (2) made in ref. [9]. The obtained curves are compared with the Gibbs–Thomson equation specified for $\sigma = f(r)$ in ref. [7].

2. Gibbs–Thomson equation for $\sigma = f(r)$ and $\sigma = f(r_2)$

If instead of σ = constant, the expression (3) is taken into account in the Gibbs–Thomson equation (1), the following equation is obtained for convex form of the drop (crystal) [7]:

$$p_r = p_\infty \exp\left[\frac{2AM}{RT\rho}\left(\frac{1}{rd_0^2} + \frac{2}{r^3}\ln\frac{d_0}{r+d_0}\right)\right]. \qquad (4)$$

On the other hand, eq. (2) gives another possibility to specify the Gibbs–Thomson equation (1) for the size dependence of σ. We shall use here the exponential approximation of Tolman's equation (2) made by Larson and Garside [9]:

$$\sigma = \sigma_\infty \exp(-2\delta/r_2), \qquad (5)$$

to obtain

$$p_{r_2} = p_\infty \exp\left[\frac{2M}{RT\rho}\frac{\sigma_\infty}{r_2}\exp\left(-\frac{2\delta}{r_2}\right)\right], \qquad (6)$$

where r_2 is the so-called radius of the particle bounded by the equimolar dividing surface and its value is determined by definition equations containing arbitrarily chosen constants [10].

In fig. 1 the Gibbs–Thomson isotherms for the formation of ice particles for σ = constant (according to eq. (1)), $\sigma = f(r)$ (according to eq. (4)) and $\sigma = f(r_2)$ (according to eq. (6)) are shown, the latter being plotted for 4 different values of δ. The curves in fig. 1 are obtained for $T = 270$ K, $d_0 = 2.76 \times 10^{-8}$ cm, $\sigma_\infty = 71.97$ erg cm^{-2}, $\rho = 0.999$ g cm^3, $A = 5.6008 \times 10^{-14}$ and $p_\infty = 8.1$ Torr. The value of the vapour pressure of ideal macrocrystal at 270 K and the value of the quantity A are calculated in ref. [7].

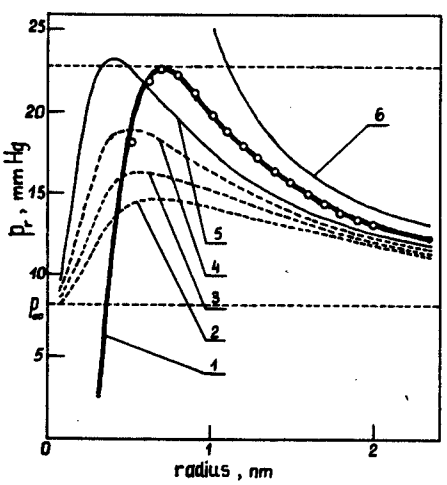

Fig. 1. Vapour pressure of ice particles, p_r, as a function of their radius. Curve 1 has been obtained according to eq. (4); (O) values calculated according to eq. (9) for $2\delta = 0.414$ nm). Curves 2, 3, 4 and 5 have been obtained according to eq. (6) for δ equal to 0.35, 0.30, 0.25 and 0.20 nm, respectively. Curve 6 has been obtained according to eq. (1) for σ = constant.

When observing the curves obtained according to eq. (4) (curve 1) and eq. (6) (curves 2–5), it is seen that all of them have a maximum, unlike curve 6 obtained according to eq. (1) in which σ = constant.

The values of δ and r_2 included in eq. (6) do not have a straightforward physical meaning and they are chosen arbitrarily. The physical meaning of the quantities included in eq. (4) is much more clear and eq. (4) can be used as a model for comparison when observing other models like the one expressed by eq. (6). As it can be seen from fig. 1, the form of the curve obtained according to eq. (6) that best of all approximates that obtained according to eq. (6) is attained at:

$$2\delta \approx 0.4 \text{ nm} \approx \tfrac{3}{2} d_0. \tag{7}$$

The obtained value of δ is more than an order of magnitude smaller than the value $\delta = 2.5$ nm accepted by Larson and Garside in ref. [9].

From fig. 1 is seen that if the difference in physical meaning of r_2 and r is taken into account the latter is of lower value than r_2 and is equal to

$$r \approx r_2 - 0.3 \text{ nm} \approx r_2 - 1.5\delta. \tag{8}$$

If we take into consideration the above, we can write instead of eq. (6):

$$p_r = p_\infty \exp\left[\frac{2M}{RT\rho}\frac{\sigma_\infty}{r_2 - 1.5\delta}\exp\left(-\frac{2\delta}{r_2 - 1.5\delta}\right)\right]. \tag{9}$$

In fig. 1 the points denoted by open circles represent the values obtained according to eq. (9). As is seen from fig. 1, the curve plotted according to eq. (9) coincides with that of eq. (4) for approximately $\delta/r < 0.5$. It is to be noted that the exponential approximation of eq. (2) made by Larson and Garside (eq. (6) in ref. [9]) holds for $\delta/r \ll 1$. We shall discuss here only the part of the curves where they coincide.

3. Discussion

Fig. 1 shows that at a given supersaturation, below that corresponding to the maximum of curve 1, two kinds of clusters exist. The clusters corresponding to the right-hand branch of the curve are in metastable equilibrium (critical clusters) – they will either grow up to a big crystal or will disperse upon a fluctuational respectively increase or decrease of their size. The cluster corresponding to the left-hand branch, however, will neither grow nor disperse upon accidental respectively increase or decrease of their size – these clusters are in a quasi-equilibrium state. This conclusion is made on the basis of two independently derived equations – eq. (4) and eq. (6) (respectively eq. (9)). As is known in the case of homogeneous condensation on ions, a maximum similar to that in curve 1 of fig. 1 is observed in refs. [41,42]. From the results in refs. [7,8] and those presented here, it follows that when taking into account the size dependence of σ, the maximum in the Gibbs–Thomson isotherm is observed in all the cases of homogeneous phase formation independent of whether the cluster is charged or not.

The size of these quasi-equilibrium clusters corresponds to tens of atoms (molecules) and will even be greater than the size observed in fig. 1, curve 1, should the forces of Born intermolecular repulsion, specific edge free energy, adsorbtion, etc. be taken into account. Therefore, statistical treatment is possible of this clustering and the laws of thermodynamics are applicable for its explanation.

We shall note here that clustering is observed experimentally upon supersaturation [14–34, 38–40] and even in saturated and undersaturated systems [35–37].

The critical supersaturation in homogeneous phase formation is usually defined as the supersaturation at which the rate of nuclei formation, I, defined by Volmer's equation [43],

$$I = A \exp(-W/kT), \tag{10}$$

is equal to unity, where I is the number of nuclei formed per unit of time in a unit volume and A is a kinetic factor determined by the transport of the substance from the parent phase to the nucleus. In practice this supersaturation is established by visual determining the appearance of the first cluster. Clearly, this subjective way of determination introduces uncertainty in the established value.

Instead of using eq. (1), another definition can be applied, similar to that in the case of homogeneous condensation on ions [42], heterogeneous phase formation at negative line tension, γ [11], and, as can be shown, also at $\gamma > 0$, i.e. the critical supersaturation in homogeneous phase formation is the supersaturation corresponding to the maximum in curve 1 in fig. 1. In terms of ref. [42], above the critical supersaturation the homogeneous phase formation is already a barrierless process. At these supersaturations the rate-determining step of the phase formation is the transport of substance from the parent phase to the cluster and the kinetic obstacles are eliminated. The latter can be understood if it is remembered that in terms of ref. [42], the barrier that should be overcome to form a nucleus at a given supersaturation is equal to the difference between the work for the formation of the critical cluster and the work for the formation of the quasi-equilibrium one. At the maximum of curve 1 of fig. 1, this work is zero.

When observing curve 1 in fig. 1 it can be seen that the conclusions in refs. [9,10] regarding clustering upon supersaturation can be extended. As it can be seen when analysing curve 1 in fig. 1, the most probable state of all atoms (molecules) in a supersaturated system in homogeneous phase formation is in the form of clusters and not of separate, single atoms (molecules). We shall only note here that this conclusion holds also for heterogeneous phase formation. Furthermore, this conclusion does not apply only for a limited region, but applies also for the whole region of supersaturations, at least where kinetic and not transport phenomena are rate-determining. The size of the quasi-equilibrium clusters is dependent on the supersaturation and a certain size of these clusters (in the above limits) corresponds to every supersaturation.

Clearly, the above conclusions should influence the derivation of the kinetic equations of phase formation since it is more probable that the elementary building particle at every supersaturation is a cluster of atoms (molecules) rather than a single, separate atom (molecule). This will lead to a somewhat "quantum" treatment of nucleation and growth with "allowed" and "forbidden" cluster sizes depending on the supersaturation. This question shall be treated in future communications.

References

[1] J.W. Gibbs, Collected Works, Vol. 1 (Longmans–Green, London, 1928) p. 219.
[2] R.C. Tolman, J. Chem. Phys. 17 (1949) 333.
[3] J.K. Lee, F.F. Abraham and G.M. Pound, Surface Sci. 34 (1973) 745.
[4] C.L. Briant and J.J. Burton, J. Chem. Phys. 63 (1975) 2045.
[5] K. Nishioka, Phys. Rev. A16 (1977) 2143.
[6] D.H. Ramussen, M. Sivaramakrishnan and G.L. Leedom, AIChE Symp. Ser. No. 125, 78 (1982) 1.
[7] C.I. Noninski, Khimia i Industria (Bulgaria) 33 (1961) 144.
[8] C.I. Noninski, Khimia i Industria (Bulgaria) 39 (1967) 208.
[9] M.A. Larson and J. Garside, J. Crystal Growth 76 (1986) 88.
[10] O. Söhnel and J. Garside, J. Crystal Growth 89 (1988) 202.
[11] A. Scheludko, Colloids Surfaces 7 (1983) 81.
[12] Spravochnik Khimika, Vol. 1 (Goskhimizdat, Leningrad, 1951) pp. 858, 880.
[13] Ya.K. Sirkin and M.E. Dyatkina, Chemical Bond and Structure of the Molecules (Goskhimizdat, Moscow, 1946) p. 317 (in Russian).
[14] E. Pozner, Zh. Fiz. Khim. 13 (1939) 889.
[15] Ya. I. Frenkel, Kinetic Theory of Liquids (Akad. Nauk SSSR, Moscow, 1945) (in Russian).
[16] M.V. Tovbin and S.N. Krasnova, Zh. Fiz. Khim. 25 (1951) 161.
[17] L.N. Matusevich and K.N. Shabalin, Zh. Prikl. Khim. 25 (1952) 1157.
[18] J.P. Borel, Helv. Phys. Acta 27 (1954) 485.
[19] M.V. Tovbin and S.N. Krasnova, Zh. Fiz. Khim. 21 (1951) 32.
[20] V.G. Khlopin, Selected Papers, Vol. 1 (Akad. Nauk SSSR, Moscow, 1957) (in Russian).
[21] M.V. Tovbin and O.V. Savinova, Nauk. Zap., Kiev Univ. 16 (1957) 45.
[22] N.M. Fletcher, Sci. Progr. 54 (1966) 227.
[23] L.N. Matusevich, Crystallization from Solutions in the Chemical Industry (Khimiya, Moscow, 1968) (in Russian).
[24] A.A. Chernov, Vestn. Akad. Nauk SSSR 11 (1968) 60.
[25] J.W. Mullin and C.L. Leci, Phil. Mag. 19 (1969) 1075.
[26] Yu.A. Serebryakov and E.V. Khamskii, Kristallografia 15 (1970) 1226.
[27] A.T. Allen, M.P. McDonald, W.M. Nicol and R.M. Wood, Nature 235 (1972) 36.
[28] A.T. Allen, M.P. McDonald, W.M. Nicol and R.M. Wood,

in: Particle Growth in Suspensions, Ed. A.L. Smith (Academic Press, London, 1973) p. 239.
[29] D.M. Rasmussen and A.P. MacKenzie, J. Chem. Phys. 59 (1973) 5003.
[30] J. Dousma and P.L. de Bruyn, J. Colloid Interface Sci. 56 (1976) 527.
[31] R.J,. Stol, A.K. van Helden and P.L. de Bruyn, J. Colloid Interface Sci. 57 (1976) 115.
[32] R.M. Heist, K.M. Colling and C.S. DuBuis, J. Chem. Phys. 65 (1976) 5147.
[33] Y.G. Russel and R.M. Heist, J. Chem. Phys. 69 (1978) 3723.
[34] G. Agarwall and R.M. Heist, J. Chem. Phys. 73 (1980) 902.
[35] G.A. Hussmann, M.A. Larson and K.A. Berglund, in: Industrial Crystallization '84, Eds. S.J. Jančić and E.J. de Jong (Elsevier, Amsterdam, 1984) p. 21.
[36] P.M. McMahon, K.A. Berglund and M.A. Larson, in: Industrial Crystallization '84, Eds. S.J. Jančić and E.J. de Jong (Elsevier, Amsterdam, 1985) p. 229.
[37] M. Nicolas and P. Joyes, Surface Sci. 156 (1985) 189.
[38] M.A. Larson and J. Garside, J. Chem. Eng. Sci. 41 (1986) 1285.
[39] Y.C. Chang and A.S. Myerson, AIChE J. 33 (1987) 697.
[40] T. Stace, Nature 327 (1987) 186.
[41] J.J. Thomson, Electrizitätdurchgang in Gasen (Teubner, Leipzig, 1901) p. 148.
[42] G. Tomford and M. Volmer, Ann. Physik (Leipzig) 33 (1938) 109.
[43] M. Volmer, Kinetic der Phasenbildung (Steinkopf, Dresden, 1939).

Small Stable Drops and Crystals in Supersaturated Homogeneous and Heterogeneous Systems at Positive Specific Linear Free Energy

VESSELIN CHRISTOV NONINSKI

Laboratory for Electrochemistry of Renewed Electrode–Solution Interface (LEPGER), P.O. Box 9, Sofia 1504, Bulgaria

Received September 30, 1988; accepted October 5, 1990

Existence during supersaturation of quasi-equilibrium clusters of atoms (molecules), conditionally called small stable drops and crystals, in homogeneous and heterogeneous phase formation is discussed. It is shown that these small stable drops can exist not only when the specific linear free energy (specific edge free energy λ, respectively line tension γ_l, is negative but also in cases when λ and γ_l are positive. It is shown that small stable drops always exist when homogeneous and heterogeneous phase formation is thermodynamically possible; the sign of the line tension does not determine the possibility that a small stable drop can exist.

Nowadays theoretical methods employing radial distribution and correlation functions are widely applied in the classical theory of capillarity (1, 2). There is another approach to this question which was foreseen by Tolman (3): "Indeed it will ultimately seem more satisfactory to continue the investigation using the concept of forces exerted by individual molecules and the more detailed methods of molecular mechanics." Using a similar approach Noninski (4, 5) was able to derive an equation for the size dependence of the specific surface free energy σ. This size dependence is important to take into account especially when observing small drops (crystals); ignoring the size dependence of σ will lead to incorrect conclusions when treating, e.g., questions of nucleation. The σ values calculated from the equation derived in Ref. (4) for different substances are in excellent concordance with experimental values. Further, it was observed (4, 5) that when the specific surface free energy in the Gibbs–Thomson isotherm is considered size dependent, which is the real case, the isotherm changes its form and far-reaching, so far unknown, conclusions can be drawn. For instance, it has been found (4, 5), that when such specified Gibbs–Thomson isotherms referring to convex and concave forms are juxtaposed, a drop (cluster) of atoms (molecules) is the thermodynamically stable formation (at zero supersaturation). Thus, at equilibrium, an ideally built structure of the crystal is hardly possible. Further specification of the Gibbs–Thomson isotherm in some cases of phase transformations, which should not be ignored when small drops (crystals) are treated, can be done also by considering the effect of the specific line free energy (slfe) (4–11).

In the present paper another type of cluster is discussed whose existence follows from the specified Gibbs–Thomson isotherm upon supersaturation. These are quasi-equilibrium formations but for simplicity here they conditionally are called small stable drops. These quasi-equilibrium clusters are not the critical nuclei of a new phase.

Another aim of the present paper is to answer the question whether quasi-equilibrium clusters (small stable drops) can exist not only at negative but also at positive slfe. For homogeneous phase formation this question has not been treated so far, while in the case of heterogeneous phase formation the existence

0021-9797/91 $3.00

of quasi-equilibrium small stable drops upon supersaturation was found by Scheludko *et al.* (6–11) only for the case of negative slfe (line tension, γ_1).

THEORY

Homogeneous Phase Formation

For the case of homogeneous phase formation the conclusions here will be based on an equation for the relationship between the specific surface free energy σ and the radius of the drop (crystal) r and the Gibbs–Thomson isotherm specified for this size-dependent σ. Derivation of this equation was carried out by Noninski (4, 5) when calculating the energy of the van der Waals interaction between a sphere and the medium of the same substance surrounding it.

Previous papers (4, 5) were published in Bulgarian; therefore, in the present paper the derivation of $\sigma = f(r)$ in Ref. (4) is outlined briefly. Here we summarize only the derivation of $\sigma = f(r)$ for a convex surface and leave for the future the discussion of the other important conclusions in Refs. (4, 5), such as the proof for the existence of a thermodynamically stable drop, the size of that drop, the influence of the above on crystal growth, and interpretation of the critical temperature of the substance.

The dependence of σ on r is derived in Ref. (4) in the following way: For simplicity the surface whose σ is to be determined is considered to be spherical. The problem in calculating σ of a sphere is reduced to the calculation of the potential energy of interaction between the sphere and the remaining (nonspherical) part of the body from which the sphere is imaginatively obtained at a moment before its tearing from the remaining (nonspherical) part. The work for reversible isothermic tearing and moving apart, up to infinity, of the parts of a body is equal to the absolute value of the potential energy of interaction between the same parts before their tearing.

The energy of interaction between two molecules is given by the expression

$$E' = -\frac{\beta}{r_1^6} + \frac{\gamma}{r_1^q} \qquad [1]$$

where β, γ, and $q > 6$ are constants, and r_1 is the distance between the centers of the molecules. The first term in Eq. [1] expresses the energy of the van der Waals attraction and the second term, the energy of Born intermolecular repulsion.

It should also be pointed out here that when the molecules of the remaining (nonspherical) part of the body are moving apart in a radial direction from the spherical part they are also moving apart from each other. Keeping in mind the latter it can easily be understood that only one surface is being obtained when the described tearing takes place, namely, the surface of the spherical drop (crystal). The work for moving apart from each other, up to infinity, of the molecules of the nonspherical part of the body has nothing in common with the work for overcoming the attraction between the sphere and the molecules that are being moved apart from it. It is the latter work that determines σ.

When solving the above problem not only the magnitude of the dispersion, the orientation, and the induction van der Waals forces of interaction between the two molecules are taken into account, but also the directions of the interaction between each molecule of the body and all the molecules of the other body are considered.

As a result and after solving some problems of a mathematical nature an equation is derived for the energy of interaction between one molecule of the spherical drop (crystal) with one molecule of the medium surrounding it (for simplicity the Born repulsion forces are neglected; such neglect is physically consistent because the repulsion forces act at a very close distance and disappear with distance much faster than the forces of attraction). This equation is integrated so that the energy of

interaction between one molecule in the spherical part of the body with all the molecules of the remaining (nonspherical) part is obtained. Then the expression obtained is integrated again for all the molecules in the spherical part of the body. Thus, the energy of attraction between the two parts of the body, spherical and nonspherical, U, is found. Now that the equation for U is known it is noted in Ref. (4) that this energy corresponds to that at the closest distance at which the body's molecules can contact each other, i.e., the distance between the centers of the separate molecules, which virtually is equal to their diameter, d_0. The work for overcoming the forces of attraction when moving the nonspherical part of the body apart from the spherical one at a distance from d_0 up to ∞ is equal to $-U$. Since in the course of this moving apart, a new surface, O, is created, of the size $O = 4\pi r^2$, the work for the creation of a unit surface which virtually is the specific surface free energy will be

$$\sigma = -\frac{U}{4\pi r^2}. \qquad [2]$$

When the expression for U derived above is substituted in Eq. [2] one obtains

$$\sigma = \frac{A}{d_0^2} + \frac{2A}{r^2} \ln \frac{d_0}{r+d_0} \qquad [3]$$

where

$$A = \tfrac{1}{15}\pi n^2 \beta$$

and d_0 is the diameter of a molecule, n is the number of molecules in a unit volume, β is the constant from the expression for the energy of attraction between two molecules, $E = -\beta/r_1^6$, r is the radius of the drop equal to the distance between the center of the drop and the centers of the outmost, peripheral molecules, situated at the cluster/parent phase interface.

As is seen, Eq. [3] contains quantities which are known from the experiment or can be calculated with sufficient accuracy. Therefore, in the cases in which the experimental value of σ is known Eq. [3] can be checked. A proof for the validity of Eq. [3] is the very good concordance between the calculated value of σ for a flat surface of pure water (73.52 erg cm^{-2}) and the experimentally established value of σ for purified water (71.97 erg cm^{-2}) (13).

While in the case of water all the three types of intermolecular interaction forces—orientation, induction, and dispersion—are available, there are simple kinds of molecules like Ar, H_2, and N_2 whose only intermolecular force of interaction is dispersion. In this case, instead of β the constant B from the Lennard-Jones (LJ) equation can be used. In Table I, just as an illustration, experimental σ values for various simple molecules are presented together with σ values calculated by the equation

$$\sigma = \frac{\pi n^2 B}{15 d_0^2} \qquad [4]$$

obtained from Eq. [3] for a flat surface and for $\beta = B$, where the B values are calculated from the virial coefficients [method of Lennard-Jones (12, p. 293)]. The other values of the constants used for these calculations are from Refs. (1, 12–14). Clearly, the result will depend strongly on the accuracy of calculation of constant B.

Taking into account Eq. [3] the Gibbs–Thomson equations are obtained for convex and concave forms, respectively, specified for $\sigma = f(r)$ (4, 5):

TABLE I

Molecule	σ (dyn/cm) Calculated	σ (dyn/cm) Experimental
Ar	11.4 (87.3 K)[a]	12.67 (87 K)
H_2	2.01 (20.2 K)	1.98 (19.9 K)
N_2	8.68 (77.2 K)	8.29 (80 K)

[a] Corresponding temperatures in parentheses.

$$\ln \frac{p_r}{p_\infty} = \frac{2AM}{RT\rho}\left(\frac{1}{rd_0^2} + \frac{2}{r^3} \cdot \ln \frac{d_0}{r + d_0}\right) \quad [5]$$

$$\ln \frac{p_{r_0}}{p_\infty} = -\frac{2AM}{RT\rho}\left(\frac{1}{r_0 d_0^2} + \frac{2}{r_0^3} \cdot \ln \frac{d_0}{r_0 + d_0}\right). \quad [6]$$

Here, T is the absolute temperature, M is the molecular weight, R is the gas constant, ρ is the density of the substance, p_r is the vapor pressure of small drops (crystals), p_∞ is the vapor pressure of the infinite drop (infinite crystal), and r_0 is the radius of the concave form. Equation [5] has a maximum and Eq. [6] has a minimum.

It was proved (4, 5) that a thermodynamically stable drop of finite size exists (having $\sigma = 0$). It was shown that the size of this thermodynamically stable drop for every substance does not depend on the nature of the intermolecular forces and is determined solely by the size of that substance's molecules. It was also shown that the volume of the thermodynamically stable drop (especially when Born forces of intermolecular repulsion, specific edge free energy, etc., are taken into account) is about 64 times greater than the volume of a single molecule. In such a volume tens of molecules are contained (approximately one and the same number for different substances). Therefore, the thermodynamically stable drop (crystal) is a particle of relatively significant dimensions for which the laws of statistics hold; therefore, the thermodynamics laws can be applied when observing it. This thermodynamically stable drop can be looked upon as an entirely differentiated entity of the new phase with a clearly delineated interface and with dimensions of the order of those of highly disperse colloid particles. These clusters are equally stable with the ideally built macrocrystal and can aggregate as building particles of a macrocrystal having a disperse structure. This disperse structure macrocrystal has inner surfaces whose vapor pressure is lower than that of the ideally built macrocrystal, and condensation will take place on that disperse structure crystal. The condensation continues until the entire ideal macrocrystal disappears.

Another proof for the validity of the above theory can be found in Ref. (5) where it is shown that the radius of the thermodynamically stable drop in Eq. [3] at $\sigma = 0$ should be equal to the value of the distance between the centers of the molecules at the critical temperature (especially after considering the intermolecular Born repulsion forces). Indeed, the value of r calculated according to Eq. [2] in Ref. (5) at $\sigma = 0$ is confirmed by the literature experimental data for the distance between the molecules at the critical temperature for 52 substances given in Table I of Ref. (5).

It should be noted here that in Refs. (4, 5) the conclusions are based on well-defined and physically clear presumptions, avoiding the use of arbitrary (conditional) notions, like Gibbs dividing surface or surface of tension. For instance, the diameter of a molecule, a basic parameter in Eq. [3], has a clear physical meaning, whereas the distance between the surface of tension and the surface of zero adsorption is an arbitrarily chosen quantity [cf. (1, pp. 31, 32)]. How the position of the dividing surface is chosen can be seen, e.g., in Ref. (15). As it concerns the physical meaning of LJ distance, the latter, since a result of an approximation, is also not too clear physically compared to the well-defined quantity "diameter of an atom."

We would like also to note that the correction term $\partial\sigma/\partial r$ in Refs. (16, 17) is also connected with the arbitrariness in choice of the dividing surface. As seen in Ref. (1, p. 33) the surface of tension, where the Gibbs–Thomson equation holds in its simplest form, is defined as a surface where the term $\partial\sigma/\partial r$ is equal to zero.

It is interesting to note that in the case of simple molecules, Eq. [4] is quite similar to the known equation (keeping the present notation)

$$\sigma = \frac{2\pi Bn^2}{(m-2)(m-3)(m-4)d_0^{m-4}} \times \left[1 - \frac{(m-4)}{(n-4)}\right]$$

which for $m = 6$ and $n = 9$ obtains the form (12, p. 850)

$$\sigma = \frac{\pi n^2 B}{20 d_0^2}.$$

In some cases of homogeneous phase formation (e.g., ice crystal/water vapor) the quantity specific linear (edge) free energy λ can also play a significant role, especially at sufficiently small crystals, although the λ value is much less than σ. As is known in this case, the Gibbs–Thomson equation for a crystal (drop) taking into account λ has the form (4)

$$p_r = p_\infty \exp\left[\frac{2AM}{RT\rho}\left(\frac{1}{rd_0^2} + \frac{2}{r^3}\ln\frac{d_0}{r+d_0}\right)\right] \times \exp\frac{\lambda}{r^2}. \quad [7]$$

The quantity λ can be both positive and negative because both concave and convex forms can be thought.

In Fig. 1 the vapor pressure of ice particles, p_r, is plotted as a function of their radius, r, according to Eq. [7] for $\lambda = 0$, $\lambda = -2 \times 10^{-15}$, and $\lambda = 2 \times 10^{-15}$ dyn and for $T = 270$ K, $\rho = 0.999$ g cm^{-3}, $d_0 = 2.76 \times 10^{-8}$ cm, $A = 5.6008 \times 10^{-14}$ [according to Ref. (4)], $M = 18$, $\sigma_\infty = 71.97$ erg cm^{-2}, and $p_\infty = 8.1$ mmHg. The value of the vapor pressure of the ideal macrocrystal at 270 K is calculated in Ref. (4). The value of the quantity A is calculated in Ref. (4) in the following way: It is taken into account that in the van der Waals forces the orientation effect (the effect of Keesom) plays the greatest role—it constitutes 77% of the forces (14). The energy of the orientation effect, E_{0r}, is given by the expression

$$E_{0r} = -\frac{2}{3}\frac{\mu^4}{r_1^6 kT} = \frac{\beta_{0r}}{r_1^6} \quad [8]$$

where μ is the dipole moment of the molecules (for water molecules $\mu_{H_2O} = 1.84 \times 10^{-18}$ esu cm (1.84 D) (13)), $k = 1.38 \times 10^{-16}$ erg K^{-1} is the Boltzmann constant, $T = 298.2$ K. Therefore, the full energy of the van der Waals interaction is

$$E = -\frac{\beta_{0r}}{0.77 r_1^6} = -\frac{\beta}{r_1^6} = -\frac{2.4116 \times 10^{-58}}{r_1^6}.$$

From this equation $\beta = 2.4116 \times 10^{-58}$; the number of water molecules in 1 cm^3 is $n = N/18.1 = 3.33 \times 10^{22}$. Therefore, $A = \frac{1}{15}\pi n^2 \beta = 5.6008 \times 10^{-14}$.

As is seen in Fig. 1 the specified Gibbs–Thomson isotherm determines the fact that upon supersaturation, even in the case of uncharged particles, two types of cluster (drops, crystals) always exist in the system. The first type is in unstable equilibrium. This cluster is known as the critical nucleus. The other type of cluster is in metastable equilibrium; this is the quasi-equilibrium cluster, conditionally called by us small stable drops. Therefore, the conclusion can be drawn that during supersaturation the most probable state of the atoms (molecules) is that of clusters and not of separate single atoms (molecules).

Figure 1 shows that with a negative value of λ, an increase in the radius of the small stable drop is observed. The region of r values in which small stable drops can exist also increases with the negative λ value, the maximum of the curve $p_r = f(r)$ decreasing at that. In the case of $\lambda > 0$ the opposite is observed;

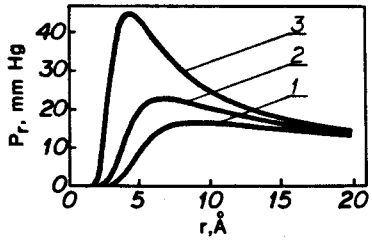

FIG. 1. Vapor pressure of small ice particles, p_r, as a function of their radius, r. (1) $\lambda = -2 \times 10^{-15}$ dyn, (2) $\lambda = 0$ dyn, (3) $\lambda = 2 \times 10^{-15}$ dyn.

with positive λ, decreases both in radius of the small stable drop and in the region where small stable drops can exist are observed, the maximum increasing at that. The latter changes are much more expressed than in the case of $\lambda < 0$. Figure 1 shows only the principal possibility for the existence of stable particles both when λ is positive and when λ is negative. Discussion of the real order of λ values is beyond the scope of this paper.

A basic conclusion can also be made from the above that in the case of homogeneous phase formation, the possibility of the existence of small stable drops is not determined by the sign of the specific edge free energy; whenever λ takes part in the phase formation small stable drops can exist both with positive and with negative λ.

Another important conclusion that can be drawn from the Gibbs–Thomson equation specified for $\sigma = f(r)$ is that critical supersaturation for homogeneous phase formation can be defined as

$$kT \ln(p/p_\infty) = \frac{2\sigma v}{r}$$

where v is the molecular volume and k is the Boltzmann constant. The following equation is obtained:

$$\ln(p/p_\infty) = \frac{2v\sigma^2}{kT\gamma_t}(\cos\Theta_\infty - \cos\Theta)\sin\Theta.$$

The values of n in Ref. (10) are obtained by expressing r from Eq. [9] and inserting it in the equation for the volume, V, of a segment of a sphere,

$$V = \frac{\pi}{3} r^3(2 - 3\cos\Theta + \cos^3\Theta),$$

and dividing by the volume of one molecule:

$$n = \frac{\pi}{3v} \cdot \frac{\gamma_t}{\sigma^3} \cdot \frac{2 - 3\cos\Theta + \cos^3\Theta}{(\cos\Theta_\infty - \cos\Theta)^3 \sin^3\Theta}.$$

In Fig. 2 the dependence of $\ln(p/p_\infty)$ versus n for water is shown as obtained in the above way for a reasonable value of $\gamma_t = 1 \times 10^{-5}$ dyn and $\sigma = 72$ dyn cm^{-1}, $\Theta_\infty = 45°$, $kT = 4 \times 10^{-14}$ erg, $v = 2.93 \times 10^{-23}$ cm^3.

One can note that unlike the first part of this paper, here, in the case of heterogeneous phase formation, we consider the specific surface free energy σ as size independent, only γ_t being considered size dependent through Eq. [9]. We apply this simplification here since it turned out that in the case of heterogeneous phase formation the $\sigma = f(r)$ dependence does not influence, in principle, the main conclusions drawn here. The effect of the $\sigma = f(r)$ dependence in the case of heterogeneous phase formation will be discussed in future communications.

Let us especially note that Fig. 2 is a more detailed presentation of the upper part of Fig. 1 in Ref. (9). This more detailed presentation leads to conclusions to be discussed now, which were unnoticed by the author of Ref. (9).

From Fig. 2 it is seen that at a given supersaturation in the region of approx $0.789 < \ln(p/p_\infty) < 0.797$ a drop exists of a given dimension (radius, r, or number of atoms, n) related with the left-hand branch, AB, of the curve ABC which will neither augment nor disappear upon an accidental increase in its dimensions. This drop will remain stable and it will represent the most probable dimension of the clusters for a given supersaturation. For clarity in Fig. 2, only the part of the whole curve corresponding to $110° < \Theta < 130°$ is represented; the slope of the two branches of

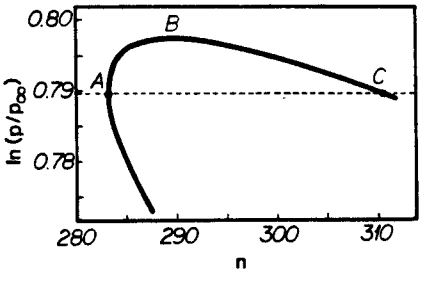

FIG. 2. Logarithm of supersaturation, $\ln(p/p_\infty)$, as a function of the number of atoms in the drop, n. See details in the text.

the curve outside these limits continues to be negative (i.e., corresponding to unstable drops) for the part of the curve below the broken line (corresponding to $\Theta < 118°$).

An important fact, also unnoticed in Ref. (9), is that according to Ref. (9, Fig. 1) at $\gamma > 0$ there are small drops of certain Θ values the existence of which is thermodynamically impossible. For instance, according to Ref. (9, Fig. 1) at a given supersaturation, unstable drops of two different dimensions exist or for a given dimension of the drop there are two differing values of the supersaturation (resp. vapor pressure). This is an evidently impossible situation: if in a closed system there are two bodies of different vapor pressures, the body with the lower vapor pressure will be thermodynamically more stable. Thus when equilibrium is reached the body with the higher vapor pressure should disappear, its vapors being condensed on the body with the lower vapor pressure. Therefore, when thermodynamic equilibrium is reached a body characterized with a single value of vapor pressure will remain in the system. These considerations lead us to the indisputable conclusion that from a thermodynamic point of view, it is impossible for the curve containing points A, B, and C (curve 1) and the curve below point A (curve 2) to exist simultaneously. Only one of these curves can exist in reality and the question is which one.

This question can be solved unambiguously only through experiments. Unfortunately, no experimental results are available so far. Nevertheless, we shall try to make some discussion and draw conclusions by applying analogy.

It is seen that in the case of $k < 0$ shown in Ref. (9, Fig. 2), a curve with a maximum is observed. In the case of homogeneous phase formation a maximum is obtained in the plot of $\ln(p/p_\infty)$ versus drop radius and according to Ref. (4, Eq. [16]) taking into account $\sigma = f(r)$ dependence, for both negative and positive specific edge free energy λ. Note that the quantity λ corresponds to k. It should especially be noted again, as was done above, that the derivations in Ref. (4) are based on quantities having strictly defined and clear physical meaning.

Proceeding from the above analogy it can be concluded that curve 1 is the physically possible one and curve 2, which is only a result of the mathematical calculations, should be ignored.

According to curve 1 in Fig. 2 only the drops having contact angle values of approx $\Theta > 118°$ (to the right of point A) can thermodynamically exist. However, we note further that in Ref. (9, Fig. 2) and in the case of homogeneous phase formation (4) there is no breaking of the curves at a point similar to point A. In Fig. 1 no curve to the left of point A is observed, probably because of some inaccuracy of the equations used to obtain the curve in Ref. (9, Fig. 2). This question, however, is beyond the scope of the present paper.

In the case of $\gamma_t > 0$ critical supersaturation can also be defined as is done in Ref. (9) for the case of $\gamma_t < 0$. In Fig. 2 point B defines the critical supersaturation for the case of $\gamma_t > 0$.

From the above it can be concluded that unlike the statements in Refs. (6–11), during heterogeneous phase formation small stable drops can exist not only when $\gamma_t < 0$ but also in cases when $\gamma_t > 0$ for $\Theta > \Theta_\infty$, the latter cases being the only possible ones when $\gamma_t > 0$.

Therefore, the possibility of the existence of small stable drops in phase formation is determined only by thermodynamic criteria. Other criteria, such as the sign of the slfe, cannot be decisive. The sign of the slfe can influence only the direction of the changes and the kinetic parameters of the process of phase formation.

REFERENCES

1. Ono, S., and Kondo, S., "Molecular Theory of Surface Tension in Liquids." Izdatel'stvo Inostrannoi Literaturi, Moscow, 1963. [in Russian]
2. Rowlinson, J. S., and Widom, B., "Molecular Theory of Capillarity." University Press, Oxford, 1982.
3. Tolman, R., *J. Chem. Phys.* **17**, (1949).
4. Noninski, C. I., *Khim. Ind. (Bulg.)*, No. 5, **33**, 144 (1961).
5. Noninski, C. I., *Khim. Ind. (Bulg.)*, No. 5, **39**, 208 (1967).

6. Scheludko, A., Toshev, B., and Platikanov, D., *in* "Modern Theory of Capillarity," pp. 163–182. Akademie Verlag, Berlin, 1981; *Ann. Univ. Sofia Fac. Chem.* **71**(1), 111 (1976/1977).
7. Scheludko, A., Chakarov, V., and Toshev, B., *J. Colloid Interface Sci.* **82**, 83 (1981).
8. Scheludko, A., *Colloids Surf.* **1**, 191 (1980).
9. Scheludko, A., *Colloids Surf.* **7**, 81 (1983).
10. Scheludko, A., Toshev, B., and Platikanov, D., "31st IUPAC Congress, Sofia (1987), Proceedings, p. 180.
11. Toshev, B. V., Platikanov, D., and Scheludko, A., *Langmuir* **4**, 489 (1988).
12. Moelwyn-Hughes, E. A., "Physical Chemistry." Izdatel'stvo Inostrannoi literaturi, Moscow, 1962. [in Russian]
13. "Short Handbook of Chemistry" [in Russian], Naukova Dumka, Kiev, 1974; "Handbook of Chemistry and Physics," 31st ed. (C. D. Hodgman, Ed.), p. 1747, Chemical Rubber Co., Cleveland, OH, 1949.
14. "Short Handbook of Chemistry." Izdatel'stvo Akademii Nauk Ukrainskoi SSR, Kiev, 1963. [in Russian]
15. Söhnel, O., and Garside, J., *J. Cryst. Growth* **89**, 202 (1988).
16. Shcherbakov, L. M., *Trudi Tul'skogo Mekhan. Inst.* **7**, 117 (1955).
17. Shcherbakov, L. M., *Koloid. Zh. (USSR)* **20**, 759 (1958).
18. Gibbs, J. W., "The Scientific Papers of J. Willard Gibbs," Vol. 1, "Thermodynamics," p. 288. Dover, New York, 1961.
19. Gretz, R. D., *J. Chem. Phys.* **45**, 3160 (1966).
20. Wesselovskii, V. S., and Pertzev, V. N., *Zh. Fiz. Khim. (USSR)* **8**, 245 (1936).

Colloids and Surfaces, 42 (1989) 205-207
Elsevier Science Publishers B.V., Amsterdam — Printed in The Netherlands

Brief Note

Stable Drop at Positive Line Tension

V.C. NONINSKI

Higher Institute of Chemical Technology, Lepger, Sofia 1156 (Bulgaria)

(Received 29 March 1988; accepted 20 June 1989)

ABSTRACT

In the present note it is shown that on supersaturation stable drops can, in principle, exist not only when the line tension, k, is negative but also in cases when $k>0$. Furthermore, it is pointed out that the decisive criteria for the existence of stable drops are thermodynamic ones, and not the sign of the line tension.

This note deals with the dependence of the logarithm of the supersaturation, $\ln(p/p_\infty)$, (where p is the vapour pressure of a small liquid drop and p_∞ is the vapour pressure of an infinite drop) as a function of the number of atoms in the liquid drop (in the case of heterogeneous phase formation), n, when the line tension [1,2] $k>0$ and the contact angle between droplet and substrate, θ, is greater than the contact angle of the large drop (for which the radius of the wetting perimeter $r\to\infty$), θ_∞.

We shall consider the case of the electrochemical deposition of mercury treated in Ref. [3], although the same conclusions also apply for other cases of heterogeneous phase formation. In Ref. [3], instead of the dependence $\ln(p/p_\infty)$ versus n the dimensionless quantity

$$\tilde{K}=(\cos\theta_\infty-\cos\theta)\sin\theta$$

versus the linear size of the drop in a dimensionless form

$$\tilde{l}=\frac{\sigma}{k}\left[\frac{3V}{\pi}\right]^{1/3}$$

is used (where σ is the surface tension and V is the volume of the drop). This exchange of the $\ln(p/p_\infty)$ versus n dependence by $\tilde{K}$ versus $\tilde{l}$ is possible because, as has been shown in Ref. [3] "the dependence $\tilde{K}$ versus $\tilde{l}$ reflects the changes in vapour pressure (supersaturation) with the change in drop size". As is claimed in Ref. [3] for the above conditions, namely $k>0$ and $\theta>\theta_\infty$, two curves of negative slope exist (Fig. 1 in Ref. [3]), so that "the states de-

0166-6622/89/$03.50

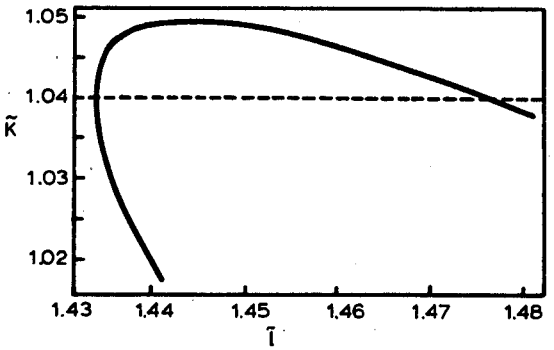

Fig. 1. Variation of $\tilde{K}$ with $\tilde{l}$ (see text) for $\Theta_\infty = 45°$, $k = 3.9 \cdot 10^{-5}$ dyn.

scribed by them are unstable: by an accidental enlargement of the equilibrium drop size its vapour pressure will diminish and the drop will continue to grow".

However, when the region of higher values of $\tilde{K}$ in Fig. 1 of Ref. [3] is observed it is seen that at a given Θ_∞ the branch of the curve with lower $\tilde{l}$ has a positive slope. This fact, unnoticed by the author of Ref. [3], can be seen in the curve presented in Fig. 1 above the broken line. This figure is obtained using the values of the constants given in Ref. [3] for a reasonable positive value of $k = 3.9 \cdot 10^{-5}$ dyn. It is necessary to note here that, because so far we are unaware of the real value of $k > 0$, if any, in the case of Hg electrodeposition, and also because the curve in Fig. 1 is plotted upon acceptance of $\sigma = \text{const}$ (note that $\sigma = \text{const}$ is accepted not only in the Gibbs–Thomson equation but also in the equation for k), which virtually does not hold for small drops, the conclusions from the figure can be drawn, for now, only in principle, utilizing only its form. In fact the conclusions from Fig. 1 in Ref. [3] were also drawn in principle because of the reasons stated above.

From Fig. 1 is seen that, above the broken line, a region of supersaturations exists where two forms of the new phase are in equilibrium: one is stable and the other unstable. The fact that such a region (although small) exists runs contrary to the claim in Refs [3–7] that a stable drop of the new phase is possible only when $k < 0$, and proves that stable drops can also exist in the case of a positive line tension ($k > 0$). Figure 1 also shows that the definition of critical supersaturation in terms of Refs [3 and 7] can be applied not only when $k < 0$ but also when $k > 0$.

REFERENCES

1 J.W. Gibbs, The Scientific Papers of J. Willard Gibbs, Vol. 1, Thermodynamics, Dover, New York, 1961, p. 288.
2 R.D. Gretz, Surf. Sci., 5 (1966) 239.

3 A. Scheludko, Colloids Surfaces, 7 (1983) 81.
4 A. Scheludko, V. Chakarov and B. Toshev, J. Colloid Interface Sci., 82 (1981) 83.
5 A. Scheludko, Colloids Surfaces, 1 (1980) 191.
6 A. Scheludko, B. Toshev and D. Platikanov, in Modern Theory of Capillarity, Akademie Verlag, Berlin, 1981, pp. 163–182; Ann. Univ. Sofia, Fac. Chem., 71 (1976/1977) 111.
7 A. Scheludko, B. Toshev and D. Platikanov, Proc. 31st IUPAC Congress, Sofia, 1987, p. 180.

Pergamon

PII: S0013-4686(96)00151-X

Electrochimica Acta, Vol. 42, No. 2, pp. 251–254, 1997

0013-4686/97 $17.00 + 0.00

Magnetic field effect on copper electrodeposition in the Tafel potential region

V. C. Noninski

Laboratory LEPGER, 149 West 12th Street, New York, NY 10011, U.S.A.

(Received 18 March 1996)

Abstract—Experimental results are reported indicating that a constant homogeneous magnetic field of 12 kGs causes a decrease of the copper deposition overpotential (increase of copper deposition rate) in the Tafel potential region. The experimental results presented in this paper were initially submitted to this journal on 13 December, 1988 as a continuation of the studies in C. Noninski *et al.*, 33rd ISE meeting, **1**, 939 (1982) [1], V. Noninski *et al.*, Elektronnaya obrabotka materialov, **1**, 50 (1986) [2]. Thus, the effect of magnetic field on copper electrodeposition in the Tafel potential region has been established prior to the paper J. P. Chopart *et al.*, electrochim. Acta **36**, 459 (1991) [3], which does not appear to have been recognized in the latter.

Key words: electrode kinetics, magnetic field, copper electrodeposition, electrode overpotential, Tafel potential region

INTRODUCTION

The effect of magnetic field (m.f.) on electrochemical reactions has been the subject of many investigations [1, 2, 4–28]. The main interest in most of these investigations is directed toward the regions where the rate-determining step of the reaction is diffusion (or at least, region of mixed kinetics). The interest in these types of electrode reactions is natural because m.f. is expected to have an effect on the concentration gradients existing in the solution at these conditions.

For the first time the effect of m.f. on the overpotential, η, in the Tafel potential region where the effect of concentration gradients on the overpotential is not expected, was reported in Refs [1, 2].

In the present paper further studies concerning m.f. effects on the copper deposition overpotential in the Tafel region are presented. Copper electrodeposition from sulfuric acid solutions is chosen for this study because of its technological significance and because of the fact that a well expressed Tafel potential region exists in which it is well established that the reasons for the overpotential are pure kinetic (see for instance the classical paper of Mattsson and Bockris [29]).

EXPERIMENTAL

In Fig. 1 the experimental set-up is shown schematically. The disc-shaped electrolytic copper cathode of 0.1 cm^2 working surface area and anode (also of electrolytic copper) of $\sim$20 cm^2 surface area are situated in a quartz cuvette of $2 \times 2 \times 3$ cm^3 dimensions. A saturated calomel electrode (*sce*) is used as a reference electrode. Sulfuric acid solutions of $CuSO_4$ were made using bidistilled water and chemicals of p.a. grade. The electromagnet used is of 12 kGs induction with a 3 cm gap between the poles.

In Fig. 2 another set-up used is shown, enabling the Luggin capillary of $\sim$30 μm diameter to be set at strictly chosen distances from the electrode surface.

The constant current is maintained using Radelkis OH-405 (Hungary) potentiostat–galvanostat used as galvanostat and the overpotential is measured using lamp millivoltmeter СП-2 (Fig. 2). The current–time transients were recorded on Endim 620.01 (GDR) X–Y recorder.

RESULTS

In Fig. 3 an example of overpotential–time transient is shown, taken while keeping constant the current passing through the electrolytic cell. The current corresponds to a potential from the Tafel potential region. From Fig. 3 it is seen that when the m.f. is turned on the copper deposition overpotential rapidly decreases to reach a minimum value. After that a slow increase of the overpotential is observed until a constant value is reached. The stationary overpotential value is much lower than the magnetic-field-off value of the overpotential. At higher currents (also corresponding to the Tafel potential region) the stationary magnetic-field-on value of the overpotential is attained much faster, shortly after the moment

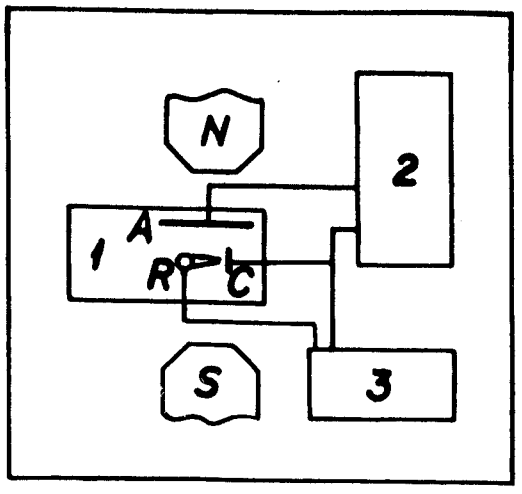

Fig. 1. Scheme of the experimental set-up for measuring the effect of magnetic field on overpotential (rate) of copper electrodeposition. 1, electrolytic cell; 2, potentiostat–galvanostat Radelkis OH-405 (Hungary): 3, X–Y and Y–t recorder Endim 620.01 (GDR). A, anode; C, cathode, and R, reference electrode. N and S, poles of the electromagnet.

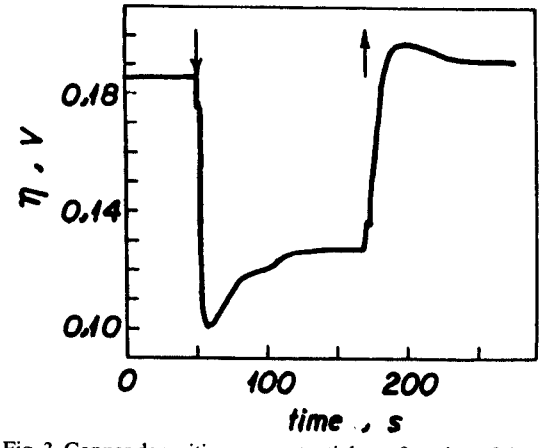

Fig. 3. Copper deposition overpotential as a function of time at current density $i = 0.05$ A cm^{-2} corresponding to the Tafel potential region. ↓, magnetic field on (12 kGs): ↑, magnetic field off. Electrolyte is 0.75 M $CuSO_4$ + 2 M H_2SO_4. The curve is obtained with the experimental set-up shown schematically in Fig. 1.

of turning the m.f. on. After turning off the m.f. the overpotential sharply increases reaching a maximum value, higher than the initial one. After a certain time, the stationary overpotential value after turning off the m.f. becomes equal to the initial overpotential value. At higher current densities (c.d.s) the maximum disappears and after turning the m.f. off the overpotential reaches its steady-state value without exceeding its initial one.

In Fig. 3 some other peculiarities in the run of the curve are seen which to a different extent appear with all the curves taken at the various c.d.s corresponding to the Tafel potential region. We shall not comment on them here.

Curves of the type shown in Fig. 3, taken at different currents, are used to obtain Fig. 4. From every such curve the stationary value of the overpotential in the presence and in the absence of m.f. is plotted against the corresponding current density.

From Fig. 4 it is seen that when the m.f. is off, the dependence between the overpotential, η, and log i is linear, *ie* it obeys the Tafel law:

$$\eta = a + b \log i \qquad (1)$$

where a and b are constants and i is the applied current density.

It is seen from Fig. 4 that the m.f. causes the overpotential to decrease (the reaction rate to increase), this decrease being higher at the higher c.d.s. The overpotential decrease observed in Fig. 4 is of the order of the decrease when applying continuous mechanical renewal (CMR) of the

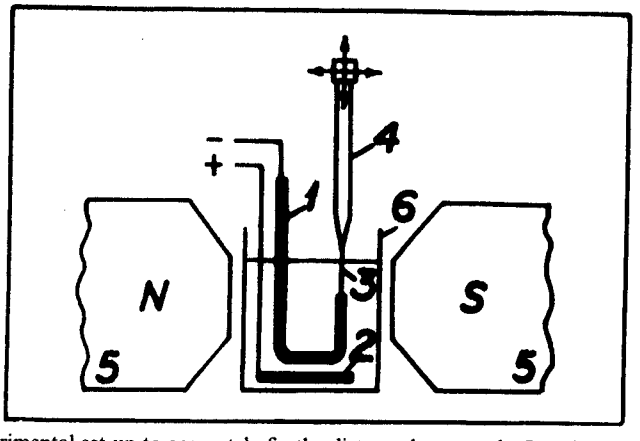

Fig. 2. Scheme of the experimental set-up to accurately fix the distance between the Luggin capillary tip and the electrode surface. 1, copper cathode ($S = 0.1$ cm^2): 2, copper anode ($S \approx 10$ cm^2); 3, Luggin capillary ($d \approx 30$ μm); 4, saturated calomel electrode attached to a micrometric table (not shown in the figure); 5, electromagnet of 12 kGs induction; 6, quartz cuvette.

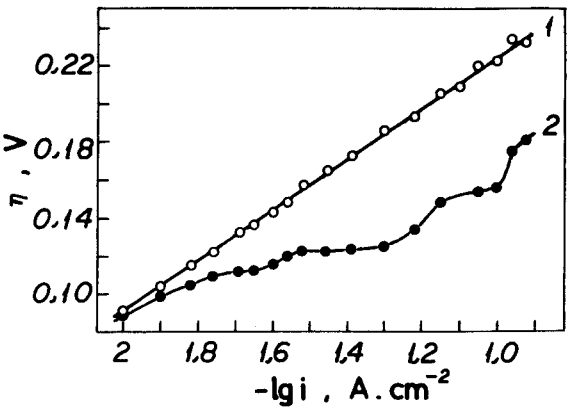

Fig. 4. Tafel plot for the electrodeposition of copper from 0.75 M $CuSO_4$ + 2 M H_2SO_4 obtained with the experimental set-up shown schematically in Fig. 1, line 1. Curve 2, η–log i dependence in the presence of a magnetic field of 12 kGs. This figure is obtained on the basis of transients similar to those shown in Fig. 3, taken at various current densities.

electrode surface—about 0.060 V at the higher c.d.s [30]. The slope of the Tafel line, b, in the absence of m.f. is ~0.130 V which is in agreement with the observed value of b in [17]. When the m.f. is on, the run of the η–log i line changes. One can hardly consider that the linear dependence is preserved any more; the line is transformed into a curve situated at lower overpotentials. Therefore, according to Fig. 4, in m.f. the Tafel dependence is no longer observed; it looks as if the Tafel dependence is being "destroyed". It is interesting to note that a similar "destroying" of the linearity between η and log i is observed (though unnoticed by the authors) in Fig. 5 of [28]. One can see in Fig. 5 of [28] that the linear η–log i dependence under m.f. is shortened and the points corresponding to the higher c.d. values do not lie on the Tafel line.

From Fig. 5 it is seen that when removing the Luggin capillary away from the electrode surface the change of the potential (overpotential) is significantly greater than that corresponding to the Ohmic drop. For distances greater than about 0.2 cm evidently it is the Ohmic component of the potential, due to the resistance of the solution, that determines the run of the η–d curve. This fact is in agreement with the earlier observed dependence between the electrode potential and d [31]. With the increase of the c.d. the change of the overpotential with the distance d is more clear. In m.f. of 12 kGs a change in the run of the η–d curve is observed which is greater the greater is the polarizing current.

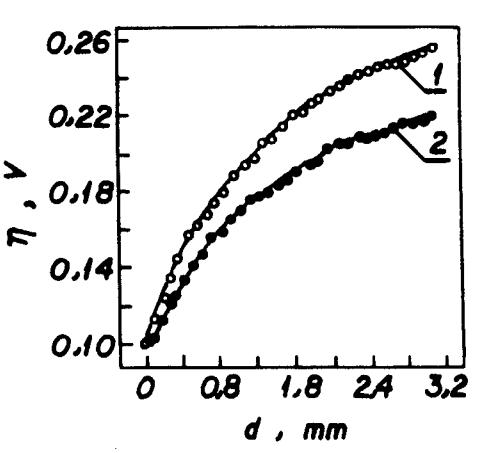

Fig. 5. Copper deposition overpotential as a function of the distance, d, between the Luggin capillary tip and the electrode surface. The curves are obtained with the set-up shown schematically in Fig. 2. Solution, 0.75 M $CuSO_4$ + 0.1 M H_2SO_4; 1, magnetic field is off; 2, magnetic field of 12 kGs is on. Current density i = 0.05 A cm^{-2}.

It is seen from Fig. 5 that at every distance, d, between the electrode and the capillary, at the given c.d. value, the overpotential value obtained in the presence of m.f. is always lower than in absence of m.f. This observation is in agreement with the conclusions from Fig. 4.

The dependencies shown in Fig. 4 correspond to a certain distance, d, between the capillary and the electrode surface. We can determine that distance at which the Luggin capillary is during the experiment. Thus, from Fig. 4, the overpotential value is determined, corresponding to the c.d. at which, say, curve 1 in Fig. 5 is obtained, and then from Fig. 5 the distance, d, to which this overpotential corresponds is worked out.

Unfortunately, because of the difference of the H_2SO_4 concentrations at which Figs 4, 5 were obtained the determination of d in the present case will not be exact. Here, we only mention the principle as a possibility for such determinations.

As is seen from Fig. 5 the effect of m.f. is felt in the bulk of the solution, beyond the double electric layer, rather than at the very electrode–electrolyte interface. This can be considered as an indication that the cause of the overpotential should be looked for on the side of the solution, at a macroscopic level. The change of the overpotential observed in Fig. 5 is connected with the decrease of the Ohmic drop in the solution layer between the capillary tip and the surface of the

cathode. The sole cause for the observed decrease of the Ohmic resistance must be the change of the solution concentration in the solution layer near the electrode (*ie* decrease of the copper ion concentration in the layer near the electrode, in the direction towards equalizing it with its concentration in the bulk of the solution at unchangeable concentration of the sulfuric acid). Evidently, under the action of the magnetic field the ions change their trajectory of movement due to the Lorentz force in such a way that their concentration in the solution layer near the electrode decreases. Discussion in more detail of how this concentration change may affect the activation overpotential will be given elsewhere.

Our experiments [1] unlike the observations in [28] showed that the m.f. influence on Cu deposition overpotential depends on the cathode surface orientation with respect to the magnetic field lines of force. When the cathode surface is perpendicular, and accordingly the lines of current are parallel to the magnetic lines of force, no influence of the m.f. on the overpotential is observed. Further, the m.f. influence on the overpotential does not depend on the mutual cathode–anode orientations (and respectively on the corresponding disposition of the current lines). It seems the influence of the m.f. is concentrated on the ions situated at a very close distance from the cathode surface, where the direction of the ion motion does not depend on the mutual cathode–anode surface orientations.

As noted, in the present paper no attempts to explain the observed effects will be made, these will be deferred to future communications. It will only be noted that the claim in [21] that the m.f. may affect the rate of both activation (charge-transfer) and mass-transport controlled processes has not been proven. In [21] a case is observed in which m.f. induces potential difference (causes current to flow) in a flowing electrolyte system. It is also to be noted that the authors of [28], who also observe m.f. effects on the activation overpotential of copper deposition (and who also fail to recognize in their paper the prior establishment of this effect in [1, 2]) look for the reasons for this effect in terms of mass-transport effects, although the nature of the overpotential is discussed by them according to the charge-transfer theory.

REFERENCES

1. C. Noninski, V. Noninski and V. Terzyiski, 33rd ISE meeting, Lyon, France, Vol. 1. p. 939 (1982).
2. V. Noninski and C. Noninski, *Elektronnaya obrabotka materialov* (USSR) **1,** 50 (1986).
3. J. P. Chopart, J. Douglade, P. Fricoteaux and A. Oliver, *Electrochim. Acta* **36,** 459 (1991).
4. E. J. Center, R. C. Overbeck and D. L. Chase, *Anal. Chem.* **23,** 1134 (1951).
5. L.. Yang, *J. Electrochem. Soc.* **101,** 456 (1954).
6. A. M. Evseev, *Zhurnal Fizicheskoi Khimii* (USSR) **36,** 1610 (1962).
7. E. Z. Gak, *Elektrokhimia (USSR)* **3,** 263 (1967).
8. D. Guerin-Ouler, C. Nicollin and A. Olivier, *C.R. Acad. Sci. Paris* **270,** 1500 (1970).
9. S. Mohanta and T. Z. Fahidy, *Can. J. Chem. Engin.* **50,** 248 (1972).
10. D. Laforgue-Kantzer, A. Laforgue and T. Cong Khanh, *Electrochim. Acta* **17,** 151 (1972).
11. J. Dash and W. W. King, *J. Electrochem. Soc.* **119,** 51 (1972).
12. M. Ammar, A. Laforgue and D. Laforgue-Kantzer, *C.R. Acad. Sci. Paris* **274,** 2140 (1972).
13. T. Z. Fahidy, *Electrochim. Acta* **18,** 607 (1973).
14. E. Z. Gak, E. H. Rokhinson and N. F. Bondarenko, *Elektronnaya obrabotka materialov* (USSR) **6,** 24 (1973).
15. S. Mohanta and T. Z. Fahidy, *Electrochim. Acta* **19,** 771 (1974).
16. S. Mohanta and T. Z. Fahidy, *Electrochim. Acta* **19,** 835 (1974).
17. E. Z. Gak, E. Kh. Rokhinson and N. F. Bondarenko, *Sov. Electrochem.* **11,** 489 (1975).
18. E. Z. Gak, E. Kh. Rokhinson and N. F. Bondarenko, *Sov. Electrochem.* **11,** 495 (1975).
19. A. P. Shorigin, G. L. Danielyan and R. Z. Alimova, *Elektrokhimia* (USSR) **11,** 1478 (1975).
20. V. N. Duradji and I. V. Bryantzev, *Elektronnaya obrabotka materialov* (USSR), **15,** 235 (1976).
21. E. J. Kelly, *J. Electrochem. Soc.* **124,** 987 (1977).
22. M. I. Ismail and T. Z. Fahidy, *Can. J. Chem. Engin.* **58,** 505 (1980).
23. G. Neite and E. Nembach, *Mater. Sci. Eng.* **52,** 169 (1982).
24. R. N. O'Brien and K. S. V. Santhanam, *J. Electrochem. Soc.* **129,** 1266 (1982).
25. A. Chiba, H. Hosokawa and T. Ogawa, *Surf. Coat. Technol.* **27,** 131 (1986).
26. A. Chiba, T. Niimi, H. Kitayama and T. Ogawa, *Surf. Coat. Technol.* **29,** 347 (1986).
27. A Chiba, K. Kitayama and T. Ogawa, *Surf. Coat. Technol.* **27,** 83 (1986).
28. A. Chiba, T. Ogawa and T. Yamashita, *Surf. Coat. Technol.* **34,** 38 (1988).
29. E. Mattsson and J. O'M. Bockris, *Trans. Faraday Soc.* **55,** 1586 (1959).
30. C. Noninski, L. Veleva and V. Noninski, *Surf. Technol.* **25,** 127 (1985).
31. C. Noninski, 33rd ISE meeting, Lyon, France, Vol. 1, p. 933 (1982).

Corrosion Science, Vol. 30, No. 8/9, pp. 839–847, 1990
Printed in Great Britain

0010-938X/90 $3.00 + 0.00

CORROSION STUDIES WITH THE SELF-CLEANING ROTATING ELECTRODE (SRE)

V. C. NONINSKI

Higher Institute of Chemical Technology, Laboratory on Electrochemistry of Renewed Interface (LEPGER), Sofia 1156, Bulgaria

Abstract—Current–time curves taken with the self-cleaning rotating electrode (SRE) are applied to study the transition from the state of continuously mechanically renewed (CMR) electrode surface to that of non-renewed surface of some steels, noble metals, Pt and Cu. These curves make it possible to characterize quantitatively both the common features and the peculiarities of that transition for different metals in corrosive media. It is also possible, on the basis of these current–time transients, to characterize quantitatively the action of inhibitors of metal corrosion in a dynamic regime, unlike the commonly used steady-state degree of protection from corrosion. The experimental findings on the basis of these curves can further be used for establishing the mechanism and kinetics of active dissolution, passive layer formation, the inhibiting of metal corrosion by different substances etc. These transients can accompany the produced metals and inhibitors and also can be gathered together in an Atlas, to help engineers choose the most suitable metal or inhibitor when their construction is to undergo mechanical stress, strain, vibrations etc., i.e. when a fresh metal surface is expected to appear.

INTRODUCTION

THE METHOD of continuous mechanical renewal (CMR) of the electrode surface with the help of the self- cleaning rotating electrode (SRE)[1] is suitable for examining the corrosion behaviour of metals in cases where there is contact of fresh metal surface with a corrosive medium. There are studies in literature of the effect of mechanical factors (scratching, wiping etc.) on the corrosion behaviour of metals[2–50] which help towards an understanding of the mechanism of passivation, stress corrosion etc. Before SRE, however, it was not possible for the effect of CMR to be studied under: (a) defined conditions of the surface—constant surface area, controllable state of renewal, renewing of the whole surface which is unscreened by the renewing device etc.; and (b) diffusion and hydrodynamic conditions of the system which both ensure high reproducibility of the results and enable effects to be observed which are difficult to observe in any other way, for example, the effect of the hydrogen evolution overvoltage decrease during the CMR of metals possessing a high hydrogen overpotential.[51] Results on studies concerning the anodic behaviour of some steels, a noble metal, Pt, Cu and of some inhibitors of corrosion in the conditions of continuous mechanical renewal (CMR) of the anode surface are presented below.

EXPERIMENTAL METHOD

Two main types of experiment have been carried out. One consisted of determining the polarization curves on non-renewed surface and comparing them with the polarization curves taken in the same conditions but during the CMR of the surface. Another was the registration of time and potential transients by applying a potential to the anode while the latter is under CMR conditions; the change of

Manuscript received 25 April 1988; in amended form 1 July 1988 and 18 April 1989.

current with time is registered. At a certain moment the renewal of the surface is suddenly stopped but the registration of the curve continues. Thus the changes in the current–time curve while the surface passes from the state of CMR to the state of non-renewed surface can be observed. To see what influence a new renewal of the surface will have for some experiments the electrode at a given moment was rotated anew.

Current–time transients upon scratching the surface of the electrode have been reported previously,[12–16,17–19,36–50] as well as earlier studies of transients connected with metal corrosion.[31–33] The potentials at which the transients were registered were obtained from the polarization curves taken at the beginning of the experiment.

EXPERIMENTAL RESULTS AND DISCUSSION

The region of active dissolution

In this region a relatively weak influence of the CMR is observed on the current–time curves of the steels Г13 and Х18АГ12, curves 1 and 2 of Fig. 1. The renewal does not remove the factors which cause an eventual retardation of the dissolution process. From curves 1 and 2 of Fig. 1 it can be seen that the behaviour of the two steels is somewhat different. At curve 1 a fast return to the state of non-renewed surface takes place. At curve 2 the transition to non-renewed surface is smooth and the steady-state is reached after a significant interval of time. The specimens of the steels manufactured by the Japanese firms show a significant influence of the CMR in this range of potentials. Though the specimens are of the same trade mark there are certain differences in the technology of their production. It should be noted that the current–time curves are taken at differing potentials though these potentials are all chosen to be near the maximum of dissolution of the different steels. This fact probably also has its influence on the curves.

For curve 1 in Fig. 2, obtained in H_2SO_4, stopping the renewal causes a fast drop of the current which becomes cathodic. However, immediately afterwards the cathodic current begins to decrease again eventually becoming anodic with a

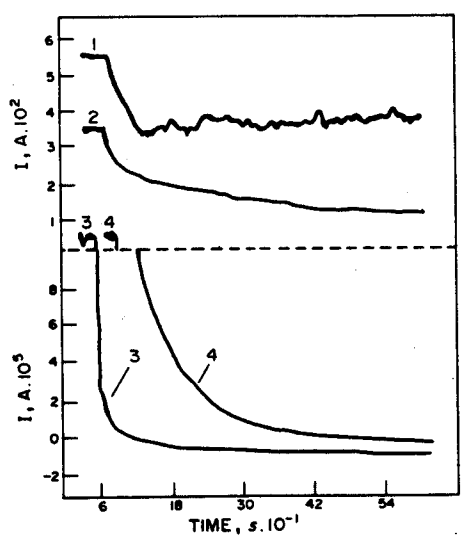

FIG. 1. Current–time transients for various steels at potentials near the maximum of the anodic dissolution in the active region: (1) Г13 (composition: C—0.95, Mn—11.88, Si—1.28, N_2—0.0254%), ϕ = −0.120 V(NHE); (2) Х18АГ12 (C—0.053, Mn—11.14, Cr—17.94, Si—0.8, N_2—0.448%), ϕ = −0.220 V(NHE); (3) AISI 304, NISSHIN Steel Co., ϕ = +0.230 V(NHE); (4) AISI 304 NIPPON JAKIN, ϕ = +0.280 V(NHE).

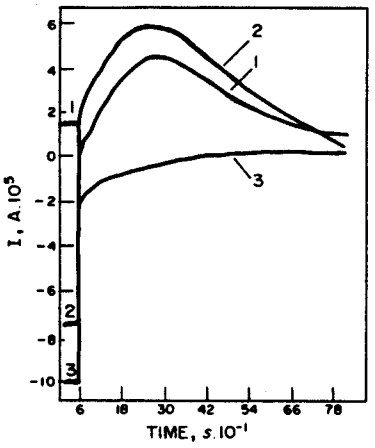

FIG. 2. Current–time dependencies obtained at potential $\phi = -0.11$ V. Anode—stainless steel 1X18H9T. (1) 8 N H_2SO_4; (2) 8 N H_2SO_4 + $K_2Cr_2O_7$; (3) 8 N H_2SO_4 + $KMnO_4$. The concentration of the inhibitors in all cases was 1%.

maximum. After the addition of $K_2Cr_2O_7$, a cathodic current passes through the electrode during CMR. After stopping the renewal the cathodic current rapidly decreases and also becomes anodic, also passing through a maximum. Curve 3 obtained after the addition of $KMnO_4$ upon CMR is situated at even higher cathodic current than curve 2 upon CMR. When the renewal is stopped curve 3 does not pass into the anodic region. Passing of the current from anodic into cathodic after ceasing of the renewal shows that the anodic dissolution entirely stops. The rapid transformation of the cathode current again into an anode one can be explained by the effect of the cathode process on the state of the electrode surface and eventually also on the inhibitor present on the electrode surface which again causes activation of the electrode. The maxima of curves 1 and 2 are connected with the fact that the changes in the state of the electrode surface at the anode process are opposite to the changes when a cathodic process takes place.

From curve 1 of Fig. 3 the Pt electrode exhibits a current of $\sim 4 \times 10^{-6}$ A which flows through the SRE. Investigation showed[52] that this anodic current at a similar potential is due to anodic dissolution of Pt. After stopping the renewal the current decreases to reach a steady-state value practically equal to zero. On re-starting the renewal the current rapidly increases reaching the starting value. Curve 2 in Fig. 3 shows that the addition of $K_2Cr_2O_7$ leads to an increase of the anode current value of almost an order of magnitude on renewal. After stopping the renewal in this case the anode current rapidly decreases to a minimum value after which it begins to increase to reaching a steady-state value greater than the one in pure H_2SO_4. Curve 3 in Fig. 3 shows that the addition of $KMnO_4$ during CMR exerts a diametrically opposite influence on the anode process in comparison with $K_2Cr_2O_7$—the anodic current decreases down to zero and even passes to the cathode, the latter having a value of about two orders of magnitude greater than the anodic current value in pure H_2SO_4. After stopping the renewal the cathode current decreases but does not pass again into anodic one. The activation of the Pt surface after the addition of $K_2Cr_2O_7$ and its passivation when adding $KMnO_4$ can be explained if it is accepted that in H_2SO_4

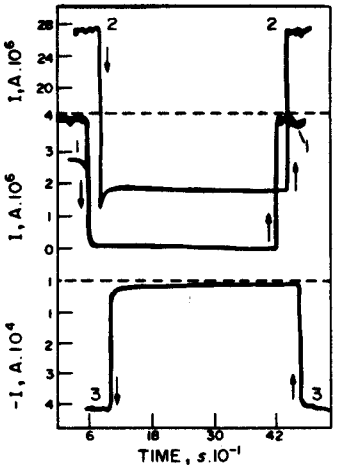

FIG. 3. The dependence of the current passing through Pt SRE on the time at potential 1.08 V(NHE). (1) N H_2SO_4; (2) 1 N H_2SO_4 + $K_2Cr_2O_7$; (3) 1 N H_2SO_4 + $KMnO_4$. Rate of SRE rotation 1000 rpm. ↓—rotation of the SRE (renewal) is ceased. ↑—rotation of the SRE (renewal) begins (1000 rpm).

solution at a potential of 1.080 V, though lower than the equilibrium potential of the oxygen electrode, the same passivating layer begins to appear on the Pt surface which preserves the latter from dissolution at potentials higher than the equilibrium potential of the oxygen electrode; the $K_2Cr_2O_7$ hinders while $KMnO_4$ helps the formation of a passivating layer. It should be expected that the presence of $K_2Cr_2O_7$ and $KMnO_4$ exerts certain influence on the composition of the passivating layer.

This suggestion is consistent with the current–time curves obtained in 1 N KOH and shown in Figs 4–6. From Fig. 4 it is seen that $K_2Cr_2O_7$ and $KMnO_4$ act directly on

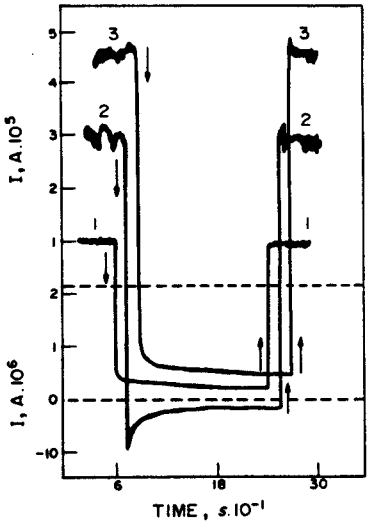

FIG. 4. Current–time dependencies on Pt SRE polarization at potential 0.14 V(NHE). (1) 1 M KOH; (2) 1 M KOH + $K_2Cr_2O_7$; (3) 1 M KOH + $KMnO_4$.

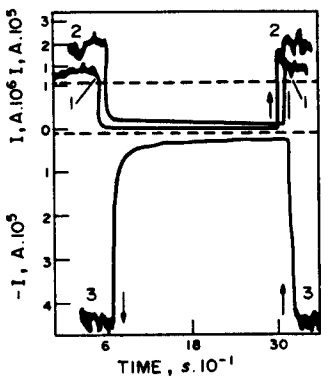

FIG. 5. Current–time dependencies on Pt SRE polarization at potential of 0.240 V(NHE). (1) 1 M KOH; (2) 1 M KOH + $KMnO_4$; (3) 1 M KOH + $K_2Cr_2O_7$.

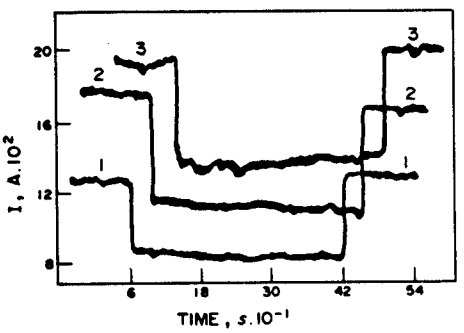

FIG. 6. Current–time dependencies on Pt SRE polarization at 1.240 V potential. (1) 1 M KOH; (2) 1 M KOH + $KMnO_4$; (3) 1 M KOH + $K_2Cr_2O_7$.

the passivating layer upon CMR as common oxidizers and accelerate the dissolution. At a potential nearer to the equilibrium oxygen the curves in Fig. 5 show that the passivating layer already begins to form and an influence on that formation adds to the direct influence on the rate of Pt dissolution. This influence is the same as in Fig. 3 though here the roles of $KMnO_4$ and $K_2Cr_2O_7$ are exchanged. At 1.24 V the formation of the passivating layer does not seem to be influenced by the presence of $K_2Cr_2O_7$ and $KMnO_4$ and they manifest themselves as common oxidizers, again accelerating, though weakly, the Pt dissolution.

From curves 1 and 4 in Fig. 7, taken at potentials from the region of active dissolution of Cu, it is seen that after stopping the renewal the transition from the state of CMR surface to the state of non-renewed is relatively slow. At a potential corresponding to the maximum of the dissolution rate—curve 2—this transition is already rapid.

The passive region

From curve 3 in Fig. 7 the transition from the state of CMR to the steady-state of non-renewed surface can be seen to take place more rapidly than the corresponding

transition in the region of active dissolution. Clearly, if passivation is promoted, by, for example, sedimentation of $CuSO_4$, as a result of the supersaturation at the anode layer, the current will decrease much more rapidly than in the absence of such a factor.

From curve 1 in Fig. 8 it is seen that the depth of passivation of X18АГ12 is the greatest for the studied steels in this figure. Despite this fact, however, for some uses

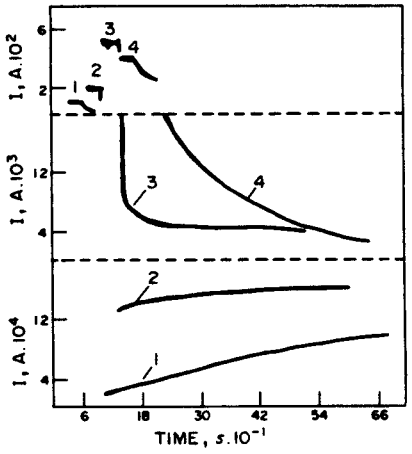

FIG. 7. Current–time transients of Cu SRE in 0.49 M $CuSO_4$ + 4 M H_2SO_4. Curve (1) is taken at 0.44 V; (2) 0.58 V; (3) 0.68 V; (4) 0.38 V.

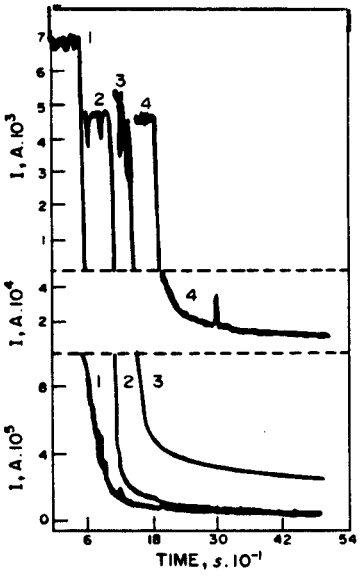

FIG. 8. Current–time dependencies for various steels, obtained with the help of the SRE in 8 N H_2SO_4 at potentials from the passive region of these steels (where the passivation is deepest). (1) X18АГ12, ϕ = +0.680 V(NHE); (2) AISI 304 NISSHIN Steel Co., ϕ = 0.780 V; (3) AISI 304 NIPPON JAKIN, ϕ = +0.730 V, (4) Г13, ϕ = +0.178 V. Compositions of the steels are the same as in Fig. 1.

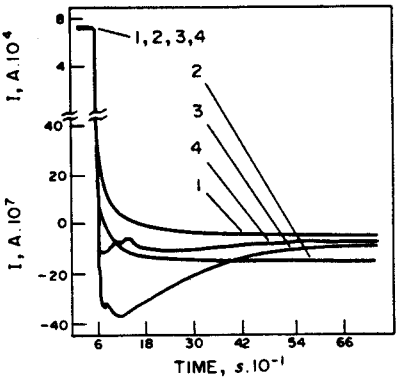

FIG. 9. Current–time dependencies obtained at potential ϕ = +0.480 V. Anode—stainless steel 1X18H9T. (1) 8 N H_2SO_4; (2) 8 N H_2SO_4 + $K_2Cr_2O_7$; (3) 8 N H_2SO_4 + $KMnO_4$; (4) 8 N H_2SO_4 + $KMnO_4$ + H_3PO_4.

the steel corresponding to curve 2 might be preferred because passivity is reached more rapidly. Peaks can be seen in curve 1 which are an indication for a certain tendency towards depassivation. Γ13 steel also exhibits a tendency towards depassivation. According to the current–time curves the steels produced in Japan do not differ much from one another but the depth of passivation of the steel produced by NISSHIN Steel Co. is greater. The curves also do not differ much in the region of CMR. In the active region a full corrosion protection of the Japanese steels takes place: the curves in Fig. 1 change from anodic to cathodic. In the passive region such an effect is not observed with these steels.

In Fig. 9, unlike Fig. 2, the current on CMR is the same in the absence and presence of inhibitors. After stopping the renewal the current rapidly decreases becoming cathodic , this change being fastest with $KMnO_4$ which also causes the cathode current to pass through a maximum. Curve 4 in Fig. 9 shows that when H_3PO_4 is added the influence of the $KMnO_4$ significantly decreases. The experiments showed that some other inhibitors such as pyridine, HNO_3, piperidine, β-naphthol, phenol, benzene, benzaldehyde, aniline, α-naphthylamine, picric acid, anthraquinone, benzoic acid, etc. do not influence the run of curve 1 of Fig. 9. The fact that at a potential in the passive region on renewal of the surface the inhibitors do not influence the current value shows that the observed current is defined practically only by the two processes: formation of the passivating layer and mechanical removal of the layer by CMR. The action of the inhibitors is negligibly small compared to that of the factors determining the formation of the passivating layer. This is seen better from the current–time curves after stopping the renewal of the surface. According to curve 1 of Fig. 9, after stopping the renewal the formation of a passivating layer decreases the current by several orders of magnitude, while according to curves 2–4 compared to curve 1 the additional change of the current under the action of the inhibitors is of the order of a thousandth part from the change due to formation of a passivating layer.

CONCLUSIONS

(1) The transients can be used to estimate the transition from the state of CMR to the state of non-renewed metal electrode surface. Furthermore, the current–time

transients can be used to examine the mechanism and kinetics of active metal dissolution, the formation of passivating layers, the inhibition of metal corrosion etc.

(2) The characteristics of transients can be an indication for the corrosion properties of metals where a fresh metal surface is created.

(3) Transients can be used for a quantitative characterization of inhibitors of metal corrosion in a dynamic regime, unlike the commonly used steady-state degree of protection from corrosion.

REFERENCES

1. C. I. NONINSKI, *Khimia i industria* (Bulgaria) **38**, 442 (1966).
2. H. ABD EL KADER and S. M. EL TANGY, *Electrochim. Acta* **30**, 841 (1985).
3. A. A. ADAMS and R. T. FOLEY, *Corrosion* **31**, 84 (1975).
4. J. R. AMBROSE and J. KRUGER, *Corrosion* **28**, 30 (1972).
5. E. V. BARELKO and B. N. KABANOV, *Dokl. Akad,. Nauk SSSR* (USSR) **90**, 1059 (1953).
6. T. R. BECK, *J. electrochem. Soc.* **115**, 890 (1968).
7. T. R. BECK, *Electrochim. Acta* **18**, 807 (1973).
8. T. R. BECK, *Electrochim. Acta* **18**, 815 (1973).
9. T. R. BECK, *Electrochemical Techniques for Corrosion* (ed. R. Baboian), p. 27, NACE, (1977).
10. T. R. BECK, *J. electrochem. Soc.* **129**, 2500 (1982).
11. M. W. BREITER, *Electrochim. Acta* **12**, 679 (1967).
12. G. T. BURSTEIN and D. H. DAVIES, *Corros. Sci.* **20**, 1143 (1980).
13. G. T. BURSTEIN and D. H. DAVIES, *J. electrochem. Soc.* **128**, 33 (1981).
14. G. T. BURSTEIN and D. H. NEWMAN, *Corros. Sci.* **20**, 375 (1980).
15. G. T. BURSTEIN and D. H. NEWMAN, *Electrochim. Acta* **25**, 1009 (1980).
16. G. T. BURSTEIN and D. H. NEWMAN, *Electrochim. Acta* **26**, 1143 (1981).
17. F. P. FORD, PhD Thesis, Univ. of Cambridge (1973).
18. F. P. FORD, *Metal Sci.* **12**, 326 (1978).
19. F. P. FORD, G. T. BURSTEIN and T. P. HOAR, *J. electrochim. Soc.* **127**, 1325 (1980).
20. N. M. GONTMAHER, V. E. GUTERMAN, V. A. SAFONOV, O. A. PETRII and V. P. GRIGORJEV, *Elektrokhimia* (USSR), **23**, 3 (1987).
21. K. GOSNER, *Z. phys. Chem.* (NF), **36**, 392 (1963).
22. K. GOSNER, *Z. phys. Chem.* (NF), **42**, 374 (1964).
23. K. GOSNER, U. FREYER and F. MANSFELD, *Z. phys. Chem.* (NF), **42**, 378 (1964).
24. T. HAGYARD and K. M. CHAPMAN, *J. electrochem. Soc.* **113**, 961 (1967).
25. T. HAGYARD and W. B. EARL, *J. electrochem. Soc.* **114**, 694 (1967).
26. T. HAGYARD and M. J. PRIOR, *Trans. Faraday Soc.* **57**, 2295 (1961).
27. T. HAGYARD and J. P. WILLIAMS, *Trans. Faraday Soc.* **57**, 2288 (1961).
28. E. KUNZE and K. SCHWABE, *Corros. Sci.* **4**, 109 (1964).
29. R. A. MACHEVSKAJA and A. V. TURKOVSKAJA, *Khimicheskoe i neftjanoe mashinostroenie* (USSR), No. 4, **32** (1965).
30. R. A. MACHEVSKAJA and A. V. TURKOVSKAJA, *Zhurnal Prikladnoi Khim.* (USSR), **38**, 335 (1965).
31. C. I. NONINSKI, R. G. RAICHEV and Z. L. GEORGIEV, *Khimia i industria* (Bulgaria), **45**, 220 (1973).
32. C. I. NONINSKI, R. G. RAICHEV and Z. L. GEORGIEV, *Khimia i industria* (Bulgaria), **45**, 311 (1973).
33. C. I. NONINSKI, R. G. RAICHEV and Z. L. GEORGIEV, *Khimia i industria* (Bulgaria), **45**, 407 (1973).
34. C. I. NONINSKI and V. C. NONINSKI, *8th International Congress on Metallic Corrosion* v. 2, p. 1251. Mainz, FRG (1981).
35. C. I. NONINSKI and V. C. NONINSKI, *Mashinostroene* (Bulgaria), No. 7, 316 (1982).
36. R. C. NEWMAN and G. T. BURSTEIN, *Corros. Sci.* **21**, 119 (1981).
37. F. OEHME and H. RHYN, *Mesures*, **34**, 81 (1969).
38. H. DIETZ and H. GOEHR, *Z. phys. Chem.* **223**, 113 (1963).
39. W. POPP, *Electrochim. Acta* **8**, 361 (1963).
40. M. PRAZAK, E. BERANEK and K. KARNIK, *J. Phys. Chem.* **214**, 299 (1962).
41. G. RADLEIN, *Z. Elektrochem.* **61**, 727 (1957).
42. K. SCHWABE, *Electrochim. Acta* **3**, 186 (1960).
43. K. SCHWABE, *Z. phys. Chem.* **214**, 343 (1960).

44. K. SCHWABE, and G. DIETZ *Z. Electrochem.* **62**, 751 (1958).
45. K. SCHWABE, *Werkstoffe Corros.* **1**, 70 (1964).
46. N. D. TOMASHOV, G. P CHERNOVA, R. M. AL'TOVSKII and G. K. BLINCHEVSKII, *Zavod. Lab.* (USSR), **24**, 299 (1958).
47. N. D. TOMASHOV, N. M. STRUKOV and L. P. VERSHININA, *Electrokhimia.* (USSR), **5**, 26 (1969).
48. N. D. TOMASHOV and L. P. VERSHININA, *Electrochim. Acta* **15**, 501 (1970).
49. N. D. TOMASHOV and L. P. VERSHININA, *Novie Metodi Issledovanija Korozii Metalov*, p. 64. Nauka, Acad. Nauk SSSR Moscow, USSR (1973).
50. R. C. NEWMAN, *Corrosion Chemistry Within Pits, Crevices and Cracks* (ed. A. Turnbull). HMSO, London (1987).
51. C. I. NONINSKI, I. P. IVANOV and M. VASSILEVA-DIMOVA, *J. electrochem. Soc.* **130**, 1836 (1983).
52. V. C. NONINSKI, Dissertation, Higher Inst. Chem. Tech. Sofia (1983).

J. Electroanal. Chem., 267 (1989) 287–290
Elsevier Sequoia S.A., Lausanne – Printed in The Netherlands

Short communication

Underpotential anodic dissolution of noble metals during the continuous mechanical renewal of their surface

V.C. Noninski

Laboratory for Electrochemistry of Renewed Electrode–Solution Interfaces (LEPGER), P.O. Box 9, Sofia 1504 (Bulgaria)

(Received 16 March 1989)

INTRODUCTION

During the anodic polarisation of Pt it is possible for anodic dissolution to take place [1–12]. Furthermore, it has been established by us [13] that, during the continuous mechanical renewal (CMR) of the anode surface, the noble metals (Pt, Rh, Au) and their alloys are dissolved anodically at rates commensurate with the rates of the anodic dissolution of the base metals whose surface is not renewed. Potential regions exist, however, where because of thermodynamic reasons, electrochemical dissolution of non-renewed Pt is impossible. During studies of the anodic evolution of oxygen during the CMR of Pt anodes it has been established [14] that at potentials lower than that at which it is thermodynamically possible for electrochemical dissolution of platinum to take place, significant anodic currents are observed. Some preliminary experiments have shown that besides the passing of a capacitance current, in this case anodic dissolution of the noble metal takes place [15]. The aim of the present communication is to present some experimental evidence for such dissolution.

EXPERIMENTAL

The experiments were carried out using the self-cleaning rotating electrode (SRE) [16]. The cone-shaped working surface of this electrode is presented against four sharp edges of a device called a sharpener, made of baked corundum. When the electrode is rotated, its conical surface is continuously renewed mechanically by these edges. The pressure of the electrode surface against the sharpener's edges can be controlled during the experiment through a scale connected to a spring or by using heavy washers of known weight. The extent of renewal is controlled by the rate of rotation of the SRE. During the renewal the surface of the electrode is practically unscreened. When the electrode is not rotated, the conical surface works

0022-0728/89/$03.50

as a common conical stationary electrode. The experiments were carried out mainly with a spectrally pure platinum (Johnson Matthey) electrode. The experimental setup was similar to that described in ref. 14, the anode compartment being isolated from the cathode one by a salt bridge to prevent the Pt ions eventually appearing from passing into the cathode compartment and being reduced there. The sulphuric acid solutions in the anodic compartment of the cell before and after the polarisation of the anode were studied by spectroscopy for the presence of Pt ions by the method of Piercy and Ryan [17,18] with a Perkin-Elmer 137 spectrophotometer. As a reagent, *p*-dimethylaminobenzylidenerhodanine (DMABR) with phenylmethyl-*p*-hexadecylammonium chloride (CETYL) added, was used. Firstly, an absorbance vs. Pt^{2+} concentration standard line was constructed by analysing a series of solutions of known Pt^{2+} concentration prepared according to refs. 17 and 18.

RESULTS AND DISCUSSION

There are different methods for determining the amount of platinum in solutions. In the present case, however, in the solution there will be Pt in the atomic state due to the mechanical scraping and eventually Pt in the ionic state due to anodic dissolution. Therefore, in order to prove anodic dissolution it is necessary to determine only the amount of Pt ions in the solution, while leaving the scraped Pt, also present in the solution, undetermined.

A reliable method for the above aim is spectroscopy in the visible region. The experiments began by applying the procedures outlined in refs. 17 and 18 to a blank H_2SO_4 probe. This probe did not show any coloration, which is a guarantee that no Pt ions exist in the solution. This initial H_2SO_4 was transferred to the cell, the electrode rotated and a potential applied. We carried out experiments at two potentials, 0.78 and 0.80 V (SHE) (at pH = 0), in the "immune" region in the Pourbaix diagram of Pt [19]. At certain moments, samples of the solution were taken and studied for the presence of Pt^{2+} according to the procedure described in refs. 17 and 18. The samples showed a pink to red coloration depending on the time of polarisation. The solutions studied demonstrated the characteristic absorption spectrum of the Pt(II)–DMABR complex with a maximum at $\lambda = 520$ nm, corresponding to different absorbance values depending on the amount of Pt^{2+} complex. The coloration was distinct and its appearance could be attributed solely to the existence of Pt ions in the solution, any other reason being excluded. For instance, the particles scraped from the electrode cannot be a source of Pt^{2+} since they are not under the applied anodic potential and the Pourbaix diagram shows the impossibility of Pt dissolution in such a state. Experiments were also carried out in which the electrode was renewed for hours in the solution without potential application. In these experiments no Pt ions were found in the solution.

In Fig. 1 the determined concentration of Pt^{2+} as a function of the time of polarisation of the CMR Pt anode is shown. Due to the mechanical wear of the sharpener's edges caused by the long duration of the experiment, the conditions of

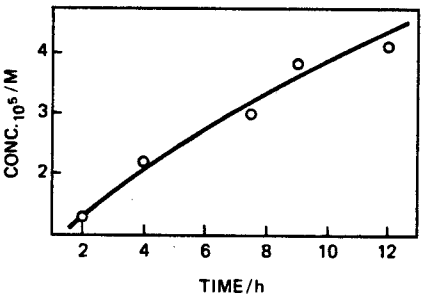

Fig. 1. Concentration of Pt^{2+} as a function of polarisation time in hours. Potential of the electrode 0.78 V vs. SHE.

renewal change, which is one of the reasons for the non-linearity of the dependence in Fig. 1.

Our experiments show [13] that the anodic current increases up to a certain limit with increasing pressure of the electrode surface against the sharpener's edges, after which there is no pressure effect on the current. The effect of the rotation speed on the observed anode current [13] is similar: with an increase of the electrode rotation rate the current increases until a certain limiting value is reached which remains constant when the rotation speed is increased further. In the present investigations the pressure of the sharpener's edges was maintained at 0.8–0.9 N cm^{-1} of edge length and was kept constant during the whole course of the experiment, while the electrode rotation speed was 1000 rpm; these values of pressure and rotation speed were chosen so as to correspond to the ones used during the experiments in ref. 14. These values were chosen because the sole aim of the present investigations was to help us understand the character of the current observed in ref. 14 at low anode potentials which fall into the so-called "immune" region of Pt. As said before, it was suggested that the above currents are due also to anodic dissolution of Pt during the CMR, although the potentials at which these currents are observed fall in a region where non-renewed Pt cannot be dissolved. To clarify the above point, which is of principal importance, it was enough just to register, with sufficient reliability (which the method of Piercy and Ryan [17,18] ensures), the appearance of Pt ions at some potentials in that region, leaving for the future detailed investigations of the phenomenon — e.g. the potential dependence of the amount of Pt ions and of the current efficiency, the temperature dependence, etc. It will be necessary to carry out such further investigations because the present findings raise many further questions — for instance, what the reasons are for the observed low current efficiency of about 10%. For now, however, even the mere coloration of the solution obtained as described above allows us to draw the important conclusion with a large degree of certainty that anodic dissolution of Pt during CMR of its surface can really take place in the "immune" potential region.

The above observations can be explained in the following way. Pourbaix diagrams are constructed on the basis of data for equilibrium states of the noble metal

(non-renewed) and in its equilibrium state Pt is thermodynamically stable. It cannot be dissolved spontaneously because its thermodynamic potential is lower than the thermodynamic potential of its ions.

In the present experiments the state of the Pt (the initial state of the system for the process of dissolution) is the one which we create and maintain artificially through CMR of the oxide layer (or the layer of adsorbed oxygen). This stationary state of Pt partially or entirely cleaned from its oxide (oxygen) is irreversible and the fact that, from this state, Pt passes spontaneously into its reversible state, in which it is covered with an oxide layer, shows that through the CMR we obtained Pt of a higher thermodynamic potential (Gibbs energy) than in its reversible state. Should the potential of the cleaned Pt become higher than the thermodynamic potential of Pt ions, the spontaneous anodic dissolution of Pt becomes possible.

REFERENCES

1 Margulis, Wied. Ann., 65 (1898) 629.
2 J. Tafel and B. Emmert, Z. Phys. Chem., 52 (1905) 349.
3 S. Gilman, Electrochim. Acta, 9 (1964) 1025.
4 A.N. Chemodanov, Ya.M. Kolotyrkin, M.A. Dembrovskii and T.V. Kudryavina, Dokl. Akad. Nauk SSSR, 171 (1966) 1384.
5 P. Malachesky, R. Jasinski and B. Burrows, J. Electrochem. Soc., 114 (1967) 1104.
6 E.I. Kruscheva, M.P. Tarasevich, N.A. Shumilova and N.I. Urisson, Zashch. Met., 15 (1979) 560.
7 D.C. Johnson, D.T. Napp and S. Bruckenstein, Electrochim. Acta, 15 (1970) 1493.
8 D.A.J. Rand and R. Woods, J. Electroanal. Chem., 35 (1972) 209.
9 Yu.M. Mironov, A.N. Chemodanov, Ya.M. Kolotyrkin, G.S. Raskin, N.S. Gorbacheva and N.A. Lyubimova, Zashch. Met., 12 (1976) 532.
10 S.Ya. Vasina, O.A. Petrii and V.A. Safonov, Elektrokhimiya, 17 (1981) 270.
11 G.M. Tagirov, I.I. Ashteulova, A.N. Chemodanov and Ya.M. Kolotyrkin, Elektrokhimiya, 17 (1981) 1103.
12 L.P. Vishnyakova, Yu.L. Golin, N.M. Danchenko, Yu.S. Usmanova and O.V. Chumakovskii, Elektrokhimiya, 14 (1978) 582.
13 V.C. Noninski, Dissertation HCIT (Sofia), 1982.
14 C.I. Noninski and V.C. Noninski, J. Electroanal. Chem., 131 (1982) 355.
15 C.I. Noninski and V.C. Noninski, 32nd ISE meeting, Dubrovnik, Yugoslavia, 1981, Ext. Abstr., Vol. 1, p. 181.
16 C.I. Noninski, Khim. Ind. (Sofia), 37 (1966) 442.
17 F. Piercy and D. Ryan, Can. J. Chem., 41 (1963) 667.
18 P. Mosheva and R. Borissova, C. R. Acad. Bulg. Sci., 35 (1982) 1085.
19 M. Pourbaix, Atlas d'Equilibres Electrochimiques, Paris, 279–383.

Hydrogen evolution on freshly generated chromium electrode surfaces

V. C. NONINSKI

The effect of continuous mechanical renewal (CMR) of a chromium electrode surface on the rate of hydrogen evolution has been investigated. The increase in steady state hydrogen evolution rate at a given potential due to CMR was found not to persist after CMR had ceased.

Manuscript received 11 April 1989; in final form 18 September 1990. *The author is in the Laboratory for Electrochemistry of Renewed Electrode–Solution Interfaces (LEPGER), PO Box 9, Sofia 1504, Bulgaria.*

INTRODUCTION

The fact that a decrease in hydrogen evolution overpotential (increase of hydrogen evolution rate) occurs during continuous mechanical renewal (CMR) of the surfaces of metals with low hydrogen evolution overpotentials has been established by Tomashov *et al.*[1-3] For metals with high hydrogen overpotentials, a decrease in this overpotential (increase in the reaction rate) and in the activation energy for hydrogen evolution during CMR occurs, as has been established by C. I. Noninski and co-workers.[4-6]

A study with the aim of determining whether the increase in hydrogen evolution rate brought about by CMR of the entire electrode surface (at a given cathodic potential) persists after renewal has been stopped is reported in the present paper. This phenomenon has been investigated[7,8] by scratching a small portion of a chromium electrode to generate fresh metal discontinuously at the surface. Large increases in hydrogen evolution rate were observed on chromium at low electrode potentials in aqueous solutions when the metal surface was freshly regenerated. This reaction was observed to continue at a rapid rate long (even indefinitely) after the fresh metal surface had been created, provided the potential remained low, an effect attributed to the formation, following scratching, of an oxide film differing in properties from the original.[7,8] Further, a decay in the cathodic current occurred, which was explained on the basis of partial reformation of an oxide film and growth of hydrogen bubbles hindering mass transfer to the scratched surface.

EXPERIMENTAL METHOD

The fresh metal surface was created by a selfcleaning rotating electrode (SRE), described in detail elsewhere.[6,9,10] Renewal of the electrode (99·9%Cr, surface area ~5 mm^2) occurs when the cone shaped working electrode, which is pressed on the four sharp edges of the sharpener (made of baked corundum), is rotated at 50 Hz. The special construction of the sharpener makes it possible to renew the entire surface of the SRE continuously at a controlled rate with practically no screening effect. Thus, a SRE allows steady state processes occurring on a continuously generated fresh metal surface to be compared with those on a non-renewed surface, i.e. when the cone surface is not being rotated. The reproducibility of results obtained during CMR is very high[11-13] – much higher than in its absence – and depends strongly on the preparation of the SRE. Because of the extended periods involved in the present experiments, it was not possible to use one electrode throughout and although the results for a given electrode are highly reproducible, the data obtained with different electrodes under the same conditions will differ slightly due to intrinsic differences. However, these variations are not significant in the context of the present investigation.

The experiments were carried out in a standard three compartment glass cell similar to that described previously.[10] Water traps, with which both the cell and the SRE were fitted, made it possible to isolate the working compartment from the atmosphere. A saturated calomel electrode was used as the reference electrode with a Luggin capillary situated <1 mm from the electrode surface, thus making any Ohmic correction of the potential virtually unnecessary. The counter electrode consisted of a platinum gauze and the anode and cathode compartments were separated by a porous membrane. The solution was saturated with argon (99·995% pure) throughout the experiment and the temperature of the cell was maintained constant at 293 ± 1 K. The working electrolyte was analytical grade 1M KOH prepared with doubly distilled water. Polarisation was controlled with a potentiostat–galvanostat Radelkis OH–405 (Hungary) and the transients recorded on an x–y recorder 620.02 (GDR).

Transients consisting of three main regions – before, during, and after CMR – were generated while a cathodic potential was applied to the electrode. However, there is a further factor that should also be considered. The electrodes were exposed to the atmosphere, usually overnight, before use, during which time oxide layer(s) were formed on the surface. While the use of a SRE makes it possible to remove this oxide from the electrode surface, so allowing measurements to be made on a virtually oxide free surface, it should be noted that several hundred rotations of the electrode are required to achieve this condition. It was therefore possible to obtain two types of transient:

(i) from electrodes having surface oxide layers, i.e. after exposure to air overnight
(ii) from electrodes that had been mechanically cleaned (while immersed in the test solution) to remove oxide layers immediately before applying the potential and commencing measurement.

RESULTS AND DISCUSSION

The transient from an experiment of type (i) is presented in Fig. 1*a*; the applied potential was −1·300 V(NHE). It can be seen that in the first few tens of seconds after application of the potential a characteristic minimum is observed in the current–time transient, after which the current increases gradually until reaching state A. Mechanical removal of the electrode surface was commenced 1060 s after application of the potential, whereupon the current increased suddenly to a maximum, then began gradually to decrease. After about a further 880 s CMR was ceased, producing a sudden drop in the current followed by a period of slower decrease. About 980 s after ceasing CMR state B was established. The reaction rate in state B is lower than that in state A.

It might appear that this result answers the question raised initially. However, it was found that if the chro-

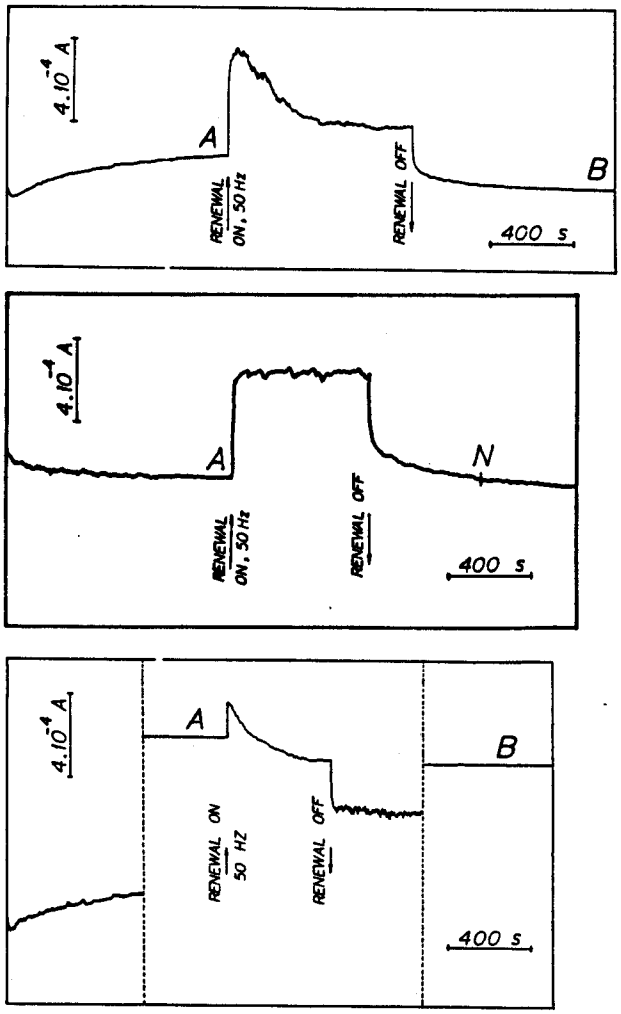

a electrode kept overnight in air at ambient temperature: *b* different electrode from *a* with surface mechanically renewed immediately before start of measurement; *c* same electrode as in *b* after exposure overnight in air at ambient temperature: broken lines indicate 20 h break in recording

1 *Cathodic current transients recorded during hydrogen evolution on chromium selfcleaning rotating electrode held at −1·300 V(NHE) in 1M KOH solution: start of curve represents application of potential; ↑ marks start and ↓ cessation of continuous mechanical surface renewal*

mium electrode surface was renewed just before starting type (ii) experiments, effects contrary to those shown in Fig. 1*a* could be observed (Fig. 1*b*). In this test the chromium surface was renewed in the solution for several minutes, after which CMR was stopped and the curve shown in Fig. 1*b* recorded. At least two types of phenomena relevant to the aims of the present study can be seen, at different stages on the curve. The current in state A of Fig. 1*b* (corresponding to state A in Fig. 1*a*) is lower than that at point N (after stopping CMR, but still maintaining the applied potential). Here, and especially in the region before N where the currents are markedly different, it would be reasonable to conclude, similarly to Burstein *et al.*[8] and C. I. Noninski,[9] that the effect of CMR *is* preserved after the process ceases.

However, at point N in Fig. 1*b* (530 s after ceasing CMR), the current is equal to that in state A. Thus, if currents are compared after point N, i.e. more than 530 s from ceasing CMR, the conclusion will be the same as that drawn from Fig. 1*a*: namely, that the effect of renewal is *not* preserved after the process is stopped.

The main reason for this apparent ambiguity lies in the fact that comparison is in some cases being made between non-steady state currents. Such non-steady state comparisons appear to have been applied by Burstein *et al.*[7,8] The transients presented in Fig. 1 of both these papers were recorded for the relatively short time of ~6 s (in Fig. 2 of Ref. 7 this period is 7 s) after cessation of scratching. In Fig. 1 of Ref. 8 a steady state regime appears to have been established several seconds after scratching is stopped, although it is relevant to note that this figure has an enlarged abscissa scale which could affect this judgement. The lowest rate of change on this figure appears to be of the order of 1 mA h^{-1}, which can reasonably be represented as a measureable value that is not indicative of steady state conditions. Thus, the claims of Burstein *et al.*[8] discussed above could be regarded as precipitate.

In an attempt to resolve the apparent ambiguity, experiments were carried out for periods sufficient to ensure that current would remain unchanged for several hours (within the limits of accuracy of the measuring system). In the present case steady state conditions were considered to have been achieved when the rate of change became <0·01 mA h^{-1}.

In Fig. 1*c* cathodic current is shown as a function of time in a type (i) experiment. It can be seen that the curve has a characteristic initial form, which, in the course of time, tends toward higher current values. This tendency was persistent and it was only after ~2 h that the rate of increase became <0·01 mA h^{-1} (A in Fig. 1*c*). After establishing a steady state current, CMR was carried out for several minutes, sufficient for the entire cathodic surface to have been renewed. This resulted (Fig. 1*c*) in a rapid increase in current to a maximum, after which a decrease to a steady state value was observed. The current recorded in Fig. 1*c* just before CMR was ceased had remained constant over a period of many hours (this is not shown in the figure for clarity) at a level that was lower than the steady state current obtained in the absence of CMR. After ceasing renewal, the current rapidly decreased to a level significantly lower than the steady state value in the absence of renewal. (Although it would appear from Fig. 1*c* that the current has reached a steady state value several minutes after stopping CMR, this value is in fact reached only after ~20 h – state B.)

It can be seen from Fig. 1*c* that the current in state B (the steady state reached after stopping CMR, but maintaining the applied potential) is lower than that in state A (steady state before CMR). This is observed not only at −1·300 V(NHE), but also at other potentials within the Tafel region when the initial condition of the chromium electrode is similar and is a difference arrived at as a result of comparing steady state currents, unlike in Fig. 1*a* and *b* where comparison of non-steady state conditions is being made. The steady state current density recorded on the filmed surface is an order of magnitude greater than that given in Ref. 8 for unscratched chromium, whereas the steady state current densities for both filmed and unfilmed chromium surfaces in Fig. 1*c* are of the same order of magnitude as the steady state scratch current density given in Ref. 8.

The increase in current during cathode polarisation of non-renewed chromium can be attributed to an increase in activity due to the decrease in thickness of the surface oxide film brought about by cathodic reduction of the latter. Differences in the processing history of the chromium electrodes (not controlled here or in Refs. 7 and 8) can lead to electrodes used in different experiments having dissimilar initial oxide thicknesses, which will affect the time necessary to achieve steady state conditions. Nevertheless, the qualitative conclusions drawn from the separate experiments should still be valid.

During CMR of the electrode surface it is probable that not only the rate of hydrogen evolution but also that of refilming is increased. Because of CMR, refilming is not

rapid enough and hydrogen evolution takes place on an activated surface. The form of the curve recorded during CMR reflects the fact that the surface state of the electrode is changed to a greater extent during CMR than is that of a non-renewed electrode because of increased catalytic activity of the electrode surface towards water molecules. It should be noted also that steady state conditions are reached several orders of magnitude faster during CMR of the electrode surface.

In considering these results it should be emphasised that several hundred rotations of the electrode are necessary for the renewal of the entire surface. This would explain the observed difference in the initial form of curves obtained during CMR for the same electrode (Fig. 1*b* and *c*), although the steady state currents during CMR practically coincide. As discussed above, the value of the steady state current is determined by competition between the processes of activation and refilming. The initial form of the curves during CMR in Fig. 1*b* and *c*, however, is determined by the processing history of the electrode. In Fig. 1*b* the CMR necessary to renew the entire surface has been applied before commencing measurement (type (ii) experiment) and no stable oxide layer has been able to form in the initial period when potential is applied without CMR. Therefore, on commencing CMR a steady state is reached rapidly – the current has a practically constant value from the very beginning of renewal.

Similarly, in the case shown in Fig. 1*c* the electrode surface was cathodically reduced for ~20 h and has reached a steady state in the absence of CMR. When CMR is applied the competing processes already mentioned eventually produce a steady state current practically coinciding, as expected, with that during CMR in Fig. 1*b*, but lower than that for the prior oxide covered chromium.

After CMR is stopped, refilming continues unopposed, as a result of which the rate of hydrogen evolution is decreased.

CONCLUSIONS

The effect of continuous mechanical renewal of the entire surfaces of chromium electrodes held at −1·300 V(NHE) in 1M KOH solution was investigated. It has been established that the steady state evolution rate of hydrogen obtained under such conditions does not persist after renewal has been stopped, even when polarisation is maintained.

REFERENCES

1. N. D. TOMASHOV, N. M. STRUKOV, and L. P. VERSHININA: *Dokl. Akad. Nauk SSSR*, 1966, **171**, 1134.
2. N. D. TOMASHOV and L. P. VERSHININA: *Electrochim. Acta*, 1970, **15**, 501.
3. N. D. TOMASHOV, N. M. STRUKOV, and L. P. VERSHININA: *Elektrokhimia*, 1969, **5**, 26.
4. C. I. NONINSKI: *Khim. Ind.*, 1972, **44**, (3), 121.
5. C. I. NONINSKI and I. P. IVANOV: *Khim. Ind.*, 1975, **47**, (2), 70.
6. C. I. NONINSKI: *Bull. Soc. Chim.*, 1976, (9–10), 1283.
7. G. T. BURSTEIN and M. A. KEARNS: *J. Electrochem. Soc.*, 1984, **131**, 991.
8. G. T. BURSTEIN, M. A. KEARNS, and J. WOODWARD: *Nature*, 1983, **301**, 692.
9. C. I. NONINSKI: *Khim. Ind.*, 1966, **37**, 442.
10. C. I. NONINSKI and V. C. NONINSKI: *J. Electroanal. Chem.*, 1982, **131**, 355.
11. V. C. NONINSKI and E. B. SOBOWALE: *Sci. Pharm.*, 1986, **54**, 105.
12. V. C. NONINSKI and E. B. SOBOWALE: *Coll. Czech. Chem. Commun.*, 1987, **52**, 66.
13. V. C. NONINSKI and E. B. SOBOWALE: *Farmacia*, 1987, **35**, 175.

EXCESS HEAT DURING THE ELECTROLYSIS OF A LIGHT WATER SOLUTION OF K_2CO_3 WITH A NICKEL CATHODE

COLD FUSION

TECHNICAL NOTE

KEYWORDS: *excess energy, electrolysis of H_2O, nickel cathode*

V. C. NONINSKI* *Laboratory for Electrochemistry of Renewed Electrode-Solution Interface (LEPGER), P.O. Box 9, Sofia 1504, Bulgaria*

Received July 5, 1991
Accepted for Publication August 19, 1991

Experimental results of differential heat loss calorimetry measurements during the electrolysis of light water solutions of K_2CO_3 and Na_2CO_3 with a nickel cathode are presented. A significant increase in temperature with every watt input, compared with the calibration experiment, is observed during the electrolysis of K_2CO_3. This effect is not observed when Na_2CO_3 is electrolyzed. No trivial explanation (in terms of chemical reactions, change in heat transfer properties, etc.) of this effect has been found so far. If the nontriviality of the observed overcoming of the energy breakeven barrier is further confirmed, this phenomenon may find application as an important new energy source.

INTRODUCTION

The studies in this paper follow the general lines of the work of Fleischmann and Pons,[1] although electrolysis of D_2O is usually considered when excess energy is claimed. Observation of excess energy production during the electrolysis of H_2O was first mentioned by Pons and later rejected.[1] Pons et al., however, explicitly state the possibility of obtaining excess energy during electrolysis of ordinary water (using nickel as a cathode, among other proposed metals) in Ref. 2. Unexplained excess heat in light water is also claimed in a paper by Bush et al.[3] Mills and Kneizys[4] claim to have obtained excess energy above the amount spent during the electrolysis of a K_2CO_3 ordinary water solution with a nickel cathode. The excess energy effect, according to these authors, is not observed when Na_2CO_3 is electrolyzed. Furthermore, unusual effects during the electrolysis of light water have also been reported by Matsumoto.[5]

This paper compares the heating coefficients for a nickel/platinum (Ni/Pt) circuit with those for a resistor heater in vacuum-jacketed dewar electrolytic cells containing K_2CO_3 or Na_2CO_3. Note that the excess energy effect from an electrochemical system containing K^+ (Li^+ is usually used in these studies) in D_2O is reported in Ref. 6.

*Visiting scholar at Franklin and Marshall College, Chemistry Department, Lancaster, Pennsylvania.

EXPERIMENTAL DETAILS

The experiments were carried out by observing and comparing the temperature difference, $\Delta T_1 = T_{electrolysis\ only} - T_{blank}$ and $\Delta T_2 = T_{resistor\ heating\ only} - T_{blank}$ referred to unit input power, between two identical 200-ml silver-coated vacuum-jacketed dewars. A calorimeter dewar having the same configuration and containing the same amount of electrolyte, same type of electrodes (nickel cathode and platinum anode), resistor heater, and thermistor (thermometer) and stirred at the same speed was used as a blank; neither electrolysis nor heating by the resistor was carried out in this dewar. Experiments were also carried out by using as a blank a dewar used in a previous experiment and vice versa. This exchange was done to ensure that the effect was not due to any difference in the thermal properties of the two specific dewars used. Each dewar had a 3-cm opening, and a 2-cm-thick tapered rubber stopper was placed 1 cm into the dewar. The experimental apparatus for the differential calorimetry used in these studies is shown in Fig. 1. Unlike the studies in Ref. 4, the resistor and the electrolytic circuit were not run simultaneously in this study; the effects of heating by the resistor and by the electrolysis circuit were studied in separate runs.

As is usual in electrochemistry, measures were taken to avoid impurities in the system, especially organic substances. While it is unclear at this point what the relationship is, if any, between the contamination effect on the hydrogen overpotential and that on the eventual excess heat, one should recall the known problems with the reproducibility of the hydrogen overpotential, which can be overcome only by ensuring the lowest possible level of impurities. Certain procedures should be applied to reproduce the excess heat effect. For instance, before starting the experiment, mechanically scour the platinum anode with steel wool, soak overnight in concentrated HNO_3, and then rinse with distilled water. Remove the nickel cathode from its container with rubber gloves, and cut and bend it in such a way such that no organic substances are transferred to the nickel surface. Preferably, dip the nickel cathode into the working solution under an electrolysis current, and avoid leaving the nickel cathode in the working solution in the absence of an electrolysis current. Clean the electrolysis dewar, and free it of organic contaminants.

After assembling the experimental setup, the nickel cathode was subjected to anodizing by a constant electrolysis current of 0.083 A for 1 h. Then, the direction of the electrolysis

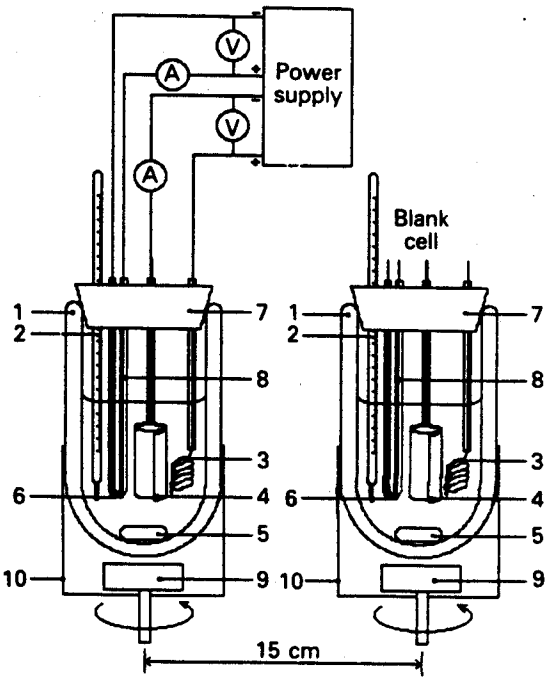

Fig. 1. Experimental setup: (1) vacuum-jacketed dewar, (2) thermometer, (3) platinum anode, (4) nickel cathode, (5) magnetic stirring bar, (6) resistor heater, (7) rubber stopper, (8) Teflon tubing, (9) magnetic stirrer, and (10) aluminum cylinder.

current was reversed (platinum anode and nickel cathode), and the electrolysis was carried out for 14 to 16 h.

The electrolysis heating power was calculated as $P_{el} = (E_{el} - 1.48)I_{el}$, where E_{el} is the applied electrolysis voltage, I_{el} is the electrolysis current (the term "electrolysis power" is used here for convenience, denoting only the power contributing to the joule heating effect during the electrolysis), and 1.48 V is the isoenthalpic voltage, which at the temperatures studied practically coincides with the thermoneutral voltage. The resistor heater power was calculated as $P_h = I_R E_R$, where I_R denotes the resistor current and E_R denotes the resistor voltage.

The cathode was a 7.5-cm-long × 4-cm-wide × 0.0125-cm-thick nickel foil (Aldrich 99.9+%) spiralled into a cylindrical form. The anode was a 0.1-cm-diam × 10-cm-long platinum wire (Johnson-Matthey). The spiral anode and the cylindrical cathode were parallel to each other. The leads were inserted into Teflon tubes to prevent any recombination of the evolving gases. The electrolyte solution in both dewars was 153 ml of 0.57 M K_2CO_3 or 0.57 M Na_2CO_3 in H_2O. The distilled water was from the common distiller of the Chemistry Department of Franklin and Marshall College. The power was delivered by a Zenith SP-2718 power supply (alternating current component <0.1%). The resistance heater was a 100-Ω, 1% precision, metal oxide resistor in a 2-mm-o.d. Teflon tube. The electrolyte solution in both dewars was stirred simultaneously (synchronized for the two dewars) by two identical spheroidal ellipse magnetic bars rotated by two magnetic stirrers at ~300 rpm. Electrolysis voltage and current were measured by two Keithley 169 multimeters, and the resistor voltage and current were measured by Extech 380198 and Micronta 22-185 A multimeters with 0.01-V and 0.001-A accuracy, respectively. The use of vacuum-jacketed dewars, rather than air-jacketed dewars or simple flasks, made the measurements more sensitive (higher heating coefficient). In a vacuum-jacketed dewar unit, input power leads to a greater steady-state temperature, thus enabling differences in steady-state temperatures (for the same configuration) to be more pronounced. The temperatures in this study were monitored continuously using the capability of the standard calorimeters (Parr P-318) to record the temperature continuously (with 0.01°C accuracy) on their strip-chart recorder (Fisher Recordall Series 5000).

RESULTS AND DISCUSSION

The results of the study are shown in Figs. 2 through 5. Figure 4 is based on the data presented in Figs. 2 and 3. Figure 2 shows the absolute change in the measured temperatures of the dewars at different conditions, while Fig. 3 shows the input powers in each case. It can be seen from Fig. 3 that while the input power with the resistors working was constant as expected, the input electrolysis power was not, and there is a time lag between the application of power and the temperature response. We compensated for this by selecting appropriate power values when calculating the heating coefficients plotted in Fig. 4 (more precisely, the term "heating coefficient" refers only to the steady-state values of the quantities in Fig. 4; the last parts of the curves in Fig. 4 can be considered to represent steady state). The heating coefficients plotted in Fig. 4 were calculated using the average power plotted in Fig. 3. Note that other reasonable ways of referring the observed ΔT to the applied power are possible; however, even the most conservative approach gives the same qualitative effect as that seen in Fig. 4. Studies currently in progress, using a data acquisition system, show sustained steady-state production of excess heat for many days. Results from these studies are presented elsewhere.

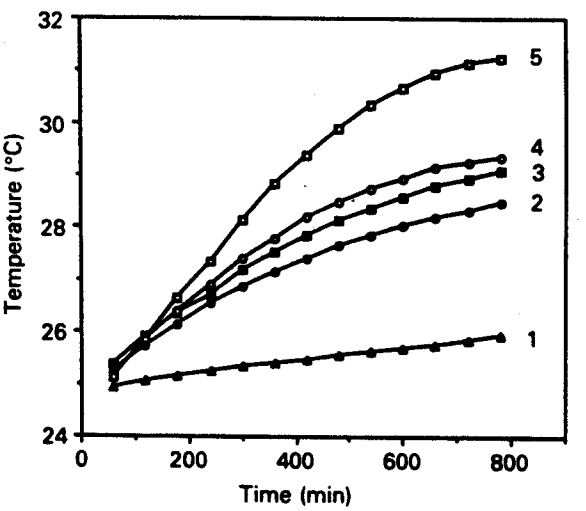

Fig. 2. Time history of temperatures: (1) blank cell (this curve is used as the blank for computing the heating coefficients of Fig. 4); (2) K_2CO_3 calibration cell (with only resistor heater working); (3) Na_2CO_3 calibration cell; (4) K_2CO_3 electrolysis cell (with only electrolysis working); and (5) Na_2CO_3 electrolysis cell.

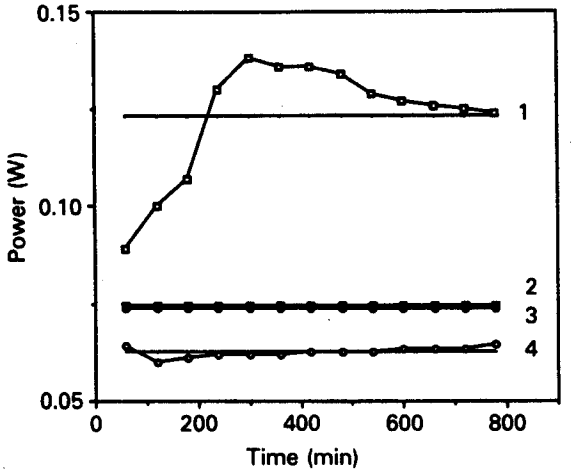

Fig. 3. Time history of the applied power: heating power with (1) electrolysis in the Na_2CO_3 cell, (2) the resistor in the Na_2CO_3 cell, (3) the resistor in the K_2CO_3 cell, and (4) electrolysis of the K_2CO_3 cell. The thermoneutral voltage is 1.48 V. For the calculations presented in this paper, mean values of the electrolysis powers in the Na_2CO_3 and K_2CO_3 cells are used, shown as solid lines in curves 1 and 4.

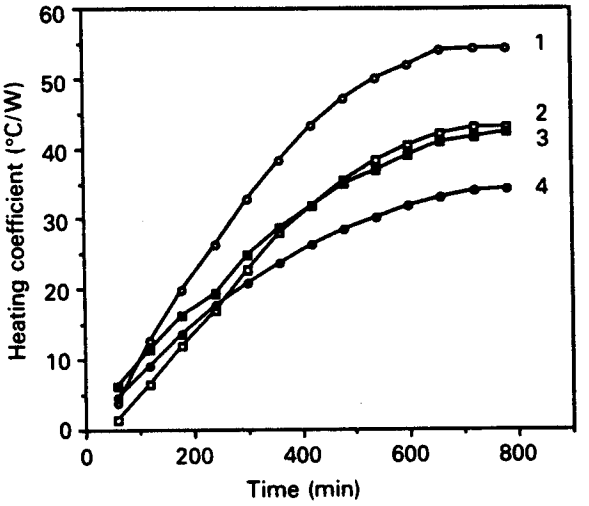

Fig. 4. Plot of the heating coefficients over time: (1) electrolysis at 0.083 A in K_2CO_3, (2) resistor working in Na_2CO_3, (3) electrolysis at 0.083 A in Na_2CO_3, and (4) resistor working in K_2CO_3.

The heating coefficient of the Na_2CO_3 cell is plotted in Fig. 4. The heating coefficient for the resistor heater only and that for the electrolysis circuit only are essentially identical. This is to be expected for a given dewar and a given electrolyte when steady state is reached: The ΔT corresponding to a unit heating power has a strictly defined value, determined by the properties of the materials through which heat is being lost. The properties of the cell are unaltered during operation. Specifically, the volume of electrolyte remains practically constant: ~0.2% of the solution volume is being electrolyzed during the 12-h operation of the Ni/Pt cell.

In contrast, the calorimeter containing K_2CO_3 showed very different behavior. The heating coefficient of the K_2CO_3 cell is plotted over time in Fig. 4. The heating coefficient-time curve of the working electrolysis cell is clearly above the curve of the dewar in which only a resistor is working. The value of the heating coefficient with the Ni/Pt circuit working is ~50°C/W, while the heating coefficient with only the resistor working is ~30°C/W. Therefore, the output power obtained through the Ni/Pt circuit is ~160% of the input power. The time-integrated power (i.e., energy) input into the system during the course of the experiment in Fig. 4 is ~4800 J compared with the output power of ~8000 J. Thus, Fig. 4 shows a significant difference in the thermal behavior of two identical systems that differ only in the positive ions of the salt.

A trivial explanation for this behavior of the K_2CO_3 cell is not straightforward. In fact, the electrolysis should be expected to lead to a decrease in the heating coefficients compared with those of the cells in which only the resistor is working ". . . consistent with additional heat losses caused by gas evolution . . . ,"[7] which is currently observed only in the Na_2CO_3 cell.

The erroneous attribution of the effect to temperature gradients was eliminated by testing for minute spatial variations of the temperature over time. Three thermistors were positioned ~2.5 cm apart at the bottom, middle, and upper part of the electrolyte. The results, shown in Fig. 5, clearly demonstrate that no difference is observed (within the limit of detection, 0.01°C).

Note that the electrolysis is always started with a newly manufactured cathode from the batch of 99.9%+ purity nickel. The use of new nickel excludes any possibility that the effect is due to the decomposition of species formed before the beginning of the electrolysis. The reaction of hydride formation is exothermic with a standard enthalpy of formation[8] of -8.79 ± 0.59 kJ·mol^{-1} H_2. However, if all of the hydrogen evolved during the run became hydride, an energy contribution would result that is more than one order of magnitude less than the excess heat that is observed according to Fig. 4. This can easily be calculated based on the amount of hydrogen evolved over ~12 to 14 h at a rate of 0.083 A. Although the overall amount of energy produced in the experiment is relatively low, it is clear that the observed effect is outside the error limit of the experiment, which is of the order of ±1°C/W, calculated from the accuracies of the measured parameters at the respective ranges.

It is not known what trivial chemical reaction might be triggered by the applied electrolysis that would be capable of producing the observed amount of excess heat. Some exotic farfetched possibilities for explaining the difference in electrochemical behavior between K_2CO_3 and Na_2CO_3 can be postulated. One such example is the formation of formic acid, e.g., by the reaction $HCO_3^- + 2H_2O \rightarrow HCOOH + 3OH^-$, or methane if $KHCO_3$ is present in the electrolyte. However, even if such possibilities are invoked, it should not be forgotten that energy is also being spent for these electrochemical reactions, which will again result in an isoenthalpic (or thermoneutral) voltage. In most cases, the value of this thermoneutral voltage may exceed 1.48 V, which will cause cooling rather than heating of the solution. This is indicative of even higher excess energy values. A reaction that readily comes to mind is oxygen reduction. It is well known, however, that nickel is a poor catalyst of oxygen reduction, and the current density of this reaction is negligibly small compared with the current density applied here (~1 mA/cm^2).

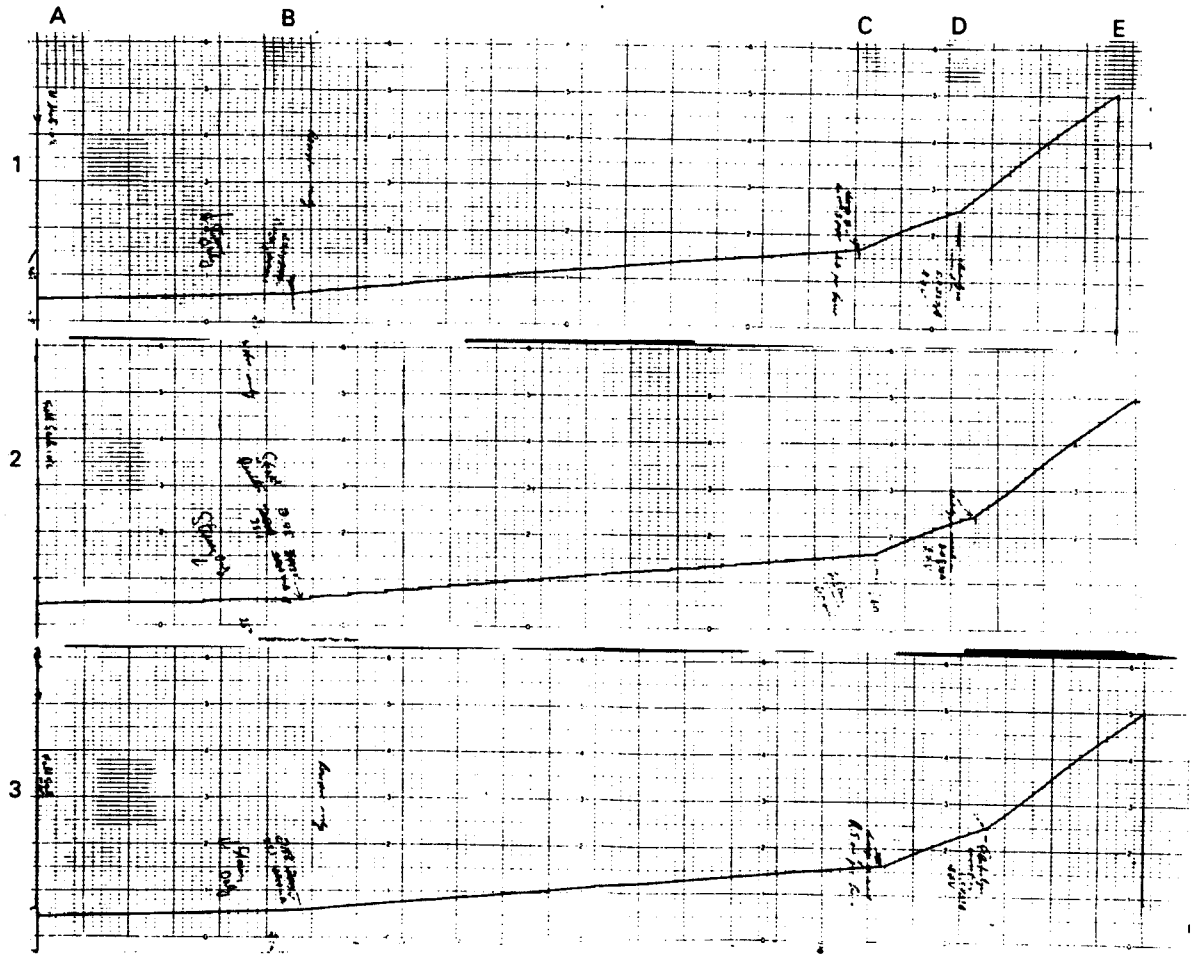

Fig. 5. Temperature changes at three points within the solution: (1) at the top, (2) in the middle, and (3) at the bottom. The setup used for this study is similar to that presented in Fig. 1, but in the working cell there are three thermistors instead of one. Section A-B: x axis scale = 30 division/h, y axis scale = 0.2°C/division, stirring only; section B-C: x axis scale = 30 division/h, y axis scale = 0.2°C/division, resistor only; section C-D: x axis scale = 5 division/h, y axis scale = 0.2°C/division, resistor only; and section D-E: x axis scale = 5 division/h, y axis scale = 0.2°C/division, electrolysis only.

These possibilities were rejected after study of the correspondence of the Faraday efficiency of the evolved H_2 and O_2 gases. This was done in a separate experiment by collecting the evolved gases and comparing the measured volume of the gases with the volume corresponding to the quantity of electricity that had passed through the cell over a given time. Note also that the absence of appreciable $H_2(D_2) + O_2$ recombination has been noted by a number of investigators, even in systems that contain metals (e.g., palladium) that are known to be good catalysts of that reaction (e.g., Refs. 9 through 14). Other preliminary studies (mass spectroscopy, pH measurements, titration) before and after the experiment showed no unexpected species or pH change. These studies should be continued further.

The problem of recombination is a crucial one in this study (note again that the excess heat here is calculated after subtracting 1.48 V), however, and it deserves special attention in any further experiments. On the other hand, as we have noted,[6] the problem of recombination (and the other connected calorimetric problems) preferably should not be solved by studying the effect in a closed cell with a recombiner. The recombiner adds new unknowns since the kinetics of the recombination of H_2 and O_2 to H_2O should be well understood through studies such as those in Ref. 15. On the other hand, since the claimed excess energy itself is a newly found, unstudied phenomenon, no additional conditions should be imposed because their eventual effect on the reproducibility of the excess energy is unknown. For instance, it is not clear whether the ability of the recombiner to recombine not only the H_2 and O_2 evolving through electrolysis but also all other quantities of H_2 and O_2 existing in the gas and the liquid phase, thus creating concentration gradients, will be a hindering factor for the appearance of excess energy.

An explanation for the increase in the heating coefficient for a Ni/Pt circuit might be that an additional source of energy of unknown nature is acting from within that adds to the energy input to the cell from without. If this nontrivial possibility is confirmed, this effect will be of great importance as an alternative energy source. Further calorimetric sophistication is necessary to further confirm the reality of the observed effect and to obtain a quantitative assessment of its magnitude. For instance, to avoid errors of a subjective nature, a data acquisition and processing system is necessary. The measurements should be carried out at constant input

power and for longer periods of time so that curves like curve 1 of Fig. 2 reach a clear and sustained steady state. Maintaining a constant ambient temperature is also a requirement in these studies. Such studies are now in progress. To fully avoid concerns connected with the peculiarities of heat transfer during bubble evolution, it is necessary, together with heat loss calorimetry measurements (including Seebeck), that this effect be observed in an adiabatic-type calorimeter (bomb calorimeter) similar to the one used in Ref. 6. Note, however, that despite the opinions of some researchers, if careful studies are carried out, calorimetric techniques are not only capable but are the only ones that can decisively prove (or disprove) the reality of the effect in question. There is also no reason to expect that time spans of tens of hours will be insufficient to definitely rule out (or conclusively confirm) a trivial explanation of the observed effect if the studies are conducted carefully. It seems, however, that the reality of the effect can qualitatively be established with the described procedure. It seems also that the reported effect is reproducible and can easily be demonstrated.

It is the author's understanding that speculations (invoking reactions of nuclear or any other origin) as to why overcoming the energy breakeven barrier might come about should be carried out only after firmly establishing the reality of the claimed effect through experiments. This circumstance is not new for science. One may recall the experimental findings of Davison and Germer, Einstein, Wien, Compton, and others, which were unexplainable at the level of knowledge at their time. These experimental findings virtually caused the birth of 20th century physics, especially quantum mechanics. Even one of the most recent scientific discoveries—high-temperature superconductivity—whose reality is undeniable, still remains unexplained, which does not make this experimentally found effect less important.

Since the problem of the reality (nontriviality) of the excess energy reported here is of primary concern, we leave open the questions for the theoretical explanation of the phenomenon.

CONCLUSIONS

The experimental results presented here show that there is more evidence than usually considered for the eventual production of excess energy during the electrolysis of water. Therefore, further efforts seem to be justified for verifying the claim of Fleischmann and Pons for overcoming the energy breakeven barrier through electrolysis.

Contrary to the opinion expressed in Refs. 16 and 17, it does not seem plausible that light water should be used as a "control" when excess energy is being sought during the electrolysis of heavy water.

ACKNOWLEDGMENTS

The author wishes to thank J. J. Farrell, Franklin and Marshall College, for his kind invitation to use his laboratory for these studies. Thanks are also due to James McBreen, Brookhaven National Laboratory; David Worledge, Electric Power Research Institute; and M. H. Miles, Naval Weapons Center, for useful discussions. The author would like to thank also W. R. Good for technical help.

The author also wishes to thank the two referees for their careful reading of the manuscript and for their useful remarks.

REFERENCES

1. M. FLEISCHMANN and S. PONS, "Electrochemically Induced Nuclear Fusion of Deuterium," *J. Electroanal. Chem.*, **262**, 301 (1989); see also Errata, *J. Electroanal. Chem.*, **263**, 187 (1989).

2. S. PONS, M. FLEISCHMANN, C. WALLING, and J. SIMONS, "Method and Apparatus for Power Generation," International Application Published Under Patent Cooperation Treaty (PCT/US90/01328; International Publication Number WO 90/10935) (Mar. 13, 1989).

3. B. F. BUSH, J. J. LAGOWSKI, M. H. MILES, and G. S. OSTROM, "Helium Peoduction During the Electrolysis of D_2O in Cold Fusion Experiments," *J. Electroanal. Chem.*, **304**, 271 (1991).

4. R. L. MILLS and S. P. KNEIZYS, "Excess Heat Production by the Electrolysis of an Aqueous Potassium Carbonate Electrolyte and the Implications for Cold Fusion," *Fusion Technol.*, **20**, 65 (1991).

5. T. MATSUMOTO, "Cold Fusion Observed with Ordinary Water," *Fusion Technol.*, **17**, 490 (1990).

6. V. C. NONINSKI and C. I. NONINSKI, "Determination of the Excess Energy Obtained During the Electrolysis of Heavy Water," *Fusion Technol.*, **19**, 364 (1991).

7. G. M. MISKELLY, M. J. HEBEN, A. KUMAR, R. M. PENNER, M. J. SAILOR, and N. S. LEWIS, "Analysis of the Published Calorimetric Evidence for Electrochemical Fusion of Deuterium in Palladium," *Science*, **246**, 793 (1989).

8. G. ALEFELD and J. VOLKL, Eds., *Hydrogen in Metals II*, p. 173, Springer-Verlag (1967).

9. V. J. CUNNANE, R. A. SCANNELL, and D. J. SCHIFFRIN, "$H_2 + O_2$ Recombination in Non-Isothermal, Non-Adiabatic Electrochemical Calorimetry of Water Electrolysis in an Undivided Cell," *J. Electroanal. Chem.*, **269**, 163 (1989).

10. R. C. KAINTHLA et al., "Sporadic Observation of the Fleischmann-Pons Heat Effect," *Electrochim. Acta*, **34**, 1315 (1989).

11. D. E. WILLIAMS et al., "Upper Bounds on 'Cold Fusion' in Electrolysis Cells," *Nature*, **342**, 375 (1989).

12. T. R. JOW, E. PLICHTA, C. WALKER, S. SLANE, and S. GILMAN, "Calorimetric Studies of Deutrated Pd Electrodes," *J. Electrochem. Soc.*, **137**, 2473 (1990).

13. D. ALBAGLI et al., "Measurement and Analysis of Neutron and Gamma-Ray Emission Rates, Other Fusion Products, and Power in Electrochemical Cells Having Pd Cathodes," *J. Fusion Energy*, **9**, 133 (1990).

14. J. DIVISEK, L. FURST, and J. BALEJ, "Energy Balance of D_2O Electrolysis with a Palladium Cathode. Part II. Experimental Results," *J. Electroanal. Chem.*, **278**, 99 (1990).

15. M. J. JONCICH and N. J. HACKERMAN, "The Reaction of Hydrogen and Oxygen on Submerged Platinum Electrode Catalysts. I. Effect of Stirring, Temperature and Electric Polarization," *J. Phys. Chem.*, **57**, 674 (1953).

16. H. FURST, cited after "Hopes for Nuclear Fusion Continue to Turn Cool," *Nature*, **338**, 691 (1989).

17. J. MADDOX, "What to Say About Cold Fusion," *Nature*, **338**, 701 (1989).

DETERMINATION OF THE EXCESS ENERGY OBTAINED DURING THE ELECTROLYSIS OF HEAVY WATER

COLD FUSION

TECHNICAL NOTE

KEYWORDS: *electrolysis of D_2O, isoperibolic calorimeter, excess energy*

V. C. NONINSKI and C. I. NONINSKI
Laboratory for Electrochemistry of Renewed Electrode-Solution Interface (LEPGER)
P.O. Box 9, Sofia 1504, Bulgaria

Received July 22, 1990
Accepted for Publication September 10, 1990

The total heat balance during the electrolysis of D_2O with a palladium cathode is determined by placing the entire hermetically sealed electrolysis system (the electrochemical cell connected with a vessel of varying volume) in an isoperibol calorimeter. Significant excess power density (excess specific rate of heating) is obtained even though a palladium cathode of thin wire (0.05-cm diam) is used, in which case a relatively low value of excess energy is expected. The method and arrangement applied remove the main causes of inaccuracies in determining the excess energy. Thus, the possibilities of using this energy seem to be greater than some researchers are inclined to consider.

INTRODUCTION

Some successful measurements of the excess energy obtained during the electrolysis of heavy water, claimed by Fleischmann and Pons,[1] are reported.

The exact determination of the quantity of heat released during the electrolysis of heavy water requires consideration of various possible causes of incorrect results, including the following:

1. Gases leaving the electrolytic cell or blown through it during electrolysis usually remove some heat through temperature increase and water evaporation. This heat may be comparable to or even greater than the excess energy, especially if the possibility of superheated gases and supersaturated D_2O vapors is considered.

2. Uncontrolled absorption and desorption of D_2 may occur.

3. Uncontrolled interaction between D_2 and O_2 may take place.

4. There may be direct heat transfer between the electrolytic cell, which is heated during the electrolysis, and the medium surrounding the calorimeter.

5. The calorimetric liquid may be improperly stirred, which enables heat to be removed from the calorimeter.

6. Inefficient stirring can cause unequal temperatures in the different regions of the calorimetric liquid.

7. A decrease or increase in the quantities of gases dissolved in the calorimetric liquid may have a measurable effect.

8. A change in the gas-phase pressure in the calorimeter may have a measurable influence on the result.

9. Processes other than those already mentioned may take place in the calorimeter, inside the electrolytic cell, or outside, together with the electrolysis of D_2O.

10. Energy expenditure or gain may be connected with changes in the palladium cathode (volume, cracking, oxidation, etc.).

Most of these possible causes of errors in the excess heat measurement seem to exist to a certain extent in the studies carried out so far. This paper presents a method to more accurately determine the excess energy and if possible to eliminate some of the possible explanations for the excess energy.

EXPERIMENTAL

In our study of the excess energy generated during electrolysis of heavy water, we used the calorimeter shown schematically in Fig. 1. It consists of an opaque dewar vessel (1) hermetically sealed with a stopper (2), in which a quantity of double-distilled water (3) is contained. The electrolytic cell (4) is entirely submerged in the distilled water. It consists of a test tube (5) hermetically sealed with a stopper (6) containing metal parts (7). The electrolytic cell is connected with a vessel (8) of a varying volume (a plastic bubble) through a spiral metal tube (9). Above and under the electrolytic cell, two copper-constantan thermocouples (10 and 11) are welded (the upper weld is used only for control). A magnetic stirrer (12) is located on the bottom of the dewar vessel. The leads (13 through 19) of the electrolytic cell, thermocouples, and the resistor (20) (for determination of heat capacity) pass through the stopper of the dewar vessel. All the wires (thermocouples, electrode, and resistor leads) situated in the dewar vessel are insulated.

The cathode is made of 0.05-cm-diam × 32-cm-long palladium wire (Koch-Light Laboratories, 99.99% pure) weighing 0.76 g, which is wrapped in a zigzag manner into an

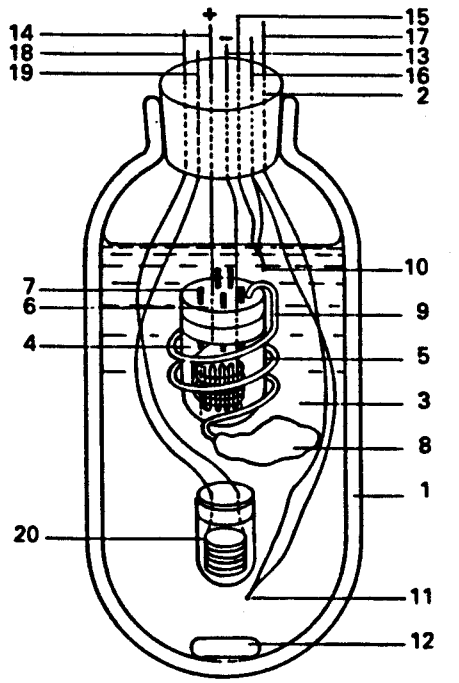

Fig. 1. Schematic of the calorimeter. See text for details.

~1.5-cm-long bundle of 21 wires. The anode is a platinum wire spirally wound around the cathode. The anode and the cathode are separated by a perforated Teflon tube.

The cathode is saturated with deuterium by a lengthy pre-electrolysis. During this time, the open cell is placed in a constant-temperature bath. The electrolytic cell contains 3 ml D_2O (Merck, 99.7% pure) plus ~0.01 M K_2SO_4. The D_2O is replenished regularly during the pre-electrolysis. The cell temperature is not measured during this time.

To begin the experiment, the pre-electrolysis current is stopped, the cell is removed from the constant-temperature bath, and it is assembled in the configuration shown in Fig. 1. The initial volume of the plastic bubble is measured in order to determine when the palladium cathode is saturated with deuterium. The cathode is ready (in the absence of electrolysis) for the experiment when the volume of $D_2 + O_2$ gas in the cell is constant with time: The deuterium is no longer being adsorbed nor desorbed by the cathode. The measurements begin when the temperatures of the cell and the calorimetric liquid are equal. Thus, we wait for >10 min after assembly of the apparatus.

We obtained the volume of the gases produced during the electrolysis by measuring the weight (volume) of water removed by the plastic bubble before and after the electrolysis. From this, we determined the character of the electrochemical reaction: possible absorption or desorption of D_2 by the palladium cathode, an interaction between D_2 and O_2, or other factors. (When the volume of the $D_2 + O_2$ did not correspond to the reaction of D_2O decomposition, the excess heat measurement was considered unsuccessful.)

A constant current I for the electrolysis of D_2O was ensured by a potentiostat-galvanostat PAR 273 serving as a galvanostat. The current was also controlled by a Hewlett-Packard 3465 B digital multimeter of $\pm 1 \times 10^{-4}$ A accuracy. The voltage was registered continuously by a Sony-Tektronix 336 digital storage oscilloscope; the accuracy of the voltage measurements below 10 V was ±0.08 V, while for measurements in tens of volts the accuracy is ±0.8 V. The time $\Delta\tau = \tau_2 - \tau_1$ of electrolysis measured by the oscilloscope was simultaneously measured by a Casio fx-7100 scientific calculator of ±0.01-s accuracy. After the completion of each experiment, the data from the oscilloscope's memory were dumped through a GPIB (IEEE 488) interface bus into the memory of an Apple IIe microcomputer, and the mean value $\bar{E}$ of the applied voltage E during the experiment was determined through numerical integration of the multiple voltage values acquired during the continuous monitoring of the voltage throughout the whole process.

The temperature of the calorimeter (thermoemf of the thermocouples) during the experiments was read at 30-s intervals using a Hewlett-Packard 3465 B digital multimeter of 1×10^{-6} V accuracy. The thermocouples were calibrated using a thermostat. It was determined that 39-μV thermoemf corresponds to 1°C.

RESULTS AND DISCUSSION

Results from the experiments are presented in Figs. 2, 3, and 4.

In Fig. 2, the temperature (thermoemf) as a function of time is shown before, during, and after passage of a 0.5990-A current through the resistor for 181.25 s at 9.76 V. From these data, the heat capacity of the calorimeter is determined to be $K = 841$ J·grad^{-1}.

In Fig. 3, the voltage-time curve $[E = E(\tau)]$ is taken before, during, and after passage of a 0.1280-A current through the electrolytic cell for an interval $\Delta\tau = \tau_2 - \tau_1 = 181.32$ s. The mean voltage obtained from Fig. 3 is $\bar{E} = 44.0$ V.

When using these data for I, $E = E(\tau)$, and $\Delta\tau = \tau_2 - \tau_1$, the energy spent for the electrolysis of D_2O is obtained from the Joule's law:

$$W = I\int_{\tau_1}^{\tau_2} E(\tau)\,d\tau = I\bar{E}\Delta\tau = 1020 \text{ J} .$$

In Fig. 4, the temperature as a function of time taken before, during, and after the electrolytic process is shown. The increase in the calorimeter temperature due to electrolysis is

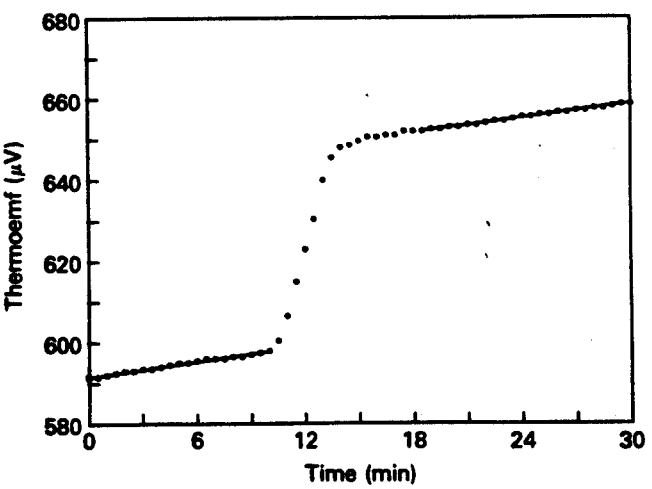

Fig. 2. Temperature (thermoemf) as a function of time for determination of heat capacity of the calorimeter.

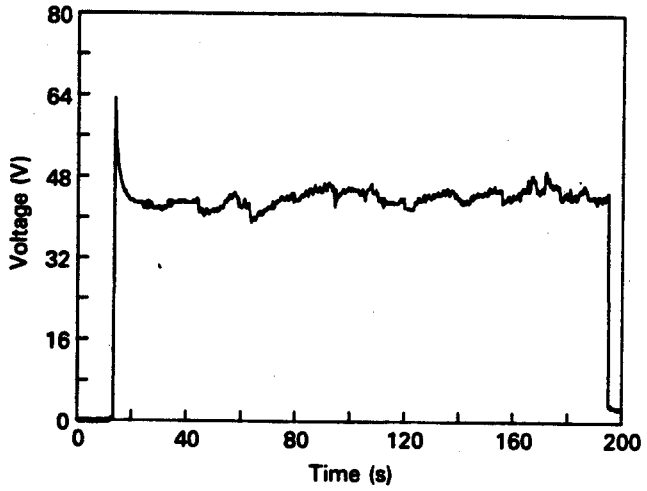

Fig. 3. Cell voltage as a function of time during electrolysis.

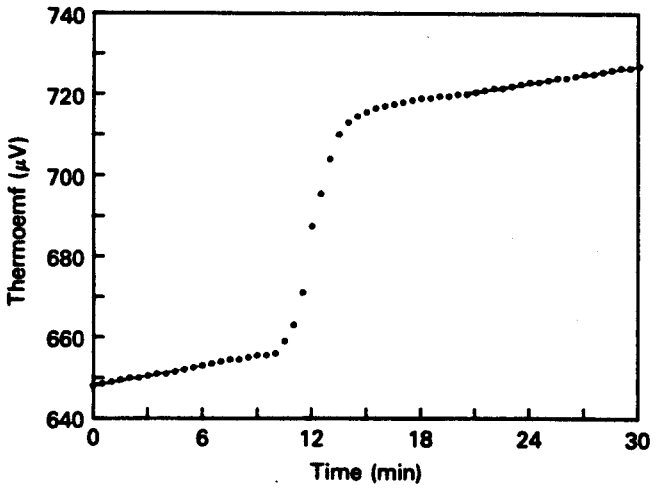

Fig. 4. Temperature (thermoemf) as a function of time during the experiment.

found to be $\Delta t = 1.44°C$. The temperature time dependence before and after electrolysis should coincide with the dependence taken when no current is passing through the system. This is the characteristic time dependence of the rate of heat dissipation from the given system toward the ambient under the given conditions. The quantity of heat Q obtained during electrolysis is

$$Q = K\Delta t = 1210 \text{ J} .$$

To compare the energy obtained with the energy spent, it is necessary to remember that the energy we obtain consists not only of the experimentally measured heat (1210 J) but also of the chemical energy that can be released if the D_2 and O_2 gases produced during the electrolysis of D_2O inversely interact (recombine) to form D_2O again. It can even be stated that this chemical energy is usually the only useful energy that results from the electrolysis of heavy water. The available data from the handbooks are generally used: This energy has been established[2] as $\Delta H = -70.4133$ Kcal/mol = -294.6 KJ/mol at 25°C. Nevertheless, this quantity should be measured directly.

The use of an internal recombiner, however, is not the most suitable for proving the existence of excess heat. An active recombiner shifts the stationary state at which the palladium cathode is saturated (possibly supersaturated) with deuterium toward another stationary state at which the palladium cathode is undersaturated with deuterium. This occurs because the active recombiner recombines virtually the entire available quantity of oxygen and deuterium, both the quantity being evolved and the quantity existing in the liquid and the vapor phases. Underpressure (slight vacuum) in the system indicates this additional recombination. Thus, the diffusion of the D_2 toward the recombiner competes with its diffusion toward the bulk of the cathode and makes saturation impossible. As has been pointed by a number of authors,[1] saturation (even supersaturation) of the cathode with deuterium is a necessary condition for the observation of excess energy. Thus, it can be concluded that whenever excess power is observed in a cell with a recombiner the effect will be only conservative. Failure to observe excess energy in recombination cells, on the other hand, cannot be considered convincing proof of the impossibility of the system's producing excess energy. Further experiments are necessary to overcome this disadvantage of the recombiner.

On the basis of the mentioned current and time values, it is determined that during the electrolysis 1.2×10^{-4} mol D_2O is decomposed. The D_2 and O_2 gases thus obtained can interact inversely (recombine) to release energy of $1.2 \times 10^{-4} \times 294\,600 \approx 35$ J. This energy should be added to the obtained heat. Note also that the quantity of gases measured using the vessel of varying volume (the plastic bubble) exactly corresponds to the expected volume calculated from Faraday's law. This observation invalidates the possible trivial explanation of the excess energy effect put forward in Refs. 3, 4, and 5. Thus, in our case the total energy obtained is 1210 + 35 = 1245 J, which exceeds by 225 J the amount of energy spent (1020 J).

When $H_2(D_2)$ is obtained electrochemically to be used as fuel, and when the question relates to the significance of hydrogen for energetics, only quantities such as the mentioned 35 J are taken into account. The energy losses due to overcoming the ohmic resistance of the solution, the leads, the electrodes, and the contacts are not considered because, in principle, these losses, which are significant in our case, are preventable to a great extent. The losses due to overcoming the D_2 and O_2 evolution overpotentials can also be disregarded because these overpotentials can be decreased,[6-8] even eliminated, as in the case of Ref. 9. The only energy expenditure that is inevitable and cannot be decreased is the quantity necessary for the electrolytic process itself [decomposition of $H_2O(D_2O)$]. In the ideal case, we reckon that the obtained chemical energy when using $H_2(D_2)$ as fuel is 100% versus the energy spent for the decomposition of $H_2O(D_2O)$. In the present case, the amount of energy that can be used (225 + 35 = 260 J) is more than seven times the usable energy expected from the electrolysis (35 J). This significant excess energy cannot be connected with the electrochemical process of decomposition of $H_2O(D_2O)$ or with any other electrochemical or chemical process.[1]

From the above data, it is seen that during the ~3-min electrolysis for the decomposition of 1.2×10^{-4} mol D_2O and for obtaining the respective quantities D_2 and O_2, 35-J energy is spent while the total available energy (excess enthalpy + enthalpy of the obtained D_2 and O_2) is 260 J. That

TABLE I

Momentary Values of Excess Enthalpy Obtained During the Electrolysis of D_2O

Experiment	Electric Energy Spent for the Electrolysis (J)	Total Energy Obtained (Heat + Enthalpy of Obtained D_2 and O_2) (J)	Excess Rate of Heating (Excess Power) (W)	Excess Specific Rate of Heating (Excess Specific Power) (W/cm^3)
1	921	1130	1.15	18.3
2	830	910	0.431	6.85
3	1090	1210	0.662	10.5
4	856	910	0.298	4.73
5	835	885	0.276	4.37
6	1440	1560	2.61	41.4
7	777	869	0.508	8.06
8	1115	1134	0.104	1.66
9	937	961	0.132	2.10
10	873	961	0.481	7.64

is, for the 181.32-s electrolysis, a mean power of 0.2 or 3.2 W/cm^3 Pd is spent for the decomposition of D_2O while the electrolytic cell has acted as an energy source (heat + chemical energy) of 1.43 W, which is 22.8 W/cm^3 Pd. If only the excess energy (225 J) is considered, 1.24 or 19.7 W/cm^3 excess power is available.

Table I presents data from some successful determinations of the excess heat obtained during the electrolysis of D_2O. Experiments 4, 5, and 6 were carried out on the same day at different times. The mean time interval between the experiments, except for experiments 4, 5, and 6 but including the intervals between them and the neighboring experiments, is ~110 h. The cathode current density for all the experiments except experiments 1 and 6 was 26 mA/cm^2. For experiment 1 the current density was 20 mA/cm^2, while for experiment 6, it was 80 mA/cm^2. In all cases except for experiment 6, the electrolysis lasted ~3 min; for experiment 6, it lasted 46.00 s.

Our method and experimental arrangement give a possibility of precise determinations of the excess heat obtained during the electrolysis of D_2O, thus ensuring a categorical answer to the important question of whether the Fleischmann and Pons effect[1] exists and, if it does exist, the exact value of the excess power during the electrolysis. However, it should be kept in mind that a comparatively short electrolysis process was carried out here after a continuous pre-electrolysis. Therefore, every excess enthalpy value obtained is valid only for a relatively short time interval—tens of seconds up to ~3 min, which we conditionally consider here as only a moment (a randomly chosen moment), compared to the tens and hundreds of hours duration of the other studies of the excess energy. As seen from Table I, the momentary values of the excess power and the excess power density (excess specific rate of heating[1]) obtained at different moments differ significantly from each other. While the result from experiment 6 is 2.61 W and 41.4 W/cm^3, experiment 8 gave values of 0.104 W and 1.66 W/cm^3, respectively, i.e., ~25 times lower values. Indeed, in experiment 6 three times greater current density was applied compared to experiment 8. In experiment 1, the current density was lower than in experiment 8; nevertheless, the values obtained for the excess power and excess power density in experiment 1 was 11 times greater than in experiment 8.

The data shown in Table I indicate that the momentary value of the excess power and excess power density do not depend on the current density. As is seen in the table, excess power density values of 1.66, 10.5, and 18.3 W/cm^3 are observed for the same current density value (26 mA/cm^2). In this experiment, the excess power density value is 19.7 W/cm^3. Evidently, the momentary values of the excess power and the excess power density are random. Therefore, one can conclude that the mean values of the excess power and the excess power density from all the experiments carried out at 26 mA/cm^2 are 0.459 W and 7.29 W/cm^3.

Since the errors from the measurements are sufficiently low and there are no significant heat losses, it cannot be accepted that the observed variation in the excess power density values is due to errors in the measurement. Therefore, it is likely that the phenomenon is of a sporadic nature. From our results, it can be concluded that the excess power and the excess power density values obtained over many hours by other authors are in fact the mean values of these quantities, which are the result of numerous differences in momentary values. Note that the moments for obtaining these values are chosen randomly.

The mean value of the excess power density obtained by us with a 0.05-cm palladium wire electrode at a current density of 26 mA/cm^2 is seven times greater than that[1] obtained after many hours with an electrode with a greater diameter (0.1 cm) and at a higher current density (64 mA/cm^2). The hermetical sealing of the calorimeter, the submersion of the entire electrolytic cell into the calorimetric liquid, keeping the obtained gases and vapors in a cell of varying volume, and the other measures taken by us seem to ensure much lower losses of the obtained excess enthalpy.

The results presented in this technical note indicate that the possibility of the practical use of the excess energy resulting during the electrolysis of D_2O are greater than is sometimes considered.

ACKNOWLEDGMENT

The authors wish to thank referee 2 for his careful reading of the paper and for the useful remarks in his report.

REFERENCES

1. M. FLEISCHMANN and S. PONS, "Electrochemically Induced Nuclear Fusion of Deuterium," *J. Electroanal. Chem.*, **261**, 301 (1989); and Erratum, *J. Electroanal. Chem.*, **263**, 187 (1989).

2. *Spravochnik Khimika, Gosudarstvennoe nauchno-tekhnicheskoe izdatel'stvo Khim. literaturi*, Leningrad, Moscow, Vol. 1, p. 792 (1963) (in Russian).

3. G. KREYSA, G. MARX, and W. PLIETH, "A Critical Analysis of Electrochemical Nuclear Fusion Experiments," *J. Electroanal. Chem.*, **266**, 437 (1989).

4. M. KEDDAM, "Some Comments on the Calorimetric Aspects of the Electrochemical 'Cold Fusion' by M. Fleischmann and S. Pons," *Electrochim. Acta*, **34**, 995 (1989).

5. N. LEWIS et al., "Searches for Low-Temperature Nuclear Fusion of Deuterium in Palladium," *Nature*, **340**, 525 (1989).

6. C. I. NONINSKI, "Theoretical and Practical Applications of a Rotating Electrode with Continuously Renewed Surface," *Bull. Soc. Chim. France*, **9–10**, 1283 (1976) (in French).

7. C. I. NONINSKI and V. C. NONINSKI, "Electrochemical Evolution of Oxygen on the Continuously Mechanically Renewed Surface of a Platinum Anode in H_2SO_4," *J. Electroanal. Chem.*, **131**, 355 (1982).

8. C. I. NONINSKI, I. P. IVANOV, and M. VASSILEVA-DIMOVA, "Hydrogen Overvoltage on Tin Self-Cleaning Rotating Electrode (SRE) in Absence and Presence of Surface Active Ions," *J. Electrochem. Soc.*, **130**, 1836 (1983).

9. C. I. NONINSKI, "Total Elimination of Electrochemical Overpotential Described by the Tafel Equation," 31st ISE Mtg., Venice, Italy, 1980, p. 179.

LETTER TO THE EDITOR

NOTES ON TWO PAPERS CLAIMING NO EVIDENCE FOR THE EXISTENCE OF EXCESS ENERGY DURING THE ELECTROLYSIS OF 0.1 *M* LiOD/D_2O WITH PALLADIUM CATHODES

A problem popularly known as "cold fusion" was brought, although in an unusual way, to the attention of the scientific community. Although much discussion was (and is still) devoted to whether this effect is connected with any *known* nuclear reactions, the latter being widely questioned, there is no doubt that the general interest in the problem was provoked by the claim of the possibility of producing excess energy, i.e., energy surmounting the energy breakeven value. Unlike the clearly negative indications so far in terms of known nuclear processes taking place, however, careful analysis reveals that the claims in the principal negative papers published so far with respect to the existence of excess energy are in disagreement with the raw experimental data whenever such is presented in those papers. This is very surprising indeed in view of the wide publicity these negative results have been given. An example of an improper analysis of their own experimental data by the authors is Ref. 1, which we have already discussed.[2] Other examples of inappropriate method and improper interpretation of their own experimental data are Refs. 3 and 4.

For convenience, denote by A the palladium/platinum (Pd/Pt) circuit working alone, that is, in the *absence* of a working resistor heater, and denote by B the combination of the Pd/Pt circuit working *together* with a resistor heater. Define E_A and E_B as the cell voltages of systems A and B, E_{tn} as the thermoneutral voltage corresponding to temperature T_1, P_h as the resistor heater power, and $\alpha(I_A)$ and $\alpha(I_B)$ as the *possible* excess powers $\alpha(I)$ produced by systems A and B, respectively, corresponding to the electrolysis currents I_A and I_B flowing through the Pd/Pt circuits of systems A and B.

In Refs. 3 and 4, to decide whether or not excess energy exists, electrolysis of D_2O was carried out with a palladium cathode and a platinum anode in the absence (case A) and the presence (case B) of a working resistor heater in the electrolysis cell, the temperature of the cell in both cases being maintained the same. This method leads to the following pairs of experimental data (see, e.g., Table 3 of Ref. 3, data couples A through E): time of electrolysis (in case A and in case B), current (I_A and I_B) or current density, electrolysis power (P_A and P_B), heater power (0 and P_h), total power [$P_{tot(A)} = P_A$ and $P_{tot(B)} = P_B + P_h$], temperature of the electrolysis cell [$T_{c(A)} = T_{c(B)}$], and heating coefficient (HC_A and HC_B), which is calculated on the basis of the data for the temperature of the cell T_c, temperature of the bath T_b, and total power P_{tot} [$HC = (T_c - T_b)/P_{tot} = \Delta T/P_{tot}$].

During isothermal calorimetry, according to Newton's cooling law in its general form,

$$P = AK(T_{cell} - T_{sur}) = AK\Delta T \ , \tag{1}$$

the heating coefficient $HC = \Delta T/P$ is given by

$$\frac{\Delta T}{P} = \frac{1}{AK} \ , \tag{2}$$

where

P = power input to the calorimeter or cell (output from calorimeter to the surroundings)

A = Newton's cooling constant

K = heat capacity of the calorimeter

T_{cell} (or T_c) = temperature of the calorimeter

T_{sur} = temperature of the surroundings = T_{bath} or T_b.

If during the electrolysis of D_2O, in addition to the electrical power P_A and P_B for the electrolysis, some other power $\alpha(I_A)$ and $\alpha(I_B)$ would have contributed to the temperature increase, then from Eq. (2) for system A [when $P = P_A + \alpha(I_A)$],

$$\frac{\Delta T}{P_A + \alpha(I_A)} = \frac{1}{AK} \quad \text{or} \quad \frac{\Delta T}{P_A} = \frac{1}{AK - \dfrac{\alpha(I_A)}{\Delta T}} \ , \tag{3}$$

and for system B, if the power of the resistor heater P_h is additionally considered [$P = P_B + P_h + \alpha(I_B)$],

$$\frac{\Delta T}{P_B + P_h + \alpha(I_B)} = \frac{1}{AK} \quad \text{or} \quad \frac{\Delta T}{P_B + P_h} = \frac{1}{AK - \dfrac{\alpha(I_B)}{\Delta T}} \ . \tag{4}$$

If only the resistor heater remains working in case B (this common case, disregarded in Refs. 3 and 4, we denote differently from A and B as A_0), then instead of Eq. (4), Eq. (2) would be valid:

$$\Delta T/P_h = 1/AK \quad \text{or} \quad AK = P_h/\Delta T \ .$$

In case A_0, ΔT (equal to ΔT in case A) and P_h (the resistor power value necessary to maintain the same difference $\Delta T = T_c - T_b$) are directly observable quantities. Thus, when P_A, ΔT, and AK obtained with systems A and A_0 are known, the value of the excess power $\alpha(I_A)$, if any, can easily be determined according to Eq. (3), and conversely, if no $\alpha(I_A)$ was produced, this also can easily be determined for sure.

However, in Refs. 3 and 4, case A, in which $\alpha(I_A) > 0$ is sought, is not juxtaposed with case A_0, in which only the resistor works in the electrolysis cell and it is *guaranteed* that $\alpha(I) = 0$. In Refs. 3 and 4, case A is juxtaposed with case B in which, as in case A, the same quantity $\alpha(I_B)$ is also to be determined since a Pd/Pt electrode is used in case B as well as in case A and in which Eq. (4), similar to Eq. (3), is used and not Eq. (2). As is seen, during what would be a proper juxtaposition of system A with system A_0, the quantity HC in Eq. (2) ($HC = \Delta T/P = 1/AK$) enables one to definitively answer the question as to whether excess power $\alpha(I)$ is obtained during the electrolysis of D_2O and, if any, what its quantity is. On the contrary, during the juxtaposition of system A with system B, accepted in Refs. 3 and 4, Eqs. (3) and (4) are obtained, comprising a system of two equations with three unknowns (and that only if the product AK is observed as a single quantity). This shows that when the particular method in Refs. 3 and 4 is applied, it is not possible to judge the value of $\alpha(I)$ from the data for the quantity HC [i.e., the data for the left sides of Eqs. (3) and (4) referring to HC]. There is, however, a way to use Eqs. (3) and (4) (referring to HC) even after finding out the obvious uselessness of HC for the purpose of determining excess energy. After some algebraic operations from Eqs. (3) and (4), Eq. (5) is obtained:

$$\frac{1}{AK - \dfrac{\alpha(I_A)}{\Delta T}} - \frac{1}{AK - \dfrac{\alpha(I_B)}{\Delta T}} = \frac{\Delta T}{P_A} - \frac{\Delta T}{P_B + P_h}$$

or

$$\alpha(I_A) - \alpha(I_B) = \Delta\alpha(I) = P_B + P_h - P_A$$

or

$$\alpha(I_A) - \alpha(I_B) = \Delta\alpha(I) = P_{tot(B)} - P_{tot(A)} \ , \qquad (5)$$

where $P_{tot(A)}$ and $P_{tot(B)}$ are the total power in cases A and B. The pairs of HC given in Refs. 3 and 4, however, are not needed to obtain Eq. (5); it is enough only to observe the very pairs of total powers themselves. One can compare the measured total power of system A,

$$P_{tot(A)} = I_A(E_A - E_{tn}) \ , \qquad (6)$$

with the corresponding total power of system B,

$$P_{tot(B)} = I_B(E_B - E_{tn}) + P_h \ , \qquad (7)$$

as the same temperature T_1 is maintained in both cells. Further, as systems A and B maintain the same temperature T_1 in the cell, we may write

$$P_{tot(B)} + \alpha(I_B) = P_{tot(A)} + \alpha(I_A) \ , \qquad (8)$$

or, substituting Eqs. (6) and (7) in Eq. (8),

$$I_B(E_B - E_{tn}) + P_h + \alpha(I_B) = I_A(E_A - E_{tn}) + \alpha(I_A) \ . \qquad (9)$$

From Eq. (9), one obtains

$$I_B(E_B - E_{tn}) + P_h - I_A(E_A - E_{tn}) = P_{tot(B)} - P_{tot(A)} = \alpha(I_A) - \alpha(I_B) = \Delta\alpha(I) \ . \qquad (10)$$

It is Eq. (10), identical to Eq. (5), on which the analysis of whether excess energy exists or not has to be based because from the data in Refs. 3 and 4, it is in fact only $\Delta\alpha(I)$ and not $\alpha(I_A)$ and/or $\alpha(I_B)$ that the authors' method can ensure and on which the authors rely entirely when drawing their conclusion of "no evidence" for excess power (enthalpy[3,4]). The authors consider that they have experimentally found this $\Delta\alpha(I)$ to be negligible (within their experimental error limits). Therefore, according to these authors, the two terms on the left side of Eq. (10) are said to be in agreement. They consider this agreement to be the ultimate proof for the nonexistence of excess power.

However, this conclusion is incorrect because even if $\Delta\alpha(I)$ were zero, it still would leave the question of the existence of excess power undetermined. The result $\Delta\alpha(I) = \alpha(I_A) - \alpha(I_B) \approx 0$ (within the error limits) is sure proof that $\alpha(I_A) \approx \alpha(I_B)$, but not that $\alpha(I_A) \approx 0$ and $\alpha(I_B) \approx 0$. The truth is that when $\Delta\alpha(I) = \alpha(I_A) - \alpha(I_B) \approx 0$, the quantities $\alpha(I_A)$ and $\alpha(I_B)$ are unknown. This result also shows that the calibration procedure applied in Refs. 3 and 4 is inappropriate—in effect, two unknown quantities are compared.

The method in Refs. 3 and 4 is unable to answer whether $\alpha(I_A)$ and $\alpha(I_B)$ were actually produced in the D_2O cell and, if they were, of what order of magnitude they might be. Therefore, to understand whether there really was any $\alpha(I)$ in Refs. 3 and 4, we must somehow rely only on the available data in those papers and compare them with the data from previous studies. Since the experiments in Ref. 3 (and Ref. 4) are "[i]n response to claims . . . " in Ref. 5, it is quite natural to refer the considerations mentioned to the latter studies. Let us see whether the only available data in, e.g., Ref. 3 concerning excess power, namely, the data for $\Delta\alpha(I)$, are in agreement with similar data in Ref. 5. From the data in Table 1 of Ref. 5 is seen that for a palladium cathode of 0.079-cm^3 volume (similar to the palladium cathode volume of 0.073 cm^3 in Table 3 of Ref. 3; note that although the correct comparison is at similar *volumes*, a similar conclusion is obtained when data at similar cathode diameters are compared) and for a similar current (a comparison at similar currents is the correct one; however, a comparison at similar current densities gives similar results!) range, an eightfold change of electrolysis current brings 0.0715 W of excess power. Therefore, since the excess power in Table 1 of Ref. 5 is at least proportional to the current density, 1.2 to 1.5 times the applied current, which is typical for Ref. 3, should be expected to bring 0.01 W of excess power. Let us compare this expected value of excess power according to Ref. 5 with the data in Ref. 3. From Table 3 of Ref. 3, the quantity $\Delta\alpha(I) = P_{tot(B)} - P_{tot(A)}$ can be found in five separate cases, and the values are, indeed, of the order of 0.01 W. The 0.01-W value may seem to be a small number. The authors of Ref. 3 even consider it within the error limits. There is, however, no more to be expected if their data are to reproduce those in Ref. 5, despite the authors' impression. The results in Ref. 5 are even more impressive when one considers that the $\Delta\alpha(I)$ is only

a part of the real amount of excess power that might have been produced in the D_2O cell.

This discussion shows that the experimental results in Ref. 3 (similar arguments can be given for Ref. 4) replicate rather than disprove the calorimetric findings in Ref. 5. The latter conclusion, however, is insufficient to provide a *decisive* answer in Refs. 3 and 4 to the question of whether $\alpha(I)$ is real or not.

V. C. Noninski

149 West 12th Street
New York, New York 10011

C. I. Noninski

Wargentinsgatan 1, tr. 1
Stockholm 11229
Sweden

November 23, 1992

REFERENCES

1. D. ALBAGLI et al., "Measurement and Analysis of Neutron and Gamma-Ray Emission Rates, Other Fusion Products, and Power in Electrochemical Cells Having Palladium Cathodes," *J. Fusion Energy*, **9**, 133 (1990).

2. V. C. NONINSKI and C. I. NONINSKI, "Comments on 'Measurement and Analysis of Neutron and Gamma-Ray Emission Rates, Other Fusion Products, and Power in Electrochemical Cells Having Palladium Cathodes,'" *Fusion Technol.*, **19**, 579 (1991).

3. N. LEWIS et al., "Searches for Low-Temperature Nuclear Fusion of Deuterium in Palladium," *Nature*, **340**, 525 (1989).

4. G. M. MISKELLY, M. J. HEBEN, A. KUMAR, R. M. PENNER, M. J. SAILOR, and N. S. LEWIS, "Analysis of Published Calorimetric Evidence for Electrochemical Fusion of Deuterium in Palladium," *Science*, **246**, 793 (1989).

5. M. FLEISCHMANN, S. PONS, and M. HAWKINS, "Electrochemically Induced Nuclear Fusion of Deuterium," *J. Electroanal. Chem.*, **261**, 301 (1989); see also Erratum, *J. Electroanal. Chem.*, **263**, 187 (1989).

LETTER TO THE EDITOR

COMMENTS ON "MEASUREMENT AND ANALYSIS OF NEUTRON AND GAMMA-RAY EMISSION RATES, OTHER FUSION PRODUCTS, AND POWER IN ELECTROCHEMICAL CELLS HAVING PALLADIUM CATHODES"

One of the best reports published so far on calorimetric measurements during the electrolysis of D_2O with palladium cathodes is Ref. 1, mainly because it contains more details of the data obtained than most publications on the subject and because of the careful way in which the experiments are carried out. However, if the raw data from the calorimetric measurements in Ref. 1 are observed more closely, a different conclusion from that expressed by the authors may be drawn. Here we briefly outline our findings, while a more detailed analysis is contained in Ref. 2. We apply, as is usually done with isothermal calorimeters,[3,4] Newton's law of cooling in its general form:

$$P = AK(T_{cell} - T_{sur}) = AK\Delta T = Am_i c_p \Delta T$$

or

$$\frac{P_i}{m_i} = Ac_p\Delta T = \frac{P}{m - \frac{I\tau M}{2F}\frac{V_{tn}^0}{V_{ie}^0}} ,$$

where

P = power input into the calorimeter (output from the calorimeter to the surroundings)

A = Newton's cooling constant

T_{cell} = temperature of the cell

T_{sur} = temperature of the surroundings

$K = m_i c_p$ = heat capacity

m = initial electrolyte mass

m_i = mass at the i'th hour

c_p = specific heat, which is practically constant throughout the experiment

M = molecular weight of D_2O

F = Faraday's constant

V_{ie}^0 = isoenthalpic voltage

V_{tn}^0 = thermoneutral voltage [at 46°C, it is 1.57 V for D_2O (Ref. 5) and 1.51 V for H_2O (Ref. 6)].

It can also be shown that if the problem is treated in terms of pure conduction heat transfer, as the authors of Ref. 1 consider,[7] similar conclusions will be reached. If we assume A = const, then P/m_i = const. If we also consider that the cell has produced no excess power at 20 h, then the quantity of excess power density $P_{x,sp}^i$ produced per unit cathode volume v_{Pd} at the following moments i can be calculated from

$$P_{x,sp}^i = \frac{P_x^i}{v_{Pd}} ,$$

where

$$P_x^i = \left(\frac{P_{20\,h}}{m_{20\,h}} - \frac{P_i}{m_i}\right) m_i ,$$

as shown in Fig. 1. It is seen from Fig. 1 that in the course of the experiment, an additional power source [greater than the sensitivity of the method—0.04 W (Ref. 1)] has acted that is of the order of, and at times even greater than, the value 0.079 W (1.01 W/cm^3) reported in Ref. 8 for the current density, similar to that used in Ref. 1. It is seen that P_x is observed exactly according to the predictions of Eq. (3) in Ref. 1.

Clearly, the above analysis gives only conservative estimates of P_x due to the assumptions that A = const, whereas A is actually increasing in time, and that no excess power has been produced at 20 h. We note that the trivial reasons for the appearance of the observed P_x asserted in Ref. 1 can hardly serve as a cause for a P_x effect, if any, of the above order. An important fact to be noted is that the electrolyte mass loss in Ref. 1 is primarily due to electrolysis only, which is confirmed by the excellent coincidence of the V_{tn} measured during the calibration with its theoretical value.[6] This finding especially invalidates the possibility adverted in Ref. 2 of unintentional $D_2 + O_2$ recombination causing the appearance of P_x. This recombination has also been observed to be negligible in other studies.[9,10] The excellent result[1] from the calibration indicates that a trivial explanation can hardly be

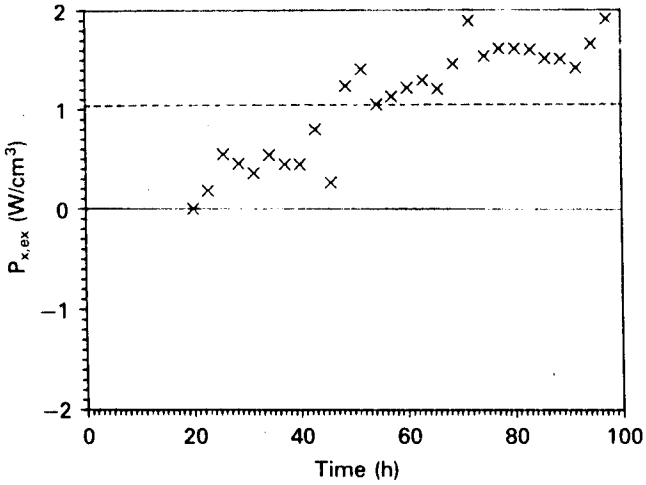

Fig. 1. Excess power density as a function of time calculated for some moments from the raw data in Ref. 1 (0.1- × 9-cm palladium cathode, 69 mA/cm^2 current density). The dotted line represents the level of $P_{x,sp}$ claimed in Ref. 8 for a 0.1- × 10-cm palladium cathode at 64 mA/cm^2 current density.

found of the fact that, despite the great sensitivity to electrolyte mass changes, at 70.5 h it was possible to maintain the required temperature of a solution containing 1.24 g more than that at 13.8 h, as seen from Figs. 5a and 6 of Ref. 1.

*V. C. Noninski**
C. I. Noninski

Laboratory for Electrochemistry of Renewed
Electrode-Solution Interface (LEPGER)
P.O. Box 9
Sofia 1504, Bulgaria

November 5, 1990

*Current address: 149 West 12th Street, Apt. #3-4, New York, New York 10011.

REFERENCES

1. D. ALBAGLI, R. BALLINGER, V. CAMMARATA, X. CHEN, R. M. CROOKS, C. FIORE, M. J. P. GAUDREAU, I. HWANG, C. K. LI, P. LINSAY, S. C. LUCKHARDT, R. P. PARKER, R. D. PETRASSO, M. O. SCHLOH, K. W. WENZEL, and M. S. WRIGHTON, "Measurement and Analysis of Neutron and Gamma-Ray Emission Rates, Other Fusion Products, and Power in Electrochemical Cells Having Palladium Cathodes," *J. Fusion Energy*, **9**, 133 (1990).

2. V. C. NONINSKI and C. I. NONINSKI, submitted to *J. Fusion Energy* (1990).

3. N. LEWIS et al., "Searches for Low-Temperature Nuclear Fusion of Deuterium in Palladium," *Nature*, **340**, 525 (1989).

4. G. M. MISKELLY, M. J. HEBEN, A. KUMAR, R. M. PENNER, M. J. SAILOR, and N. S. LEWIS, "Analysis of Published Calorimetric Evidence for Electrochemical Fusion of Deuterium in Palladium," *Science*, **246**, 793 (1989).

5. J. BALEY and J. DIVISEK, "Energy Balance of D_2O Electrolysis with a Palladium Cathode, Part I: Theoretical Relations," *J. Electroanal. Chem.*, **278**, 85 (1989).

6. R. L. LeROY, C. T. BOWEN, and D. J. LeROY, "The Thermodynamics of Aqueous Water Electrolysis," *J. Electrochem. Soc.*, **127**, 1954 (1980).

7. Private communication from the authors of Ref. 1 above.

8. M. FLEISCHMANN and S. PONS, "Electrochemically Induced Nuclear Fusion of Deuterium," *J. Electroanal. Chem.*, **261**, 307 (1989); see also M. FLEISCHMANN and S. PONS, Erratum, *J. Electroanal. Chem.*, **263**, 187 (1989).

9. V. J. CUNNANE, R. A. SCANNELL, and D. J. SCHIFFRIN, "$H_2 + O_2$ Recombination in Non-Isothermal, Non-Adiabatic Electrochemical Calorimetry of Water Electrolysis in an Undivided Cell," *J. Electroanal. Chem.*, **269**, 163 (1989).

10. D. E. WILLIAMS et al., "Upper Bounds on 'Cold Fusion' in Electrolytic Cells," *Nature*, **342**, 375 (1989).

Scientia Pharmaceutica (Sci. Pharm.) 54, 105–110 (1986)

Anodic Polarographic Determination of Analgin and Amidophen in Drugs with the Help of the Self-Cleaning Rotating Electrode (SRE)

V. C. Noninski[a]* and E. B. Sobowale[b]

[a] Higher Institute of Chemical Technology, LEPGER, Sofia 1156, Bulgaria
[b] Medical Academy, Faculty of Pharmacy, Department of Pharmaceutical Chemistry, Sofia 1000, Bulgaria

(Received October 23, 1985)

Anodic polarograms of analgin and amidophen are presented obtained with gold self-cleaning rotating electrode (SRE). Due to the continuous mechanical renewal of the electrode surface in strictly defined hydrodynamic, diffusion etc. conditions the polarograms are continuously reproducible without the pretreatment of the SRE. Good reproducibility and linearity between the wave height and concentration is observed both with low concentrations (of the order of 4.10^{-6} M) and with relatively high concentrations (of the order of 1.10^{-3} M) of the substances. It was found that the half-wave potentials, $E_{1/2}$, of analgin and amidophen and the shape of the waves are not influenced practically by the additives of the drugs. Therefore preliminary procedures like extraction, filtration etc. are unnecessary. The mentioned substances can be determined directly by polarography using inexpensive routine apparatuses. This polarographic method eliminates the use of the hazardous mercury. The difference between the $E_{1/2}$ of the two substances allow a simultaneous determination. Results of the determination of analgin and amidophen in tablets, analgin in tablets of bellalgin, analgin-chinin, anapyrin and amidophen in tablets of anapyrin and sedaphen are presented.

Anoden-polarographische Bestimmung des Analgins und Amidophens in Arzneimitteln mit der selbstreinigenden rotierenden Elektrode (SRE)

Es werden anodische Polarogramme des Analgins und Amidophens, erhalten mit der selbstreinigenden rotierenden Elektrode (SRE), vorgestellt. Durch eine kontinuierliche mechanische Erneuerung der Elektrodenoberfläche in streng definierten Bedingungen sind die Polarogramme ohne Vorbereitung der Elektrode stets reproduzierbar. Die gute Reproduzierbarkeit und Linearität zwischen der Wellenhöhe und der Konzentration der Substanzen kann sowohl bei niedriger Konzentration ($4{,}10^{-6}$ M) als auch bei relativ hohen Konzentrationen ($1{,}10^{-3}$ M) beobachtet werden. Es konnte festgestellt werden, daß weder das Potential der Halbwelle des Analgins und Amidophens noch ihre Form von den Balaststoffen in den Arzneimitteln beeinflußt werden. Daher können einleitende Operationen wie Extraktion, Filtration usw. unterlassen werden. Die vorgestellte Methode bietet die Möglichkeit, mit geringem Aufwand und routinemäßiger Apparateausstattung die obengenannten Substanzen einzeln und/oder gemeinsam zu bestimmen. Diese Methode vermeidet die Anwendung des giftigen Quecksilbers.

(Keywords: Anodic polarography, analgin and amidophen determination, self-cleaning rotating electrode (SRE), in drugs)

Introduction

Analgin (1-phenyl-2,3-dimethyl-4-methylamino pyrazol-5-one-N-methansulphonate sodium) and amidophen (1-phenyl-2,3-dimethyl-4-dimethylamino-pyrazol-5-one) are some of the analgesics – antipyretics of the pyrazolone series widely used in medical practice. In drug combinations they are usually determined after preliminary extraction, filtration and other time-consuming procedures. Our studies showed the possibility of direct and presice determinations by applying anodic polarography with

gold self-cleaning rotating electrode (SRE). An advantage of SRE in comparison to other solid electrodes is the possibility to avoid pretreatment of the electrode before each determination without influence on the reproducibility of the results. Another advantage of the SRE is the absence of the noxious mercury usually applied in polarography. Polarographic determination of combinations of analgin and amidophen in drugs has not been carried out by now.

Experimental

Apparatus

In the present paper the experiments are obtained with a cone shaped gold SRE[1] as working electrode. It should be noted that SRE can be a disc as well. However, application of a cone with an angle at the top less than 180° (disc is a special case of a cone with an angle at its top = 180°) as in our case has certain advantages – the mechanical renewal is improved because of the special construction of the cleaning device, leakage underneath the side cylinder surface is avoided as well as the side wobbling of the electrode, because the cleaning device plays also the role of a sliding bearing, etc. With the use of the SRE it is possible to maintain strictly defined diffusion, hydrodynamic etc. conditions, which also ensures reproducible results. The working electrode rotation rate used for the present investigations is 50 Hz. All the polarograms are taken versus saturated calomel electrode (SCE). A large surface platinum wire was used as counter electrode. Part of the investigations were carried out in a three compartment glass cell. Experiments were carried out also in a common laboratory 50 ml glass which gave satisfactory results. The anode potentials were applied with the help of a potentiostat-galvanostat RADELKIS OH-405 (Hungary). The potential sweep rate was 10 mV/s. The polarographic waves were registered on PHILIPS PM 8210 X–Y recorder at room temperature. It should be noted that instead of the mentioned RADELKIS and PHILIPS type apparatuses any other potentiostat and X–Y recorder available in the laboratory can be used. Any common polarographic apparatus can be used instead.

Reagents

The chemicals used were of analytical grade. The solutions were prepared with bidistilled water. However, our experiments showed that the common distilled water can be used with the same success. The tablets studied were: analgin (analgin 0.5 g, tabletting material – quantum satis), amidophen (amidophen 0.1 g, tabletting material – quantum satis), amidophen-granules for syrup (amidophen 3.75–4.25 %), bellalgin (analgin 0.25 g ± 5 %, anaesthesin 0.25 g ± 5 %, $NaHCO_3$ 0.10 g ± 10 %, extract from belladonna), analgin-quinine (analgin 0.18–0.22 g, quinine hydrochloride 0.045–0.055 g), anapyrin (analgin 0.25 g ± 5 g, amidopyrin 0.25 g ± 5 %, caffeine sodium benzoat 0.10 g ± 5 %), sedaphen (caffeine purum 0.05 g ± 10 %, phenacetin 0.15 g ± 5 %, amidophen 0.15 g ± 5 %, adalin 0.12 g ± 5 %). These tablets were obtained from PHARMACHIM, Sofia. A stock solution for every sample was prepared immediately before the experiment. Britton-Robinson buffer (BRB) was used as supporting electrolyte. If necessary the pH of the buffer was adjusted with 2 *M* NaOH.

Procedure

The determinations were carried out as follows. Ten tablets of a given drug were weighed to determine the average weight of a single tablet. Then the tablets were powdered in a mortar. 100.0 mg of this powder were then placed in a 50 ml volumetric

flask (in the case of amidophen-granules for syrup 2.5 g were taken) and 30 ml of BRB were added. The contents were stirred for 5 min and then more buffer was added to the mark. The concentration of the studied substances in thus prepared solution was determined by polarography of five aliquots (usually of 0.5 ml). The quantity of analgin or amidophen contained in a single tablet was calculated from the quantity determined in 100 mg of the powder by using the average weight of a tablet.

Results and Discussion

In Fig. 1 direct current (dc) polarographic waves of analgin (A) and amidophen (B) and analgin and amidophen in combination (C) are shown. They are recorded successively one after the other without pretreatment of the SRE. Fig. 1 shows good reproducibility of the obtained waves. Recording of such reproducible waves can be continued. The same reproducibility of the waves was observed in all our experiments.

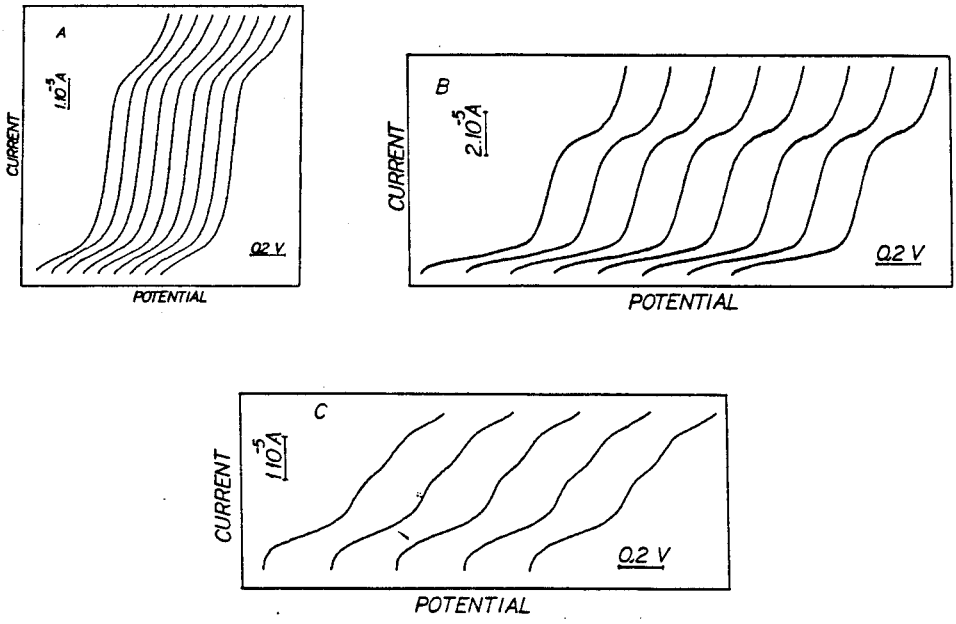

Figure 1: Polarograms of $2.3 \cdot 10^{-4}$ M analgin (A), $1.6 \cdot 10^{-4}$ M amidophen (B) and combination of $5.3 \cdot 10^{-5}$ M analgin and $8.2 \cdot 10^{-5}$ M amidophen (C) in Britton-Robinson buffer on gold SRE. Starting potential 0.0 V vs. SCE.

Because of the good shape and reproducibility of the obtained dc waves we called the method applying SRE "polarography", in contrast to the term "voltametry" normally used in the case of solid electrodes.

From the polarograms in Fig. 1 A and B half-wave potentials, $E_{1/2}$, of 0.410 V and 0.580 V for analgin and amidophen resp. are established. The same values of $E_{1/2}$ were obtained in all other studied cases. It was found that the additives and other substances present in the studied tablets practically do not change the $E_{1/2}$ of analgin and amidophen at constant pH of the medium. Neither did these additives and substances change the shape of the analgin and amidophen waves. These are important facts which enabled us to carry out the determination of these substances in

various drug combinations containing analgin and amidophen. Another favourable fact is the difference between the $E_{1/2}$ values of analgin and amidophen which allows their simultaneous determination. A solution of both substances shows two waves in the polarogram (see Fig. 1 C).

In Fig. 2 A and B some of the obtained polarogrphic waves of analgin and amidophen resp. in BRB recorded at different concentrations are shown. The investigations showed that a linear dependence exists between the wave height and the concentration of both analgin and amidophen in a wide range of concentrations – from 4.10^{-6} up to 1.10^{-3} M. (The latter was the highest concentration studied by us.) The high concentration of the studied substance does not influence the determination by adsorbtion or by other modification of the electrode surface, a fact which distinguishes SRE in comparision to other solid electrodes.

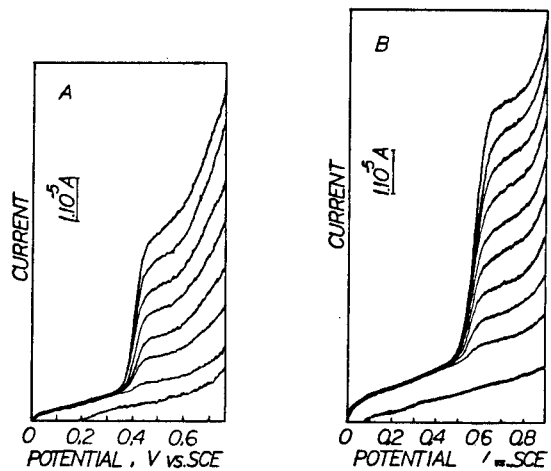

Figure 2: Polarograms of analgin (A) and amidophen (B) on gold SRE. The concentrations of analgin are in the range from $1.3 \cdot 10^{-5}$ M to $3.9 \cdot 10^{-4}$ M and of amidophen – from $1.9 \cdot 10^{-5}$ M to $3.2 \cdot 10^{-4}$ M. The first curve from the bottom shows the polarogram of the supporting electrolyte.

From Fig. 2 can be seen that the $E_{1/2}$ value of analgin does not change with the concentration while the $E_{1/2}$ of amidophen is slightly shifted to values more positive (about 20 mV). Nevertheless, it can be considered that in both cases $E_{1/2}$ practically does not depend on their concentration which is favourable for their qualitative determination. The half-wave potentials of the studied substances showed strong dependence on the pH of BRB. The waves of the two substances in combination are better separated (the difference between the half-wave potentials is greater) when the pH of the buffer is low. Thus in Fig. 1 C the waves are taken at pH = 1.5 and the $E_{1/2}$ values of the two substances (0.420 V and 0.610 V for analgin and amidophen resp.) differ from those in Fig. 1 A and B where the pH = 2.

In the Table some of the obtained results of the determination of analgin and amidophen in tablets and in some drug combinations are presented. The Table shows that the relative standard deviation, RSD, varying from 0.52 to 1.64 shows good reproducibility of the method in all the studied cases. In the case of anapyrin the mentioned ability to determine analgin and amidophen simultaneously is demonstrated. The method is more sensitive than the approved titrimetric method by the

Table: **Precision data for the determination of analgin and amidophen** (in tablets and in drug combinations) **by polarography and titrimetry**

	Polarography				Titrimetry			
Substance	Quantity found for a tablet, mg	SD*, mg	RSD, %	Confidence limits**	Quantity found for a tablet, mg	SD*, mg	RSD, %	Confidence limits**
Analgin (tab.)	521.8	2.73	0.52	521.8 ± 3.39	549.5	7.00	1.27	549.5 ± 8.7
Analgin in:								
Bellalgin (tab.)	220.6	2.00	0.91	220.6 ± 2.49	247.6	26.80	10.80	247.6 ± 33.3
Analgin-chinin (tab.)	205.0	3.48	1.42	205.0 ± 4.33	183.9	2.10	1.20	183.9 ± 2.6
Anapyrin (tab.)	249.9	3.08	1.23	249.9 ± 3.82	219.4	7.00	3.19	219.4 ± 8.7
Amidophen (tab.)	99.3	0.58	0.59	99.3 ± 0.72	105.0	2.50	2.30	105.0 ± 3.1
Amidophengranules for syrup	106.1	1.74	1.64	106.1 ± 2.24				
Amidophen in:								
Anapyrin (tab.)	245.0	2.55	1.04	245.0 ± 3.17	253.9	16.90	6.65	253.9 ± 21.0
Sedaphen (tab.)	156.2	1.25	0.80	156.2 ± 1.55	156.1	7.08	4.50	156.1 ± 8.9

* For five determinations
** Probability level = 0.95

Pharmacopoeia[2]. In the Table we present also the results obtained from titrimetric determinations. It shows that the proposed method is of the same, if not better, accuracy and precision as the official one. The detection limit of the method is found to be about 4.10^{-6} M.

References

[1] C. I. Noninski: Khim. i Ind. (Sofia), **10**, 442 (1966).
[2] State Pharmacopoeia, USSR, Volume 10, bulgarian translation, "Medizina i fizkultura", Sofia, 1970, pp. 118 and 105.

ANODIC VOLTAMMETRY OF PYRAZOLONE DERIVATIVES WITH THE HELP OF THE SELF-CLEANING ROTATING ELECTRODE

Vesselin C. NONINSKI[a] and Emanuel B. SOBOWALE[b]

[a] *Higher Institute of Chemical Technology, LEPGER, Sofia 1156, Bulgaria and*
[b] *Medical Academy, Faculty of Pharmacy, Department of Pharmaceutical Chemistry, Sofia 1000, Bulgaria*

Received November 7th, 1985

Nine pyrazolone derivatives have been studied by anodic voltammetry using gold self-cleaning rotating electrode (SRE). Voltamograms of good reproducibility are presented. On the basis of voltammetric data a mechanism is proposed for the electrochemical oxidation of sodium 1-phenyl--2,3-dimethyl-4-(N-methyl amino)pyrazol-5-one-N-methansulphonate and 1-phenyl-2,3-di-methyl--4-(dimethylamino)pyrazol-5-one in protic medium.

Voltammetric method has been used for the analytical study of 1-phenyl-2,3-dimethyl-4-(dimethylamino)pyrazol-5-one in protic medium[1] and cyclic voltammetry has been applied for the electrochemical study of 1-phenyl-2,3-dimethyl-4-(methylamino)pyrazol-5-one, 1-phenyl-2,3-dimethyl-4-(methylamino)pyrazol-5-one, 1-phenyl -2,3-dimethyl-4-aminopyrazol-5-one, and 1-phenyl-2,3-dimethyl-pyrazol-5-one to establish the mechanism of electrooxidation of 1-phenyl-2,3-dimethyl-4-(dimethylamino)pyrazol-5-one in aprotic medium.

However, a systematic study of the pyrazolone group has not been carried out in protic media in view of establishing the mechanism of electrooxidation, influence of substituent groups and pH of the medium on their electrochemical behaviour.

In the present paper results and some theoretical considerations are presented for the electrochemical oxidation of nine pyrazolone derivatives using gold self-cleaning electrode (SRE)[3]. The studied compounds are presented in Table I and shall be denoted henceforth in the text by roman figures as in Table I.

EXPERIMENTAL

Reagents. All chemicals used are of analytical grade. In the preparation of the solutions bi-distilled water was used. It was found out that ordinary distilled water is also suitable. For every sample a stock solution of $1 . 10^{-3}$ mol l^{-1} concentration was prepared immediately before the experiment. The supporting electrolyte was Britton–Robinson buffer. The pH of the buffer was adjusted with NaOH of 2 mol l^{-1} concentraiton. The pyrazolone derivatives listed in Table I were obtained from Pharmachim, Sofia, except for *III* which was obtained from the Bulgarian Academy of Sciences.

Apparatus. The experiments were carried out in a three compartment glass cell. The working electrode was gold SRE[3]. Saturated calomel electrode (SCE) was used as reference electrode. As counter electrode a large platinum wire was used. The volume of the glass cell was 150 ml. However, the same results can be obtained by using a common laboratory glass *e.g.* of 50 ml. This makes the method easily applicable in serial analysis. The anodic potentials were applied by Radelkis OH-405 (Hungary) potentiostat-galvanostat. The potential sweep rate was 10 mV/s. The voltammograms were recorded by a Philips PM 8120 X–Y recorder. The working electrode

TABLE I

Compounds examined

Basic structure ($R^1 = R^2 = H$) 1-phenyl-3-methylpyrazol-5-one

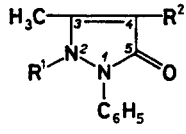

Compound	Substituents		Half-wave potential, $E_{1/2}$, V
	R^1	R^2	
I	$-CH_3$	$-H$	1·200
II	$-H$	$-H$	0·695
III	$-CH_3$	$-CH(CH_3)_2$	1·050
IV	$-CH_3$	$-NH_2$	0·560
V	$-CH_3$	$-NHCH_3$	0·410
VI	$-CH_3$	$-NHCHO$	0·920
VII	$-CH_3$	$-N(Na)-CH_2OSO_2Na$	0·590
VIII	$-CH_3$	$-N(CH_3)-CH_2OSO_2Na$	0·400
IX	$-CH_3$	$-N(CH_3)-CH_3$	0·560

rotation rate in most of the cases was 50 Hz. The voltammograms were taken at room temperature.

Procedure. To obtain reliable data 100·0 mg of the studied substance were taken and dissolved in 100·0 ml of distilled water. By voltammetric determination of the studied substance in five different aliquots of the above solution the quantity of the studied substance in this solution was found.

Coulometric studies. Firstly the voltammogram of the sample was recorded in Britton–Robinson buffer pH 2. Then the potential corresponding to the wave plateau was applied to the SRE. The current passing through the cell was recorded by a *X–t* recorder. After integrating the area of the current-time curve the quantity of electricity that passed through the cell was calculated. At the end of the experiment a voltammogram was recorded to determine the quantity of the remaining compound.

RESULTS AND DISCUSSION

In Fig. 1 voltammograms of $2{\cdot}3 \cdot 10^{-4}$ mol l^{-1} of *VIII* recorded one after the other without pretreatment of the electrode are presented to demonstrate good reproducibility of the waves. The same reproducibility (without the need of electrode pretreatment) was obtained also for the other compounds studied. Linear dependence is obtained between the wave height and the square root of the SRE rotation rate, $n^{1/2}$, which is an indication for the diffusion character of the obtained waves. The depedence between the concentration of the substance (pH 2) and their wave height is linear in a wide concentration range (10^{-5}–10^{-3} mol l^{-1}); the half-wave potentials, $E_{1/2}$, of the studied substances do not change with concentration.

In Fig. 2 $E_{1/2}$ of *VIII* and *IX* as a function of the pH of the medium are shown. Well formed voltammograms of *VIII* could be obtained up to pH about 7·3 while for *IX* up to pH about 8·6. With the increase of pH above 3 for *IX* and 3·9 for *VIII* splitting of their waves is observed. The second wave of amidophen with the more positive $E_{1/2}$ disappears at about pH = 6·5 and only the first wave remains. At pH = 3 the $E_{1/2}$ – pH plot of *IX* having a slope of 0·064 V/pH unit changes after a discontinuity into a line of 0·047 V/pH unit and of 0·020 V/pH at pH = 4·9. From pH = 6·5 the $E_{1/2}$ of *IX* is independent of pH which indicates that in this pH region its oxidation proceeds without the participation of protons. Protons participate in the oxidation of *VIII* in the whole pH range where its oxidation can take place. Since our coulometric investigations showed one electron oxidation of both *VIII* and *IX* in acidic medium (pH = 2) fractional numbers for the protons participating in the reaction are obtained. This fact might be an indication of the irreversibility of the obtained voltammograms. Even more complicated is the explanation of the obtained $E_{1/2}$ – pH dependences at higher pH values; additional data are necessary which are not available now. It should be stated here that the $E_{1/2}$ – pH line of *V* (not presented in Fig. 2) showed a slope similar to that of *VIII*.

From the voltammetric data obtained we made some conclusions concerning the mechanism of the electrochemical oxidation of *VIII* and *IX*. We also studied some

of the intermediate products during their synthesis and also some substances having a structure that can help us in evaluating the mechanism. In Table I the half-wave potentials, $E_{1/2}$, of the studied nine pyrazolone derivatives in Britton–Robinson buffer (pH = 2) at 50 Hz rotation rate of the gold SRE are shown. It is seen that a close relation exists between the strcture of the pyrazolone derivatives and their electrochemical oxidation. It should be noted that the existence of a substituent on C-4 in the pyrazolone ring plays the main role. If there is no substituent on C-4 (*I*) a wave of high positive $E_{1/2}$ value appears (1·2 V). With the introduction of an alkyl group the electrochemical reactivity does not increase significantly. Thus, the compound with the isopropyl group on C-4 (*III*) has the $E_{1/2}$ value 1·050 V which is only 0·150 V lower as compared with *I*. From the $E_{1/2}$ values in Table I it follows that amino group substituents on C-4 increase the electrochemical reactivity of pyrazolones. In the case of a primary amino group on C-4 (*IV*) the $E_{1/2}$ = 0·560 V, *i.e.* about half of the $E_{1/2}$ value of *I*. The substituents in the amino group are of important significance with respect to the electroreactivity. If the substituent has a positive induction effect as it is in the case of V, $E_{1/2}$ has a lower value (about 0·150 V lower) than that of *IV*. Disubstituted *IV* (*IX*) has the same value of the half-wave potential as that of *IV*. Probably due to steric effect the $E_{1/2}$ of *IX* is higher than that of *V*.

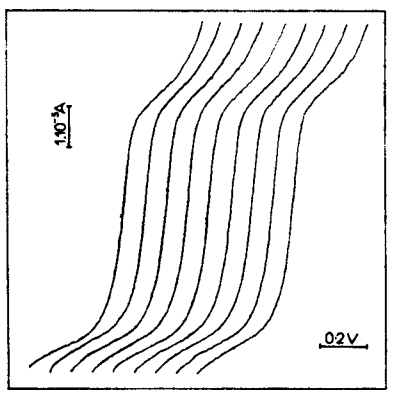

FIG. 1

Voltammograms of sodium 1-phenyl-2,3-dimethyl-4-(N-methylamino)pyrazol-5-one-N-methansulphonate in Britton–Robinson buffer on gold SRE taken successively one after the other. Starting potential 0·0 V *vs* SCE

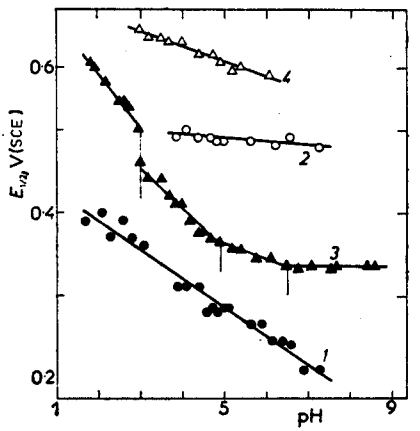

FIG. 2

Half-wave potential, $E_{1/2}$, of some pyrazolone derivatives as a function of pH. The substances are denoted with roman figures as in Table I. *1* first wave of *VIII*; *2* second wave of *VIII*; *3* first wave of *IX*; *4* second wave of *IX*. Concentration of *VIII* 1·7 . 10^{-4} mol l^{-1} and of *IX* 2·6 . 10^{-4} mol . l^{-1}

Similar to $E_{1/2}$ of *V* is the $E_{1/2}$ of *VIII*. The reason for this is probably the hydrolysis of *VIII* in acidic medium leading to the formation of *V*. The latter is oxidized electrochemically showing an $E_{1/2}$ similar to that when pure *V* is oxidized. In ref.[2] a mechanism is proposed for the electrooxidation of *IX* in aprotic medium (acetonitrile). Unlike the results reported in ref.[2] our studies revealed that the $E_{1/2}$ of the tertiary amine *IX* is more negative than that of the secondary amine *V* but equal to that of the primary amine *IV*. However, when the substituent in the amino group is exerting negative induction effect (*VI*) the oxidation is hindered and the $E_{1/2}$ has a relatively very high positive value (0·920 V) compared to that of *VIII*, *IX*, and *V*. On the other hand the $E_{1/2}$ of *VI* is relatively less positive as compared to $E_{1/2}$ of *I*. Similar observation was made for *VII* ($E_{1/2}$ = 0·590 V) due to the negative induction effect of sodium. Interesting was the electrochemical oxidation of *II*. Its oxidation is much easier and compared to *I* its $E_{1/2}$ is almost twice as low. It is to be noted that in its pyrazolone ring there is a secondary nitrogen where the oxidation can take place.

From the relations established between the structure and the electrochemical oxidation of the pyrazolone derivatives it can be concluded that the latter takes place in a different way compared to the chemical oxidation. For instance, it is known that during the oxidimetric determination of *IX* the double bond in its pyrazolone ring is broken and dioxopyramidon is obtained. However, it is known also that the chemical oxidation of the pyrazolone ring at the —C=C— bond needs four electrons[1,4–6]. This mechanism is improbable here because according to the mentioned coulometric investigations in the electrochemical oxidation of both *VIII* and *IX* only one electron participates. Analysis of the slopes of the voltammograms points also to a one electron electrooxidation. Furthermore, during the oxidimetric determination of *VIII* it is the sulphite anion which is oxidized. In our studies we did not observe the wave of the oxidation of the sulphite anion in *VIII* which indicates that this anion is not oxidized electrochemically. Therefore, unlike the chemical oxidation of *VIII*, the voltammogram of this substance only reveals the oxidation of *V* remaining after its hydrolysis. Probably the mechanism of the electrochemical oxidation of *VIII* and *IX* is similar to the mechanism of the chemical oxidation of amino groups with H_2O_2 in which one electron and one proton participate[7,8]. Therefore, we propose the following mechanism for the electrochemical oxidation of *VIII* (*A*) and *IX* (*B*):

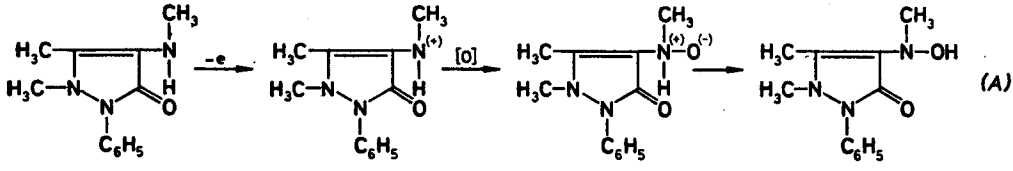

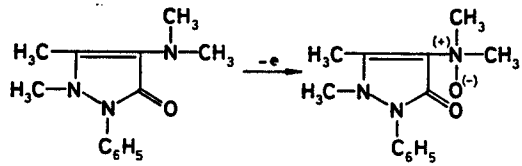

(B)

The method of anodic voltammetry using gold SRE has been observed to be favourably applicable for routine determination of pyrazolone derivatives.

REFERENCES

1. Lugovoi S. V., Ryazanov I. P.: Zh. Anal. Khim., *22*, 1093 (1967).
2. Sayo H., Masui M.: J. Chem. Soc., Perkin Trans. 2, *1973*, 1641.
3. Noninski C. I.: Khim. Ind. (Sofia) No *10*, 442 (1966);
   Noninski C. I.: Bull. Soc. Chim. Fr. No *9—10*, 1283 (1976).
4. Böhme H., Hartke K.: *Deutsches Arzneibuch*, 7. Ausgabe, 1968. Kommentar Wissenschaftlische Verlagsgesellschaft, MBH, Stuttgart, GOVI-Verlag, Frankfurt 1970.
5. Awe W., Traeht H. G.: Pharmaz. Ztg. *107*, 429 (1962).
6. Schulec E., Menyharth P.: Z. Anal. Chem. *89*, 426 (1932).
7. Norman R. O. C.: *Principles of Organic Synthesis*, p. 531. Science Paperbacks, London 1972.
8. Patai S. (Ed.): *The Chemistry of Amino Group*, p. 320. Interscience, London 1968.

Anodic polarographic determination of Etamcylate (Dicynone) with the help of the self-cleaning rotating electrode (SRE)

V. C. Noninski — Higher Institute of Chemical Technology LEPGER, Sofia 1156, Bulgaria

E. B. Sobowale, L. A. Dryanovska-Noninska — Medical Academy, Faculty of Pharmacy, Department of Pharmaceutical Chemistry, Sofia 1000, Bulgaria

SUMMARY *Results are presented for the anodic behaviour of diethylamine of 2,5-dihidroxybenzensuluhonic acid known as Etamcylate or Dicynone on gold self-cleaning rotating electrode (SRE). Two waves are observed on the anodic polarogram of this substance which can be applied for analytical purposes.*

INTRODUCTION

Diethylamine of 2,5-dihydroxybenzenesulphonic acid known as Etamcylate or Dicynone is an efficient antihaemorrhagic substance for whose determination thin layer chromatography (TLC), UV spectroscopy, cerimetry (1) and high performance liquid chromatography (HPLC) (2) are applied. A possibility to determine this substance gave the anodic polarographic method using the self-cleaning rotating electrode (SRE) which has already been successfully applied by us for the determination of other pharmaceutical substances (3). Polarographic method has not been used until now for the determination of Etamcylate though papers on voltammetry of various hydroquinones are known (4—6).

The experimental set-up was described in (3). The chemicals used were of p.a. qualification. The pure Etamcylate was in powder form. The tablets of Etamcylate were obtained from the Technology Department of the Faculty of Pharmacy, Medical Academy, Sofia. As supporting electrolyte mainly Britton-Robinson buffer (BRB) was used. When necessary the pH of the buffer was corrected with 2 M NaOH.

The procedure for the preparation of the stock solution was the following : 100,0 mg of pure Etamcylate were weighed and then placed in 50 ml volumetric flask containing about 30 ml BRB. The content was stirred for about 5 minutes, more buffer was added to the mark and again stirred.

The determination of Etamcylate tablets began by weighing five tablets and the mean weight of a single was determined. Then the five tablets were ground in a mortar and 100,0 mg of the obtained powder was weighed. The weighed powder was dissolved in 50 ml BRB.

After the polarogram of the supporting electrolyte was obtained starting from 0,0 V, 0,5 ml of the stock solution was added to obtain the next polarogram starting again from 0,0 V. From the obtained waves the standard line of the wave height versus the concentration was constructed.

Coulometric investigations similar to those described in (3) were also carried out.

RESULTS AND DISCUSSION

The polarograms of Etamcylate obtained on gold SRE consist of two waves whose half-wave potentials, $E_{1/2}$, are 0,400 V and 0,835 V resp. In fig. 1 five waves of Etamcylate are shown, taken one after the other without the pretreatment of the electrods. From fig. 1 is seen thal the polarograms of this substance obtained with the SRE are very well reproductible. The good reproductibility of the obtained waves gave us the base for calling the method when using SRE polarography, unlike the term voltammetry commonly used for solid electrodes in such cases.

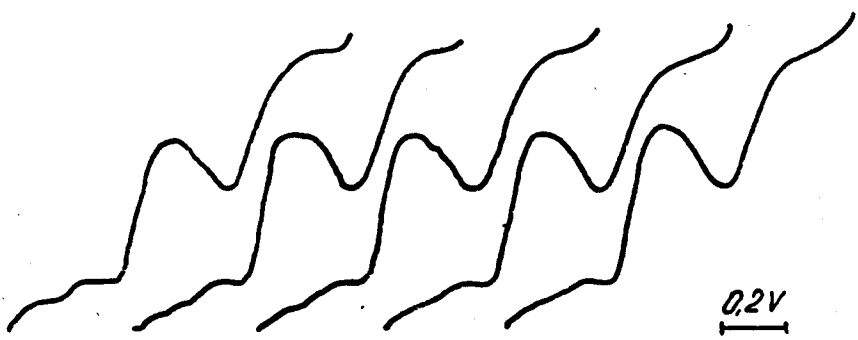

Fig. 1 — Polarograms of 1.10^{-4} M Etamcylate (Dicynone) in Britton-Robinson buffer taken on gold SRE at 50 Hz rotation rate and 10 mV/s potential sweep rate.

To determine the character of the current of these waves polarograms were taken at different rotation rates, *n*, of the SRE shown in fig. 2a. From fig. 2b is seen that the dependence of the height of the waves, *h*, as a function of $n_{1/2}$ of the first 1 and second 2 waves separately as well as the sum of the two wave heights 3 are linear. This fact is an indication of the diffusion limitation of the current of both waves.

In fig. 3 waves taken at different concentration of Etamcylate are presented. The dependence of the wave heights as a function of Etamcylate concentration is linear and these waves can be used for quantitative determinations. For such either the first or second or the combination of both waves can be used. Polarographic waves of Etamcylate can be observed down to concentration of the order of 10^{-6}M.

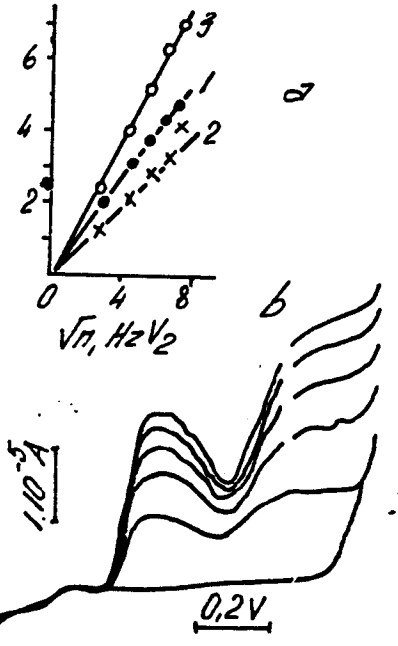

Fig. 2 — Polarograms of Etamcylate of 1.10^{-4} M concentration in BRB at SRE rotation rate resp.: 10, 20, 30, 40 and 50 Hz. The first wave from the bottom is the curve of the supporting electrolyte. The insertion in the figure shows the height of the first 1, the second 2 and the sum of the first and the second 3 waves as a function of the square root of the SRE rotation rate.

Fig. 3 — Polarograms of Etamcylate of different concentration (from $2{,}2.10^{-4}$ M to $1{,}2.10^{-3}$ M) on gold SRE in BRB. Rate of the SRE rotation — 50 Hz.

Some investigations were carried out in connection with the study of mechanism of Etamcylate electrooxidation. To determine the number of electrons participating in this reaction coulometric investigations were carried out. They showed that during the electrooxidation of Etamcylate one electron is involved both with the first and the second wave.

In fig. 4a and b the $E_{1/2}$ of Etamcylate waves as a function of buffer pH are shown. $E_{1/2}$ of the first and the second waves do not depend on pH up to pH = 2,4 and 3,5 resp. After these pH values $E_{1/2}$ show strong dependence on pH which is linear. From the slopes of these dependences and from the coulometric investigations showing one electron electrooxidation the participation of one proton with each wave is obtained.

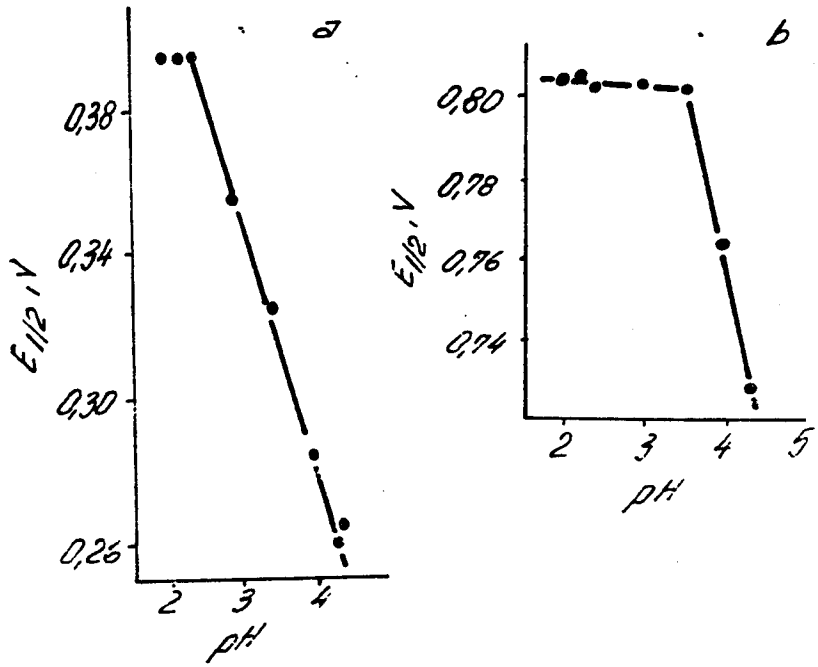

Fig. 4 — Half-wave potentials, $E_{1/2}$, of the first wave *(a)* and of the second wave *(b)* as a function of pH. Concentration of Etamcylate in the solution — $1{,}10^{-4}$ M. Supporting electrolyte — BRB.

In table I results are presented from the determination of Etamcylate in tablets by anodic polarography using SRE and by UV spectroscopy. It was found that the additives in the tablets (avicel PH 101, aerosil, PVP K-25, talc and magnesium stearate) practically do not interfere in the determination of the substance by the proposed method. From the table is seen that the anodic polarographic method is good reproductibility. The detection limit of the method is about 5.10^{-6}M. We should also note that in this method the hazardous to health mercury usually applied in polarography is not used. By the proposed method Etamcylate can be determined directly — no additional procedures such as extraction, filtration, pretreatment of the SRE or pur-

ging with inert gas are necessary. It makes the method suitable for serial determinations.

Table 1

Precision data for the determination of Etamcylate in tablets by anodic polarography using SRE and UV spectroscopy

Method	*Quantity found for a tablet, mg*	*SD**, mg	RSD, %	Confidence limits**
Polarography	248,3	2,92	1,18	248,3±3,13
UV spectroscopy	243,9	6,41	2,63	243,9±6,88

* For five determinations
** Probability level = 0,95
N.B. A tablet was stated to contain 250,0 mg Etamcylate.

REFERENCES

1. NEGRITESCU S., BELU D., DRĂGOI R., SISMAN E., COSMIN A., CANDIDATU A., GREGORESCU D. — *Rev. Chim. (Bucharest)*, 1979, *30*, 912.
2. JANWEN MA, LIU YUPO, YAOWU — *Fenxi Zazhi*, 1984, 4(4), 209.
3. NONINSKI V. C., SOBOWALE E. B. — *Farmacia (Sofia)*, in press.
4. MEIER E. P., CHAMBERS J. D., CHAMBERS C. A., EGGINS B. R., LIAO C. S. — *J. Electroanal Chem.*, 1971, *33*, 409.
5. BAILEY S. I., RITCHIE I. M. — *Electrochem. Acta*, 1985, *30*, 3.
6. SASAKI K., TAKEHIRA K., SHIBA H. — *Electrochem. Acta*, 1968, *13*, 1 623.

Articol intrat în redacție la 21.X.1985

Indicele de clasificare : 615.778.474—017.715 :545.33

РЕЗЮМЕ

В. К. Нонински, Е. Б. Собозале, Л. А. Дрянovска-Нонинска — ПОЛАРОГРАФИЧЕСКОЕ АНОДНОЕ ОПРЕДЕЛЕНИЕ ЭТАМЕЙЛАТА (ДИЦИНОН) С ПОМОШЬЮ САМООЧИЩАЮЩЕГОСЯ ВРАЩАЮЩЕГОСЯ ЭЛЕКТРОДА (SRE)

Сообщаются результаты в связи с анодным образом действия 2,5 дигидроксибензенсульфонового диэтиламина, т.е. кислоты известной под наименованием Этамцилата или Дицинона, при помощи золотого вращающегося и самоочищающегося электрода (*gold self- cleaning rotating electrode SRE*).

На анодной полярограмме этого вещества было отмечено наличие двух извилин. Метод может быть использован в аналитических целях.

REZUMAT

V. C. Noninski, E. B. Sobowale, L. A. Dryanovska-Noninska — DETERMINAREA ANODICĂ POLAROGRAFICĂ A ETAMCYLATE-ULUI (DICYNONE) CU AJUTORUL ELECTRODULUI ROTATIV AUTOPURIFICATOR — *SELF-CLEANING ROTATING ELECTRODE (SRE)*

Sînt prezentate rezultatele asupra comportării anodice a diethylaminei 2,5-dihidroxybenzensulfonic, acid cunoscut ca Etamcylat sau Dicynone cu electrod de aur rotativ autopurificator (*gold self-cleaning rotating electrode — SRE*).

S-au observat două ondulații pe polarograma anodică a acestei substanțe care poate fi aplicată în scop analitic.

АНОДНО ПОЛЯРОГРАФСКО ИЗСЛЕДВАНЕ НА МОРФИН С ПОМОЩТА НА САМОПОЧИСТВАЩ СЕ РОТИРАЩ ЕЛЕКТРОД

В. Нонински, Е. Собовале

Висш химико-технологичен институт — София
ВМИ — София, Фармацевтичен факултет, Катедра по фармацевтична химия
ръководител проф. Л. Дряновска-Нонинска

Полярографският метод се използва за определяне на морфин, като се редуцира неговото нитрозопроизводно (1, 3). Правени са опити за анодно определяне на морфин върху твърди електроди, при което се извършва окислителна димеризация на морфина (4, 5). По време на окислението електродът от твърд метал изменя свойствата си и се получават невъзпроизводими поляро-

графски вълни, което налага преди всяко определяне специално да се почисти електродът. Това затруднява и забавя произвеждането на анализа.

Целта на настоящата работа бе да се проучат възможностите за директно определяне на морфин в анодната област от потенциала, като се използва самопочистващ се ротиращ електрод (2), характеризиращ се с това, че по време на работата границата електрод—разтвор непрекъснато се подновява и по такъв начин се осигурява възпроизводимост на резултатите и възможност за бързи серийни определяния.

Експериментална част

В настоящата работа самопочистващият се ротиращ електрод имаше конусна форма. Той може да бъде и дисков (2). Дисковият електрод всъщност е конусен, но с ъгъл при върха на конуса 180°. Прилагането на конус с ъгъл при върха, по-малък от 180°, какъвто е нашият случай, има редица предимства: подобрява се подновяването поради специалната конструкция на острилката, избягват се утечките под изолацията на страничната цилиндрична повърхност, както и страничното биене на електрода, тъй като острилката играе ролята и на плъзгащ лагер и т. н. С използването на самоочистващия се ротиращ електрод е възможно спазване на строго определени дифузионни, хидродинамични и други условия, което осигурява получаването на възпроизводими резултати в полярографията.

Всички поляризационни криви бяха снети, като електродният потенциал се измерваше спрямо наситен каломелов електрод.

Като противоелектрод беше използвана платинена жица с голяма повърхност (около два порядъка по-голяма в сравнение с повърхността на работния електрод).

Част от изследванията бяха проведени в електрохимична клетка от стъкло, при която сравнителният електрод се монтира посредством шлифт странично на работния самопочистващ се ротиращ електрод, за да се осигури минимално разстояние между лугиновата капиляра и повърхността на самопочистващия се ротиращ електрод. В същото отделение беше монтиран (също с помощта на шлиф) и спомагателният електрод. Бяха проведени експерименти и в обикновена отворена лабораторна чаша от 50 ml, в която бяха поставени работният самопочистващ се ротиращ електрод, сравнителният електрод и противоелектродът. Нашите изследвания показаха, че за целите на настоящата работа и особено за аналитични определения последната клетка дава напълно задоволителни резултати.

Анодните потенциали бяха задавани с помощта на потенциостат-галваностата „Radelkis"—ОН-405. Скоростта на разгъването на потенциала беше 10 mV/s. Полярографските вълни бяха регистрирани с помощта на Х-У записвач „Philips" PM 8120. Полярограмите бяха снемани при стайна температура.

Използваните химикали бяха квалификация ч. з. а. морфин HCl . $3H_2O$ и кодеин $1H_2O$ — производство на Химико-фармацевтичния завод — София, а папаверин HCl и наркотин — производство на „Мерк". Разтворите бяха приготвяни с дестилирана вода.

Като фон бяха използвани 0,01 М сярна, фосфорна и перхлорна киселина, 2 М натриева основа, 0,5 М калиев нитрат, 1 М амониев нитрат, натриев сулфат, както и Бритън—Робинзонови буферни разтвори.

Полярограмите се снимаха, като се започваше с потенциал 0,0 V. Представените полярограми са от 0,4 V за прегледност.

Зависимостта на $E_{1/2}$ от pH определяхме, като започвахме от ниските стойности на pH, които се увеличаваха с добавяне на 2 M натриева основа.

Кулонометричните изследвания бяха проведени по следния начин. Найнапред се снемаше полярограма на морфин с определена концентрация в разтвор на Британ—Робинзонов буфер (pH=2). След това на работния електрод се подаваше потенциал, съответстващ на платото на поляризационната крива.

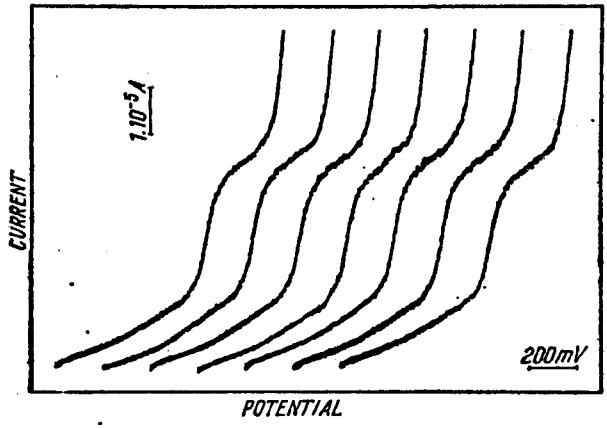

Фиг. 1

Протичащият през електрода ток беше регистриран във времето с помощта на X-Y записвач. След интегриране на площта под регистрираната крива ток-време се изчисляваше количеството електричество, протекло през клетката. В края на опита се снемаше полярограма, от която се съдеше за намалението на концентрацията на деполяризатора вследствие на електролизата (с продължителност около 20 min).

Резултати и обсъждане

На фиг. 1 са представени полярографски вълни на морфин с $1{,}9 . 10^{-4}$ M концентрация, снети една след друга с помощта на самопочистващ се ротиращ електрод в 0,01 M сярна киселина. Показваме един пример за високата възпроизводимост на резултатите от нашите изследвания.

Добрата форма и възпроизводимостта на вълните ни дадоха основание да наречем метода с използване на самопочистващ се ротиращ електрод полярография за разлика от обикновено прилагания в такива случаи за твърди електроди термин волтаметрия или волтамперометрия.

На фиг. 2 са показани някои от получените вълни на морфин в 0,01 M сярна киселина (от концентрация $4{,}9 . 10^{-4}$ до $1{,}3 . 10^{-3}$M) при една и съща скорост на въртене на самопочистващ се ротиращ електрод. Нашите изследвания показаха, че линейната зависимост между концентрацията на морфина и височината на вълната се наблюдава в областта на концентрации от $4 . 10^{-6}$

до 1.10^{-3} М. На фиг. 3 е показана стандартната права на морфина. На нея са представени стойностите на височината на вълната при относително по-високите концентрации, но същата права е валидна и за най-ниските концентрации. Същата линейна зависимост бе установена при стандартните прави, снети и в останалите фонови електролити.

На фиг. 2 може да се види, че с увеличаване на концентрацията на морфина $E_{1/2}$ се изменя към по-положителни стойности. Така например при концентрация 4.10^{-6} М $E_{1/2}$=0,580 V, а при $1{,}1.10^{-3}$ М той вече е 0,695 V. По-

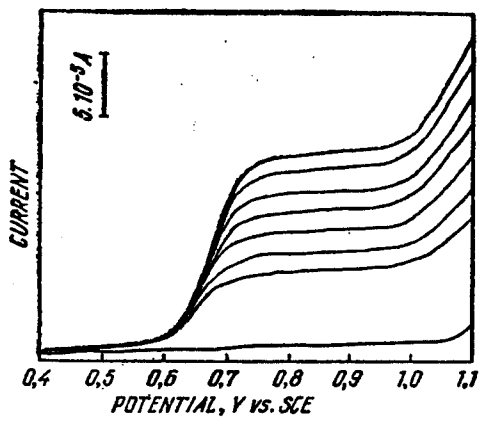

Фиг. 2

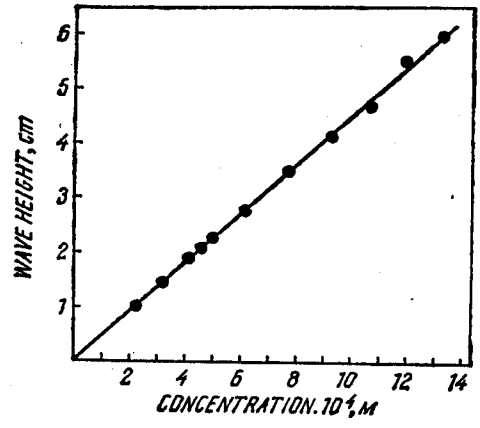

Фиг. 3

положителен с около 0,020 V (за областта от концентрации от порядъка на 10^{-4} М) става $E_{1/2}$, когато оборотите се увеличат от 10 до 50 Hz. Подобно отместване на потенциала на полувълната се наблюдава и в останалите фонове. Отместването към по-положителни стойности на $E_{1/2}$ на морфина с увеличаване на неговата концентрация установихме и при други твърди електроди в публикациите (4, 5), но авторите на тези работи не са обърнали внимание на този факт.

Беше изследвана зависимостта на пределния дифузионен ток от квадратния корен от броя на оборотите за единица време в 15 разтвора с различни концентрации на морфин от порядъка на 10^{-4} М и се установи, че във всички случаи тя е линейна. На фиг. 4 показваме някои от получените прави. Тази зависимост показа, че получените полярограми имат чисто дифузионен характер и че самопочистващият се ротиращ електрод притежава същите свойства по отношение на дифузията, каквито има ротиращият дисков електрод.

Беше изучена също зависимостта на височината на вълната и $E_{1/2}$ на морфина от pH. С увеличаване на pH височината на вълната се намалява, което води до намаляване на точността на определенията. За увеличаване на точността при ниските pH стойности допринася по-доброто оформяне на вълните в сравнение с това при по-високите pH. На фиг. 5 е представена зависимостта на $E_{1/2}$ от pH при една и съща концентрация на морфин. При преминаване към алкалната област от pH (от около pH=6,8) се получава раздвояване на вълната. При увеличаване на концентрацията на морфина се увеличава височината само на първата вълна и тя би могла да се използва за аналитични цели. При още по-високи стойности на pH (над pH=8,5) втората вълна, отго-

варяща на по-положителни потенциали, изчезва. Следователно аналитичното определяне на морфин е възможно във всички области на pH, но за практически цели е за предпочитане определянето да се извършва в област с ниски стойности на pH.

Както се вижда от фиг. 5, $E_{1/2}$—pH зависимостта до pH=10 се състои

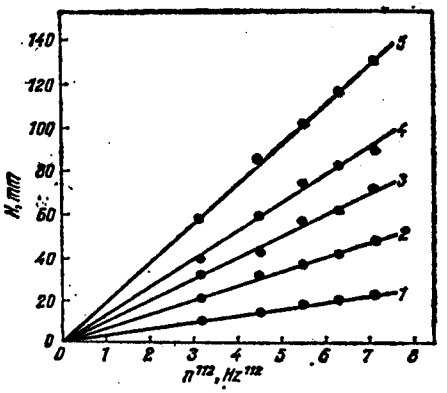

Фиг. 4

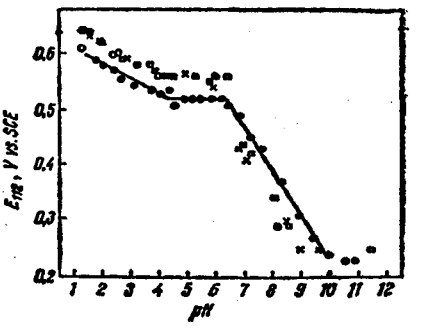

Фиг. 5

от три линейни части. Първата права има наклон 0,026 V/pH. При pH=4,3 тя пресича линията, показваща успоредна на абсцисата, която продължава до pH =6,3. След тази pH стойност $E_{1/2}$—pH зависимостта има наклон 0,80 V/pH. От кулонометричните изследвания беше намерено, че в кисела среда при pH=2 при окислението на морфина участва един електрон. Едноелектронното окисление на морфина се потвърждава и от анализа на наклона на полярографската вълна. Ако вземем предвид този факт, за броя на протоните, участващи в окислението до pH=4,3, се получава число, което е по-малко от 1. Това вероятно е указание за необратимия характер на получените полярографски вълни. От pH=4,3 до pH=6,3 протони не участват в окислението, защото $E_{1/2}$ не зависи от pH. От pH=6,3 до pH=10 наклонът на линейната зависимост е 0,080 V/pH. Ако приемем едноелектронно окисление, за броя на протоните се получава 1,35 (това число може да се апроксимира до 1). След pH=10 $E_{1/2}$ на морфина също не изглежда да зависи от pH. Ходът на $E_{1/2}$ зависимостта, снета в Британ—Робинзонов буфер, разгледан в статията, се потвърждава също от отдел експерименти в други фонове електролити (HNO_3, H_2SO_4) при различни концентрации на морфина. Ходът на зависимостта $E_{1/2}$—pH е все още без обяснение и по-специално съществуването на област от pH, където при окислението на морфин не вземат участие протони. Тя се намира между две други pH области, при които в окислението вземат участие протони.

Бяха проведени изследвания от алкалоидите кодеин, папаверин и наркотин при същите условия на анодно определяне на морфин. И при трите алкалоида, при които фенолната група не е свободна, се получиха вълни с много висок потенциал на полувълната (над 1000 V). В настоящата работа няма да разглеждаме подробно тези вълни. Изследвано бе влиянието на кодеин, папаверин и наркотин върху полярографската вълна на морфина. Резултатите показаха, че кодеинът не влияе върху височината на вълната на морфина, даже и при

високи негови концентрации (сравними с тези на наличния в разтвора морфин). При такива концентрации кодеинът отмества потенциала на полувълната на морфина към по-положителни стойности (с около 0,050 V). Подобно на кодеина влияе и наркотинът. Папаверинът в малки количества (в каквито той се съдържа в опиума) също не влияе върху височината на вълната на морфина, но силно отмества $E_{1/2}$ към по-положителни стойности. При по-високи концентрации той силно видоизменя вълната на морфина, а при сравними концентрации с тези на морфина може да я потисне. Тези изследвания показват, че окислението на морфин се извършва с участието на свободната фенолна група.

Книгопис. 1. Нонински, Хр., Л. Дряновска-Нонинска, Л. Ст. Илиев. *Фармация*, 19, 1969, 24. — 2. Нонински, Хр. *Химия и индустрия*, 10, 1966, 443 — 3. Baggesgaard, H. C. Kasmussen. *Halm. Jlerk Dansk Tidssks, Farm.*, 19, 1955, 41. — 4. Devs, H. P. *Pharm Weekblad*, 99, 1964, 737. — 5. Rashid, A., R. Kalvoda. *Cesk farm.*, 20, 1971, 143.

В. Нонински, Е. Собовале — **Анодное полярографическое исследование морфина при помощи самоочищающегося ротирующего электрода (СРЭ)**

Резюме. Предложенный полярографический метод непосредственного определения морфина в анодной области потенциалов при помощи самоочищающегося ротирующего электрода имеет ряд преимуществ в сравнении с существующими подобными методами с применением твердых электродов. Впервые установлена хорошая воспроизводимость полярографической волны при электроокислении органического соединения в анодной области с твердыми электродами. Определение морфина проводится в более широких границах концентраций и при более высокой чувствительности. Метод легко выполним и быстрый, обеспечивает непрерывность при проведении серийных анализов.

Noninski, V., E. Sobovale — **Anode Polarographic Investigation of Morphine with the Help of Selfcleaning Rotating Electrode**

Summary. A polarographic method for direct determination of morphine in anode region of potentials with the help of selfcleaning rotating electrode is proposed. It has many advantages in comparison with the same methods with solid electrodes. Good reproducibility is obtained for the first time of the polarographic wave on electrooxidation of organic compounds in the anode region with solid electrodes. Determination of morphine is carried out in wider concentration limites and at higher sensitivity. The method is prompt and ensures continuous process which is suitable for serial analysis.

Фармац., XXXV, 1985, 4
Farmac., XXXV, 1985, 4

Постъпила — май 1985
Received — May 1985

Journal of Scientific Exploration, Vol. 9, No. 2, pp. 201–206, 1995 0892-3310/95

Experiments on a Possible γ-Ray Emission Caused by a Chemical Process

V. C. NONINSKI, J. L. CIOTTONE, P. J. WHITE

Fitchburg State College, Department of Chemistry, Fitchburg, MA 01420

Abstract — We report here results from Geiger-Mueller and NaI(Tl) γ-ray counting of a mixture of several chemicals before and after burning compared with a control sample of KNO_3. The experimental results did not show non-trivial increase in γ-emissions after burning of the mixture.

Introduction

Enhancement in the low-energy end of the γ-ray spectrum incited by non-nuclear processes is increasingly being reported. Probably one of the first to report such non-trivial low energy γ-ray emissions was Matsumoto (1990). Unfortunately, in addition to the experimental results he has presented an obviously untenable theoretical explanation of three-body collision of deuterons and protons. He has also misinterpreted the $^{208}_{81}$Tl (2.615 MeV) peak, interpreting it incorrectly as a $^{208}_{83}$Bi (2.615 MeV) peak. Other groups also report low-energy (Karabut *et al.*, 1992; Scott *et al*, 1990; Takahashi, 1990) and high-energy (Prelas *et al.*, 1990) γ-ray emissions induced in an unexpected way. Recently Bockris and collaborators reported unexpected effects during burning of a mixture of chemicals. Bockris and colleagues' reports caused a certain controversy (cf. Bishop, 1993) and some further scientific inquiry into the problem is warranted. In this paper we present some experimental results with regard to the claimed increased γ-ray emission as a results of a chemical process. No experiments were carried out concerning other claimed effects (Bishop, 1993; Sundarasan & Bockris, 1994) in this system.

Experiments

The experiment was carried out by mixing of 300 g C, 900 g KNO_3, 80 g S, 120 g SiO_2, 100 g $FeSO_4$, 30 g Cd, 100 g Hg_2Cl_2, 50 g PbO, 5 g Ag and 30 g CaO. The resulting mixture was burned in a hood. We performed five burns, four of which were successfully completed (burn #2 contained approximately one-half the amount of KNO_3 resulting in very slow burning and was discarded). The burning was vigorous and lasted from about 30 s (burn #1) to about 3 min (burn #3). After burning was complete and the sample was cooled down, random samples were taken from the bulk and were ground in a mortar with a

pestle. The initial experiments were carried out by transferring the sample into a crucible. To ensure that the configuration (area, thickness, and geometry) of sample viewed by the detector was the same for all samples, the same size crucible was used, and care was taken to level each sample in the same way. The crucible was then inserted under the active window (≈1 cm diameter) of a Radalert Geiger-Mueller counter. The Radalert was connected to a laptop IBM PC, where a special program was written to monitor the counts every minute throughout many hours. In the initial experiments the Geiger-Mueller counter was surrounded by a 0.2 cm lead shield. Later, in addition to the Geiger-Mueller counter a NaI(Tl) scintillation detector (3 cm x 3 cm) was set up. The sample, prepared according to the above procedure, was transferred into a watch-glass, levelled using a piece of glass and inserted into the gap below a NaI(Tl) scintillation detector. The configuration (area and thickness geometry) of the sample in this case was also the same for all samples used; the watch-glass was the same throughout. The detector and the sample were surrounded by 5 cm thick lead bricks. The detector was connected to a Model 35 Canberra Multichannel Spectrum Analyzer. In all experiments measures were taken to maintain the same counting geometries. The obtained spectra were dumped through the serial port of an IBM PC, where they were observed and analyzed using MathCad 5.0. Besides the natural calibration of the NaI(Tl) detector system by the prominent $^{40}_{19}$K line appearing at 1.460 MeV in the background and the 0.511 MeV e^+-e^- annihilation γ-ray, we also calibrated the system using $^{60}_{27}$Co (1.33 MeV and 1.17 MeV) and $^{22}_{11}$Na (0.511 and 1.274 MeV) sources. Although a Ge(Li) detector would have given better resolution, we believe that the NaI(Tl) detector available in our laboratory should be considered capable of giving reliable results.

Experimental Results

The typical Geiger-Mueller count rate per minute of the sample before burning was 19.07 ± 0.86 over a 24-h period. This was clearly lower than that after burning which was 24.64 ± 0.43. The control sample, KNO_3, exhibited 22.85 ± 0.32 counts per minute. It is to be noted that these determinations were carried out on random days during February and March, 1994, thus influences of cosmic events on the results were expected to be excluded. The increase in counting rate after burning provoked our interest and we continued our studies with a NaI(Tl) detector.

In Figure 1 we show the background taken for 12 hours starting on March 13, 1994 at 11:32 am (curve 1). In the background trace the prominent $^{40}_{19}$K peak at 1.460 MeV, the e^+-e^- annihilation peak at 0.511 MeV, the $^{214}_{83}$Bi at 1.12 MeV, the smaller peaks of $^{214}_{83}$Bi at 1.764 MeV, $^{214}_{83}$Bi at 2.117 MeV, and $^{208}_{81}$Tl at 2.615 MeV are observed. In Figure 1 the γ-ray spectrum from the sample before burning (curve 2), after burning (curve 3), and the control KNO_3 sample (curve 4) are also shown.

Figure 1 shows that the background counts at all energies are lower than the

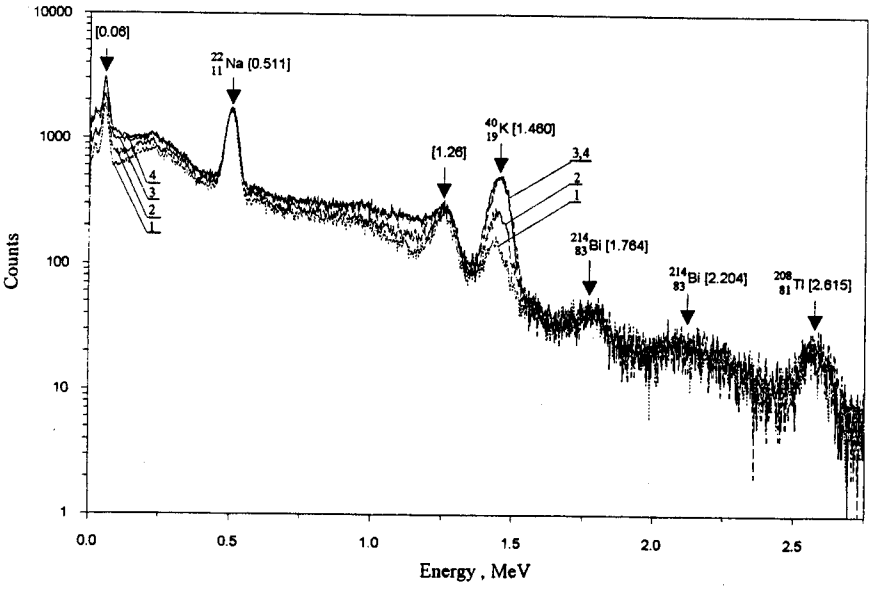

Fig. 1. The γ-ray spectrum measured with a 3 cm x 3 cm NaI(Tl) detector. Curve 1 — background, curve 2 — mixture before burning, curve 3 — mixture after burning, curve 4 — pure KNO_3.

counts of the studied samples. Even the mixture before burning (curve 2) shows higher counts vs. background, especially at energies corresponding to the $^{40}_{19}$K peak and the low-energy γ-ray peak (0.06 MeV). This fact, however, is easily explainable by the higher concentration of $^{40}_{19}$K in the mixture. As expected from the results of the preliminary Geiger-Mueller experiments, the curve corresponding to the sample after burning (curve 3) lies at still higher counts at almost all energies compared to background and the mixture before burning. Practically no change is observed for the e^+-e^- γ-ray annihilation peak at 0.511 MeV and for energies higher than that of $^{40}_{19}$K peak. The higher counts for the mixture after burning were confirmed during several independent trials. We believe that the obtained data (of which Figure 1 is only one example) contains a statistically significant number of counts for this difference to be considered real.

Discussion

In order to explain the above increase in the γ-ray emission after burning of the sample, we carried out some additional experiments. For clarification, standard isotope data references were used to determine if any significant

decay of the observed γ-ray peaks would occur (Walker *et al.*, 1989). The NaI(Tl) detector was mounted vertically inside the lead-brick housing and a weighed amount of the burned sample #5 (several hours after the burn) was placed directly on top of the detector. The sample was monitored during the course of one month. No decay was observed during the period of study which indicates that no radioactive isotopes of short lifetime were created during the burn of the sample.

Of all the elements initially present in our mixture K is the most important since it has a naturally occurring radioactive isotope ($^{40}_{19}$K) with a long half-life. Other elements that have naturally occurring radioactive isotopes are $^{199}_{80}$Hg (16.9%), $^{204}_{82}$Pb (1.4%), $^{207}_{82}$Pb (22.1%), $^{107}_{47}$Ag (51.8%), $^{109}_{47}$Ag (48.1%), $^{111}_{48}$Cd (12.8%, half-life 48.5 min) (Walker *et al.*, 1989). These elements have isomeric transitions (states) which usually decay through γ-emissions but $^{107}_{47}$Ag and $^{109}_{47}$Ag decay by β^-. The half-life of $^{199}_{80}$Hg is 42.6 min, $^{207}_{82}$Pb is 0.8 s, $^{204}_{82}$Pb is 1.12 hours, $^{107}_{47}$Ag is 44.2 s, $^{109}_{47}$Ag is 39.8 s (Walker *et al.*, 1989). Isotopes with even numbers of neutrons may decay through β^- to $^{17}_{8}$O and neutrons (delayed neutrons) are emitted with a half-life of 4.17 s. Thus, the short half-lives of the naturally occurring isotopes of elements other than $^{40}_{19}$K cannot account for the observed effect. Therefore, we focused our attention on the concentration of K in the samples. As is already observed from Figure 1 an enhancement of the intensities of all peaks is seen after burning of the mixture. This, however, is a trivial effect due to concentrating the amount of available K (resp. $^{40}_{19}$K). Increase of K concentration was independently confirmed by atomic absorption analysis using Perkin-Elmer 3100 Atomic Absorption Spectrometer (AAS). One gram of the mixture before and after burning was dissolved in 50 ml HNO_3, and the solution was diluted to 1 l. Of these, 5 ml were diluted to 50 ml, and the absorbances of the diluted solutions were determined using AAS with a K lamp at λ=766.5 nm. For our purposes it was sufficient to just compare the AAS absorbance signals rather than to determine the exact concentrations of the two studied samples. Since, as mentioned, it was 1 g of each sample that was used for the AAS determinations, a difference in density of the two studied samples might have resulted in differences in K concentrations due to differences in volumes of samples. The increase in K concentration was not due to differences in sample density, because the density of the burned sample was at least of the same order of magnitude as that of the mixture before burning. We have noticed, however, that during weighing of the burned sample constant weight was not able to be reached, because of a certain hygroscopicity of the burned sample. Obviously, the mentioned difficulty due to hygroscopicity even further enhances the conclusion that the increased γ-ray emission signal is due to increased K concentration in the burned sample.

In another experiment designed to explain the above effect, the γ-ray spectrum of pure KNO_3 was taken under the same conditions as used for previous experiments. Figure 1 (curve 4) shows the γ-rays from this experiment. Comparison of curve 3 and 4 shows that there is practically no difference between

these curves. It was also determined that the density of the ash was slightly lower than the density of the KNO_3 by weighing equal volumes of these substances on a five-place electronic balance. It was determined by AAS that the concentration of K was practically the same both in the ash and in the pure KNO_3.

Conclusions

The above experimental results provide no basis to conclude that any unexpected effects, such as appearance of radioactive isotopes not present initially, are occurring due to a chemical process (burning of the sample).

Although we did not observe non-trivial effects during the present studies there are several conclusions which we were able to draw. First, we now understand that the results are very reproducible. The methods we apply are sensitive enough for the purpose and we would have been able to observe effects should there have been such. Secondly, we do not exclude the possibility that we have overlooked some hidden effects since we were looking for the broad picture of the events. Also, there may be some intricacies, unknown to us, for preparation of the samples which may cause positive results to appear. We also note that such claimed effects should be resolved only experimentally and no theoretical arguments should supercede or prevent the carrying out of experiments. Theoretical arguments should in general be used as mere guidelines and should be suspended once effects contrary to theoretical expectations are observed. This is not unusual in science. In this respect even experiments such as the above, the negative outcome of which can be predicted based on contemporary knowledge, are worth carrying out because the boundaries of those parts of contemporary knowledge that constitute absolute truths are not always clear cut.

Acknowledgement

The authors would like to thank the three reviewers for their valuable comments.

Email addresses of the authors:
V. C. Noninski: vnoninski@fscvax.fsc.mass.edu
J. L. Ciottone: ciottone@fscvax.fsc.mass.edu
P. J. White: pwhite@fscvax.fsc.mass.edu

References

Bishop, J. E. (1993). Alchemists ancient dreams hover over 'cold fusion' parley in Maui. *Wall Street Journal*, December 10, p. B5.

Karabut, A. B. and Ya. R. Kucherov, I. B. Savvatimova (1992). Nuclear product ratio for glow discharge in Deuterium. *Physics Letters*, A 170, 265.

Lin, G. H. and R. Bhardwaj and J. O'M. Bockris (1995). Observation of β radiation decay in low energy nuclear reaction. *Journal of Scientific Exploration*, 9, 2.

Matsumoto, T. (1990). Cold fusion observed with ordinary water. *Fusion Technology*, 17, 490.

Prelas, M. and F. Boody, W. Gallaher, E. Leal-Quiros, D. Mencin, S. Taylor (1990). Cold fusion experiments using Maxwellian plasmas and sub-atmospheric deuterium gas. *J. Fusion Energy*, 911, 309.

Scott, Charles D. and J. E. Mrochek, T. C. Scott, G. E. Michaels, E. Newman and Milicia Petek (1990). Measurement of excess heat and apparent coincident increases in the neutron and gamma-ray count rates during the electrolysis of heavy water. *Fusion Technology*, 18, 103.

Sundarasan, R., J. O'M Bockris (1994). Anomalous reactions during arcing between carbon rods in water. *Fusion Technology*, 26, 261.

Takahashi, A. (1990). Neutron Spectra from D_{20} Pd Cells and Possibility of Multi-Body Fusion, lecture presented at National Cold Fusion Institute on September 10, 1990.

Walker, F. W., Parrington, J. R., and Feiner, F. (1989). *Nuclides and Isotopes*. 14th Edition. San Jose: General Electric Co.

Journal of Scientific Exploration, Vol. 9, No. 3, pp. 317–321, 1995 0892-3310/95

Experiments on Claimed β-Particle Emission Decay

V. C. NONINSKI, J. L. CIOTTONE, AND P. J. WHITE

Fitchburg State College, Dept. of Chemistry, Fitchburg, Massachusetts, 01420-2697

Abstract — In a previous paper (Noninski, 1995) we reported comparative results of γ-ray measurements before and after burning of a mixture of chemicals. Increase of γ-ray activity after burning was claimed by some colleagues to be an indication of the fact that certain nuclear processes can be induced simply by carrying out chemical reactions. Although we observed an increase in the γ-ray counts after burning of the sample, we concluded that the reasons for this increase are trivial and are due to concentrating, as a result of burning, of the naturally occurring isotopes of some elements, especially ^{40}K. We noted, however, that there may be certain conditions, unknown to us, which may bring about the purported changes of nuclear character due simply to chemical reactions. In follow-up of our manuscript, (Lin, 1995), presented data of β-particle decay when using a mixture whose composition includes fewer chemicals than those in the mixture studied by us. Also, the amounts of the various ingredients in the mixture differed from those used in (Noninski). We carried out a series of measurements of the β-particle emission activity with this new recipe and are reporting the results from these studies in the present communication.

Experimental

Nine separate burns were carried out. The composition of the mixture used was: C – 100 g, Johnson Matthey, Carbon Graphite Powder, 300 mesh, 99.0%; KNO_3 – 300 g, Fisher, ACS grade Mallinckrodt; S – 30 g, Johnson Matthey, Sulfur Powder, Sublimed USP; SiO_2 – 30 g, Fluka, Seesand, 40-200 mesh, acid purified; FeS – 40 g, unknown origin, granular; Hg_2Cl_2 – 10 g, Merck, USP; PbO – 10 g, Fisher certified lead monoxide. All chemicals are from the stockroom of the department.

For measurement of the β-particle emission activity a Ludlum 44-1 Beta Survey Detector consisting of a plastic scintillator of 0.010 thickness with 11.6 cm^2 window area was used. The window was covered by 0.8 mg/cm^2 metalized mylar for light tightness. The plastic scintillator (crystal itself), 1 inch in diameter, was NE102. The operating range/efficiency is from C^{14}/15% to P^{32}/60%. The PM tube used was the 10 stage head-on type. The detector was attached to a Ludlum Model 2200 Scaler Ratemeter whose settings were as follow: Window 3.02; Threshold 6.0; Range x1k; set for 60 min intervals; meter readings 200 cpm; Window ON. The ratemeter was typically set to acquire counts in the course of one hour. The number of counts acquired for one hour (from burn 4 on) were dumped into the memory of a computer through a

serial port. A larger paint pail (leaktite paint pot #5) from HQ was used as a vessel. As also required by the recipe, two 6 inch galvanized framing nails were placed in the reaction vessel. Counting was carried out by placing the detector-sample combination in a dark space. Initially the detector and the sample were placed simply in a bench cabinet. The room background count was approximately 8 cpm. Later a specially prepared wooden enclosure was used. In the latter configuration sample and detector were placed in the box which was covered with lead sheets. The sample was placed in a 50 ml beaker and the detector was suspended at about 5 mm from the surface of the sample. Experiments with and without dessicant in the enclosed space were carried out. Finally the sample and detector were placed in a glass vessel painted black on the outside. The cover of this vessel had provisions for maintaining vacuum conditions (~30 inch underpressure) internally — Figure 1.

Simultaneous temperature measurements within the sample were also carried out with some experiments. A thermistor in a glass tube was placed within the sample and resistance readings determined by a Fluke 8840A DMM were averaged over an hour and dumped through a GPIB (IEEE-488) bus into the memory of a computer.

One of the samples after burning was brought to MIT on the same day of the burn for observation of the γ-emission spectrum. The Ge(Li) detector showed an overwhelming signal of ^{40}K in the sample and it was found that further studies are necessary if one is to use a Ge(Li) detector to determine whether any unusual nuclear events have occurred due to burning.

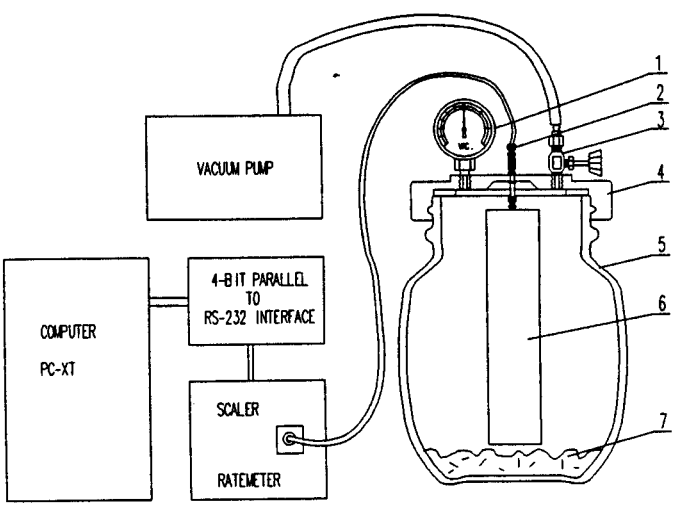

Fig. 1. Schematic diagram of the vacuum β-counting system. 1 — vacuum gauge, 2 — BNC feed through connector, 3 — valve, 4 — aluminum lid, 5 — glass vessel externally painted black, 6 — Ludlum 44-1 Beta Survey Detector, 7 — sample.

Neutron activation analysis of samples before and after burning was performed and a comparison was made of the γ– spectra. The peak at 411.7 keV, originally thought to be due to ^{198}Au, was determined in reality to be the double escape peak of ^{52}V. The photopeak at 1434 keV and the single escape peak at 923 keV were also present in the spectrum. Observation of the decay rate of these peaks verified the identification. Details of these studies will be reported in a separate communication.

Discussion

In Figure 2 the β-counts as a function of time are presented of a sample prepared according to the above recipe. The β-counting of that sample was done in a manner similar to that by which the data in (Lin) were obtained. As seen from Figure 2 a decrease of the β-counts in time, similar to that reported in (Lin), is clearly observable. The question which then had to be answered is whether this decrease is due to nuclear decay or to some trivial reason. One trivial reason may be the hygroscopicity of the sample, as mentioned in our previous publication (Noninski). One of the sources of β-emission from the sample is the decay of the naturally occurring radioactive isotopes such as ^{40}K. Absorption of water vapors would be an attenuating factor for this naturally

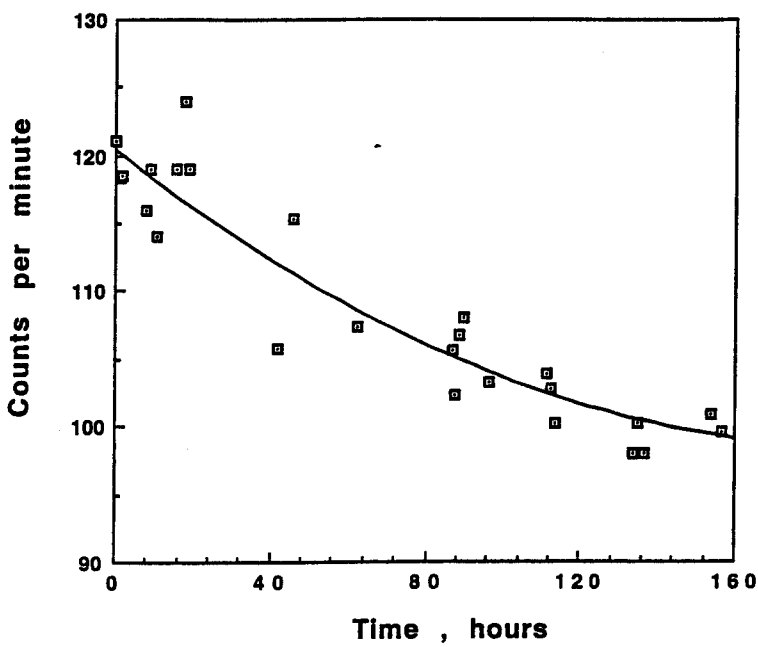

Fig. 2 Plot of β-counts vs. time of a sample after burning. The sample was prepared according to the recipe in (Lin) and counting was carried out in air. β-detector and sample were placed in a bench cabinet to avoid external light.

occurring β-emission. Thus, any decrease of β-emission activity due to such cause should be considered an artifact. Another factor which may cause attenuation is oxidation of the ashes from the burn. Instead of further exploring whether absorption of water vapors or oxidation is the trivial cause for β-emission decrease we decided to measure β-emission under conditions where any such cause would be eliminated. The measurement of β-emission activity of the burned sample was carried out in a container from which a continuous evacuation of the air was performed as described above — Figure 1. An example of the results from these measurements is shown in Figure 3. As is seen from Figure 3 no decrease of the β-counts is observed when measures are taken to avoid oxidation and/or absorption of water vapors by the sample. It was found that variations over time, if any, of the β-counts are in good concordance with room temperature changes.

We conclude from the above studies and from the studies reported in (Noninski) that at the level of accuracy of our apparatus and methods and the precision of our determinations we were not able so far to determine signatures of unusual nuclear events invoked by burning of the proposed sample.

Acknowledgements

The authors would like to thank Dr. Peter Hagelstein from Massachusetts Institute of Technology and Leo Bobek of Worcester Polytechnic Institute for providing use of their facilities and the useful discussions.

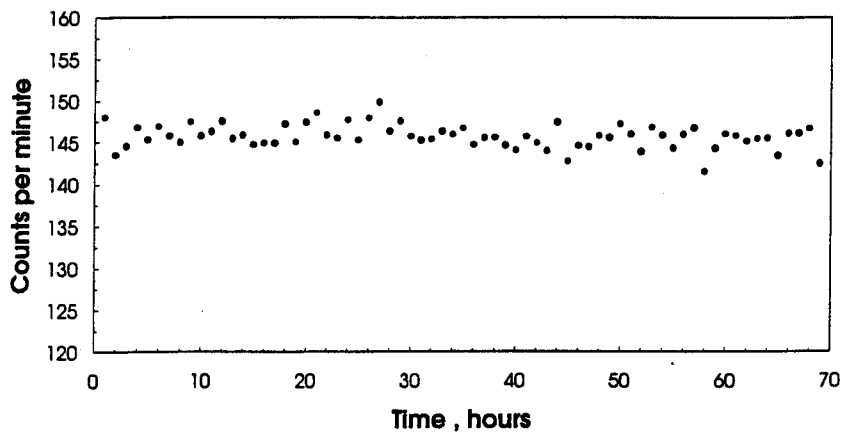

Fig. 3 Plot of β-counts vs. time of a sample after burning. The sample was prepared according to the recipe in (Lin). β-counting was carried out in the vacuum system shown in Figure 1.

Email addresses of the authors:
N. C. Noninski: vnoninski@fsc.edu
J. L. Ciottone: ciottone@fsc.edu
P. J. White: pwhite@fsc.edu

References

Noninski, V. C., Ciottone, J. L., and White, P. J. (1995). *Journal of Scientific Exploration*, 9, 201.
Lin, G. H., Bhardwaj, R., and O'M.Bockris, J. (1995). *Journal of Scientific Exploration*, 9, 207.

Journal of Scientific Exploration, Vol. 10, No. 2, pp. 249–252, 1996 0892-3310/96

Experiments on Claimed Transmutation of Elements Caused by a Chemical Process

V. C. Noninski, J. L. Ciottone and P. J. White

Fitchburg State College, Department of Chemistry, Fitchburg, MA 01420
email: ciottone@falcon.fsc.edu, pwhite@falcon.fsc.edu

Abstract — Results are presented for neutron activation analysis of a mixture of several chemicals before and after burning. The experimental results do not show any unexpected appearance of new elements after burning of the mixture.

Introduction

In a recent publication, Bockris and collaborators have reported unexpected effects during burning of a mixture of chemicals (Lin *et al.*, 1995). In this paper we present some experimental results of our studies with regard to claimed creation, as the result of a chemical process, of elements different from those initially present in the sample.

In previously published papers (Noninski *et al.*, 1995a,b), we have studied some other aspects of claimed nuclear effects due to chemical processes, such as increase of γ-ray emission after burning and β decay after burning. This communication is intended to wrap up our studies on this matter.

Experiments

Studies were carried out using two different recipes. The first mixture (A), used mainly for the determination of γ-emissions, consisted of 300g C, Cambosco; 900g KNO_3, Fisher Certified ACS grade; 80g S, Johnson Matthey, sulfur powdered, sublimed USP; 120g $Si0_2$, Fluka, Seesand, 40-200 mesh, acid purified; 100g $FeSO_4$, Fisher Certified; 30g Cd; 100g Hg_2Cl_2, Merck, USP; 50g PbO, Fisher Certified lead monoxide; 5g Ag and 30g CaO. The second mixture (B) contained fewer chemicals and lesser amounts of each. Mixture B, used primarily for β-counting and neutron-activation analysis, consisted of 100g C, Johnson Matthey, carbon graphite powder, 300 mesh, 99%; 300g KNO_3, Fisher Certified ACS grade; 30g S powder, sublimed USP; 30g $Si0_2$, Fluka, Seesand, 40-200 mesh, acid purified; 40g FeS unknown origin, granular; 10g Hg_2Cl_2, Merck USP and 10g PbO, Fisher Certified lead monoxide.

For all burns, performed in a chemical fume hood, the vessel used was a large paint pail (leaktite paint pot #5). As also required by the recipe two 6 inch galvanized framing nails were placed in the reaction vessel.

A total of 16 burns were carried out. Burn procedure is described elsewhere (Noninski *et al.*, 1995a).

Neutron activation analysis of samples, before and after burning as well as each individual chemical component of the mixture, was performed in a 10 kW open-pool reactor at Worcester Polytechnic Institute, and a comparison was made of the γ-spectra, which were obtained using a Germanium detector. The samples studied were irradiated for approximately 3 min. at 1 kW power.

Results and Discussion

The neutron activation analysis was specifically performed on burns #13 through #16 from mixture B and their γ-spectra were compared to the spectra of the same samples before burning. An amount equal to 3.6166 g of mixture B before the 13th burning was placed in a small plastic vial. The small plastic vial was then placed in a larger one, transported into the reactor core and irradiated with neutrons for 3 minutes. Similarly, 2.8855 g of the 13th burned mixture B was irradiated. After irradiation of each sample a γ-ray spectrum was recorded using a Ge detector shielded with Pb, Cd and Cu. A segment of these γ-spectra is presented in Figure 1. It is seen from Figure 1 that peaks such as the ones corresponding to, e.g. $^{144}_{58}$Ce, at 133.55 keV or $^{203}_{80}$Hg at 279.19 keV initially present in the mixture B before burning are seen to disappear in the γ-spectrum of the burned sample. Some of these disappearances can easily be explained by the fact that the high temperatures of the burn may be causing the evaporation of the respective elements. Upon careful scrutiny of the spectra one may notice appearance of small additional peaks after the burn (this part of the spectrum is not shown in Figure 1). These peaks, however, were established in the γ-spectra of the nails and the vessel after carrying out neutron activation, and therefore, should be considered trivial.

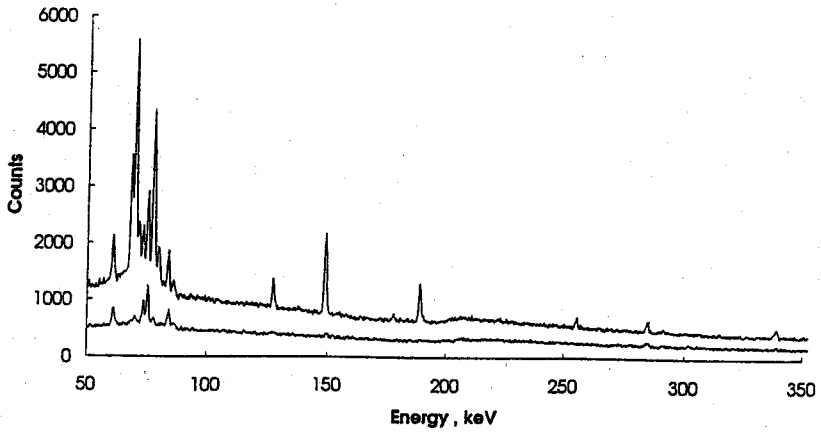

Fig. 1. Part of the γ-spectrum of irradiated mixture B before burning (Burn #8). Upper trace — before burning; lower trace — after burning.

The peak which attracts the most attention is the one at 411.70 keV which may appear to be due to the presence of $^{198}_{79}$Au. The part of the γ-spectrum containing this specific peak is presented in Figure 2. It is seen from Figure 2 that the peak which may ostensibly be due to $^{198}_{79}$Au at 411.70 keV is present almost at the same level in the burned and unburned samples. Nevertheless, calculations show that the amount of what appears to be Au in the burned sample is 3.43×10^{-5} grams of the element per gram of sample. One may speculate that because of these stated differences in the amounts of the irradiated samples it may appear that the burned sample contains an unexpected large quantity of an element showing a γ-peak at 411.70 keV. It should not be forgotten, however, that a peak at 411.70 keV was initially present in the mixture and might have been concentrated in the sample during the burn. Special efforts were applied to understand the nature of the peak at 411.70 keV. Several additional neutron-activation studies were carried out on the graphite samples used. At all times during these studies it was found that after irradiating the sample of Alfa graphite in the core of the reactor for three minutes at 1 kW power the peak at 411.70 keV was present. It turned out, however, that after leaving the sample for about an hour and recounting it this peak completely decayed. This shows that the peak in question cannot be due to $^{198}_{79}$Au since its half-life is 2.7 days. Upon careful observation of the γ-spectrum it was found that the peak at 411.7 keV is due to the second-escape peak of $^{52}_{23}$V whose photopeak is at 1434 keV and whose half-life is 5 min. This explains the disappearance of the peak at 411.70 keV in about an hour. In all samples where there was the peak at 411.70 keV the photopeak of $^{52}_{23}$V was also present (as well as the first-escape peak). In the samples where there was no photopeak at 1434 keV no peak at 411.70 keV was observed.

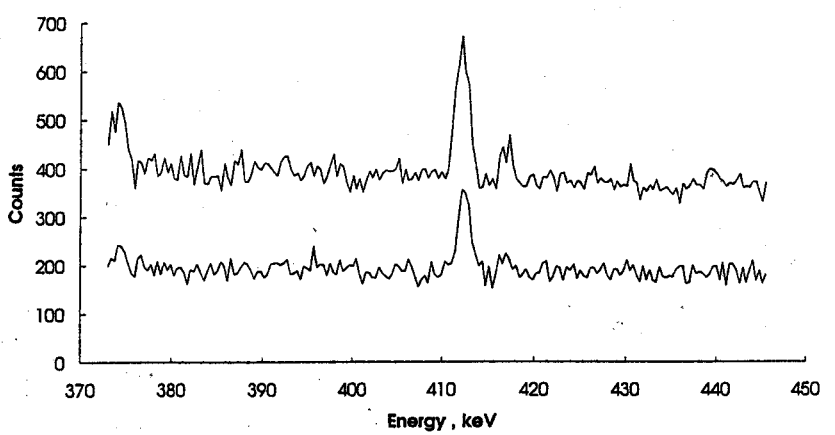

Fig. 2. Expanded region from γ-spectrum containing the 411.70 peak (Burn #8). Upper trace — mixture B before burning; lower trace — mixture B after burning.

Conclusions

We did not observe non-trivial effects during our studies such as the appearance, as a result of a chemical process, of elements different from those initially present in the sample. One may wonder what may have caused us to carry out the above studies. These problems, one may argue, have been resolved long ago. However, it is obvious from the above results that there may be cases such as the ostensible increase of the γ (Noninski *et al.*, 1995a) and the decrease of the β counts (Noninski *et al.*, 1995b) due to burning, which may tempt some to abandon these previous conclusions. If left unresolved, these effects may lead some to unsubstantiated far-reaching conclusions. This may be as much detrimental to the scientific process as the deliberate ignoring of facts, which occasionally occurs. As we mentioned previously (Noninski *et al.*, 1995a), because the boundaries of what are considered to be absolute truths in science are not always clear cut, sometimes mere theoretical arguments, based on contemporary understanding, should not be the only guiding lights in scientific research. Although rare, it is not unusual in science to find experimental facts in clear contradiction with the accepted view of nature. Therefore, we remain critically open-mined and will be happy to be shown experimental evidence contrary to what we have found.

References

Lin, G. H., Bhardwaj, R., and Bockris, J. O'M. (1995). Observation of β radiation decay in low energy nuclear reaction. *J. Scientific Exploration*, 9, 2, 207.

Noninski, V. C., Ciottone, J. L., and White, P. J. (1995a). Experiments on possible γ-ray emission caused by a chemical process. *J. Scientific Exploration*, 9, 2, 201.

Noninski, V. C., Ciottone, J. L., and White, P. J. (1995b). Experiments on claimed β-particle emission decay. *J. Scientific Exploration*, 9, 3, 317.

LETTER TO THE EDITOR

ON AN EXPERIMENTAL CURIOSITY THAT IF UNDETECTED MAY LEAD TO ERRONEOUS FAR-REACHING CONCLUSIONS

Recently, a renewed interest has been observed among some colleagues of the possibilities of inducing nuclear effects by carrying out only chemical reactions.[1] Undoubtedly, this interest is a result of the still unresolved problem of "cold fusion," and some colleagues tend to see a clear connection, and even an extension of the studies, between cold fusion and the alleged chemical transmutation of elements. While we have already published thorough reports (negative so far) of our studies with regard to the claimed increase of gamma-ray emission and beta decay after burning of a mixture of chemicals,[2,3] in this letter, we wish to inform the *Fusion Technology* readership of an experimental curiosity that we encountered during similar studies that initially led us to an erroneous conclusion. We believe that sharing this information with those interested in the question is important so that errors of a similar character are avoided, which may avert the making of unsubstantiated far-reaching conclusions.

As in the previous studies,[2,3] we compared certain radiochemical properties of a mixture of chemicals before and after a chemical reaction (burning). Under discussion here is a peak that we observed in the range of 412 keV in the gamma spectrum of one of our burned samples after neutron activating it for 3 min at 1 kW. This peak was ostensibly not present in the same sample unburned. Because $^{198}_{79}$Au has a gamma peak at approximately this energy (411.8 keV), our attention and interest increased. This finding, if true, would have meant that the mercury, which the unburned sample contained, had "transmuted" into gold, which was not initially present in the unburned sample. This further would have meant that the highly unexpected "transmutations" of this sort, claimed by others,[1] would have been confirmed.

Determination of the true nature of this peak was somewhat accidental. In a subsequent burn, we again observed the peak at 411.7 keV immediately after neutron activation. Approximately 1 h after the neutron activation, we wanted to see the peak again, but when the sample was counted at this time with a germanium detector, the peak had completely disappeared. Because the aforementioned $^{198}_{79}$Au has a half-life ($t_{1/2}$) of 2.7 days (Ref. 4), the peak seen at ~412 keV could not have been due to the presence of this element. Another exotic possibility for the peak in the range of 411 keV, formation of $^{152}_{63}$Eu, was also excluded because its $t_{1/2}$ is 13.33 yr (Ref. 4) and its photopeak lies at 411.1-keV energy, which is somewhat lower than the energy we observed. It was speculated then that the observed peak at ~412 keV could be due to a single or a double escape peak of some other element. We noted from the data in Ref. 4 that $^{52}_{23}$V [$t_{1/2}$ = 3.75 min (Ref. 4)] has a photopeak at 1434.1 keV, which would provide a double escape peak fortuitously coinciding almost exactly with the peak of gold at 411.8 keV but having a much shorter half-life. Indeed, a photopeak of $^{52}_{23}$V was found in the gamma spectra after neutron activation of both burned and unburned samples. Figures 1 and 2 present parts of the gamma spectrum containing the photopeak and the second escape peak of $^{52}_{23}$V decaying in time.

To verify further the foregoing conclusion, we again neutron activated the samples before burning and determined that in the gamma spectrum taken immediately after irradiation, all three peaks (photopeak at 1434.1 keV, single escape peak at 923.1 keV, and double escape peak at 412.1 keV) due to vanadium were indeed present. Some 15 min after the irradiation, the peaks disappeared. In this way, our initial observation of the "unusual" event found its explanation. After the unburned sample had been neutron activated, obviously we inadvertently delayed the taking of its gamma spectrum, and the double escape peak had decayed; this led us to the erroneous conclusion that no peak in the range of 412 keV had ever existed in the unburned sample. Conversely, we accidentally took the gamma spectrum of the burned sample right after its neutron activation; this did not give enough time for the peak at ~412 keV to decay. We noticed this peak, and erroneously concluded that the appearance of a peak at 412 keV, fortuitously coinciding almost exactly with the value of the $^{198}_{79}$Au peak, was due to burning of the sample.

We encourage all our colleagues who have done neutron activation of such samples and claim to have seen similar transmutations, but still claim their reality, to check again their gamma spectra and note whether their findings can have a trivial explanation similar to ours.

Vesselin C. Noninski
Judith L. Ciottone
Paul J. White

Fitchburg State College
Department of Chemistry
Fitchburg, Massachusetts 01420

February 12, 1996

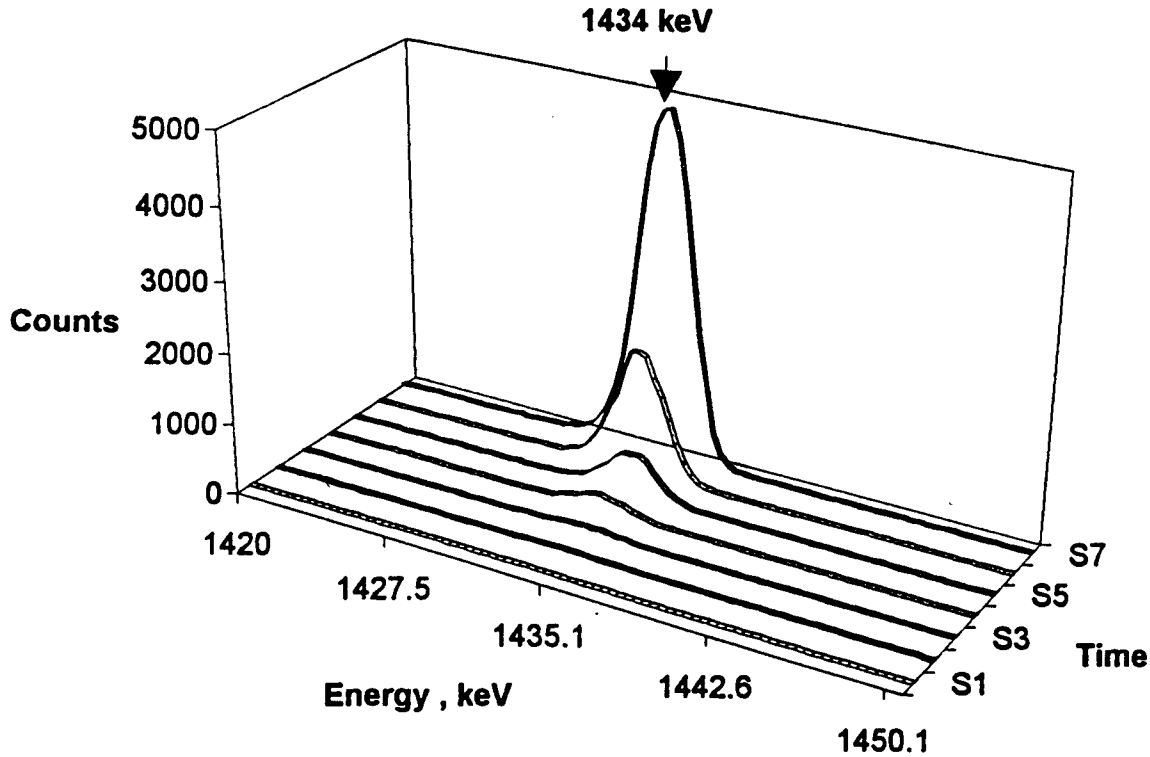

Fig. 1. Time variation of a part of the gamma spectrum of a neutron-activated burned sample containing the photopeak of $^{52}_{23}V$. The gamma spectrum was taken with a germanium detector, and the nuclear reactor power was 1 kW. The time of activation was 3 min. The S7 through S1 spectra were taken successively at 5-min intervals after the neutron activation.

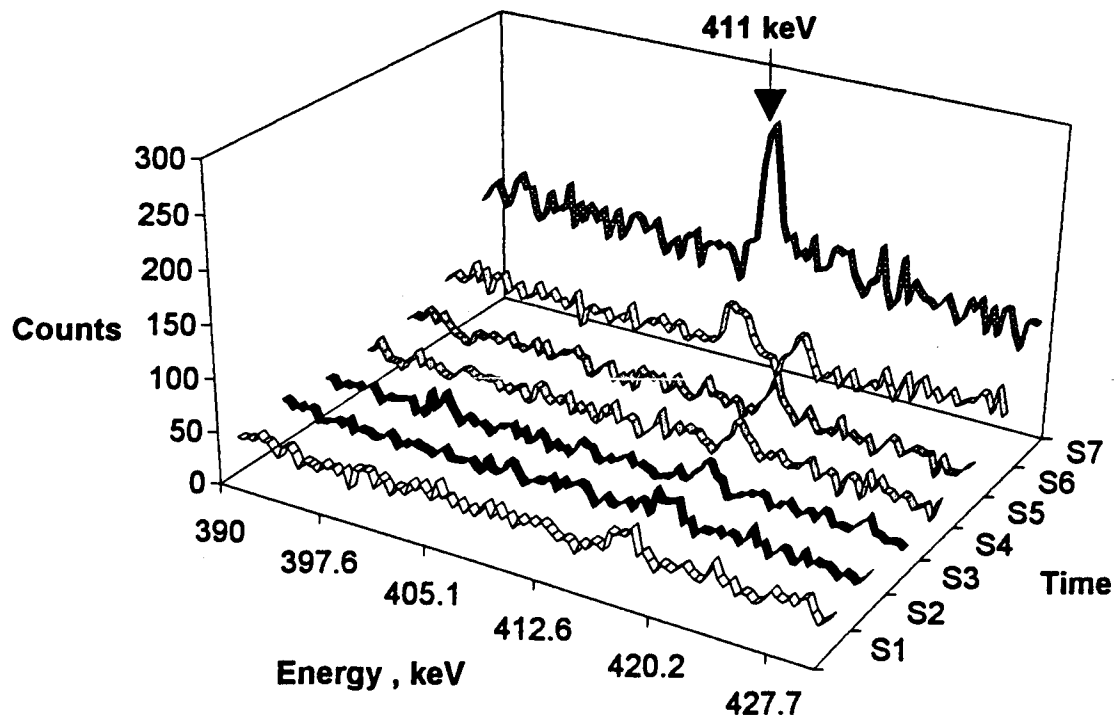

Fig. 2. Time variation of a part of the gamma spectrum of a neutron-activated burned sample containing the double escape peak of $^{52}_{23}V$. The conditions are the same as in Fig. 1.

ACKNOWLEDGMENTS

The authors acknowledge the technical help from and the useful discussions with L. Bobek and E. Billingsley, from the Worcester Polytechnic Institute.

REFERENCES

1. "Abstracts, Meeting at Texas A&M University," J. O'M. BOCKRIS, Ed. (June 1995).

2. V. C. NONINSKI, J. L. CIOTTONE, and P. J. WHITE, "Experiments on a Possible γ-Ray Emission Caused by a Chemical Process," *J. Sci. Exploration*, **9**, 201 (1995).

3. V. C. NONINSKI, J. L. CIOTTONE, and P. J. WHITE, "Experiments on a Claimed β-Particle Emission Decay," *J. Sci. Exploration*, **9**, 317 (1995).

4. M. D. GLASCOCK, *Tables for Neutron Activation Analysis*, 3rd ed., University of Missouri (Mar. 1991).

В. Хр. Нонински, Хр. Ив. Нонински

г. София (НРБ)

Влияние магнитного поля на распределение потенциала при осаждении меди в тафелевской области потенциалов

В последние годы экспериментально был установлен макроскопический энергетический барьер в приэлектродном слое в процессе электролитического выделения меди в тафелевской области потенциалов, объясняющийся скоплением ионов в этом слое под воздействием электрического поля [1]. Имея в виду затруднения, которые возникают в теории электродного перенапряжения при выяснении тафелевской зависимости [2], необходимо обратить внимание на указанный выше факт, дающий основание для нового подхода к обоснованию тафелевской зависимости. В [1] было установлено влияние на макробарьер размешивания приэлектродного слоя посредством соскабливания электродной поверхности. В настоящем сообщении представлены результаты некоторых опытов влияния магнитного поля на этот макробарьер.

Рис. 1. Схема опытной установки (пояснения в тексте)

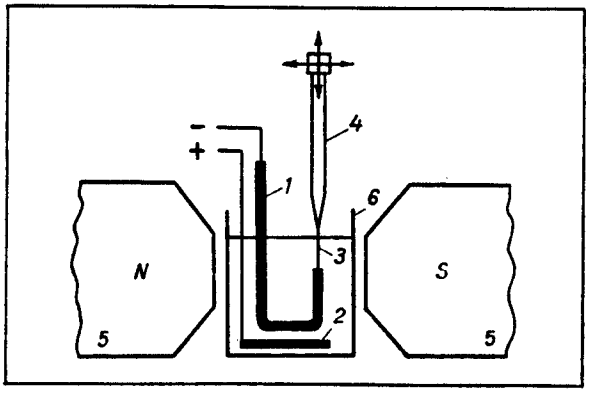

На рис. 1 схематически показана экспериментальная установка, с помощью которой получены результаты, представленные в настоящей статье. Установка включает микрометрический столик (на рис. 1 не указан), к которому прикреплен насыщенный каломельный электрод *4* с капилляром Луггина *3* диаметром ~30 мкм. Капилляр погружен в раствор 0,75 М $CuSO_4$+0,1 М H_2SO_4, находящийся в стеклянной кювете *6* размерами 2×2× ×3 см. В кювету вмонтированы медный катод *1* с поверхностью 10 мм² и медный анод *2* с поверхностью на два порядка больше поверхности катода. Кювета расположена между полюсами электромагнита *5* с индукцией поля 12 кГс. Постоянный ток через электролитическую ячейку поддерживался при помощи потенциостата-гальваностата Radelkis OH-405 (Венгрия), а величина перенапря-

жения отсчитывалась при помощи лампового милливольтметра СП-2.

На рис. 2, *б* представлены зависимости перенапряжения η от расстояния *d* между концом капилляра и поверхностью электрода при протекании тока 2, 4 и 5 мА. Равновесный потенциал медного катода составляет 360 мВ (н. в. э.). Упомянутые значения тока соответствуют потенциалам тафелевской области, что подтверждается полулогарифмической зависимостью между током и перенапряжением.

Из рис. 2 видно, что при удалении капилляра от электродной поверхности изменение потенциала значительно больше того, которое соответствует омическому падению (наблюдается до расстояний *d* немного бóльших 0,2 см). Для больших расстояний определяющим, очевидно, является омическая составляющая потенциала, обусловленная сопротивлением раствора. Этот факт находится в полном соответствии с наблюдаемой ранее зависимостью между потенциалом электрода и *d*. Необходимо отметить, что с увеличением плотности тока изменение перенапряжения с расстоянием *d* проявляется более резко. Зависимость между *d* и измеряемой величиной потенциала, очевидно, связана с упомянутым макроскопическим барьером, преодоление которого ионами является главной причиной перенапряжения выделения меди. При наличии магнитного поля (12 кГс) наблюдается изменение хода кривой η от *d*, которое тем больше, чем больше поляризующий ток. Это изменение связано с уменьшением омического падения в слое раствора между концом капилляра и поверхностью катода. Единственной причиной наблюдаемого снижения омического сопротивления может быть изменение концентрации раствора в приэлектродном слое (уменьшение концентрации ионов меди в приэлектродном слое в направлении выравниваний концентрации во внутренней части раствора при неизменной концентрации серной кислоты). Очевидно, что при включении магнитного поля ионы изменяют свою траекторию движения под воздействием лоренцевой силы таким образом, что их концентрация в приэлектродном слое уменьшается.

Из рис. 2 видно, что при любом заданном расстоянии между электродом и капилляром при указанных значениях тока величина перенапряжения, полученного в магнитном поле, всегда меньше, чем без него. Это наблюдение согласуется с нашими, ранее опубликованными данными [3], которые показали, что магнитное поле с индукцией 12 кГс уменьшает перенапряжение выделения меди на ~60—100 мВ.

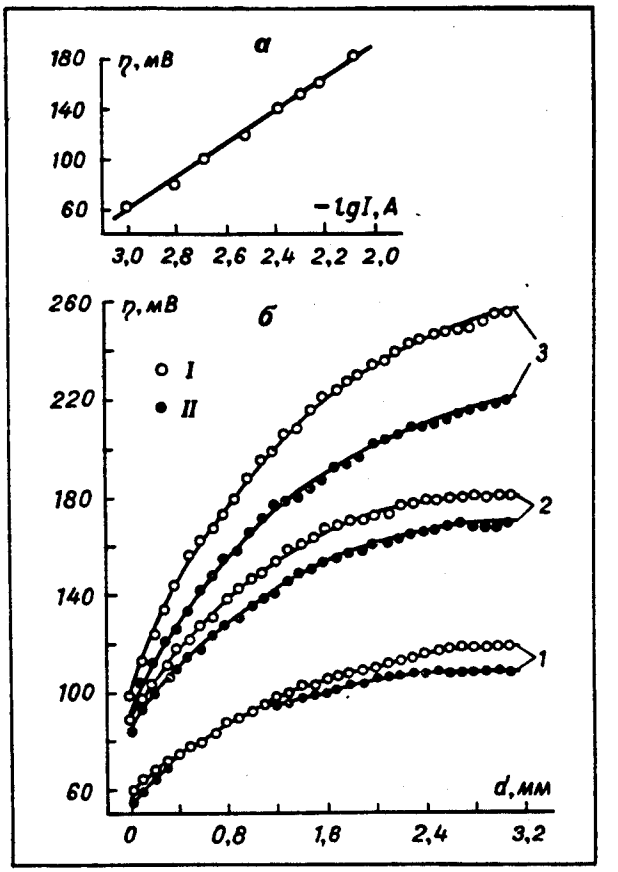

Рис. 2. Зависимость потенциала катода от расстояния между концом капилляра и электродной поверхностью.

I — в отсутствие магнитного поля; II — после введения магнитного поля индукцией 12 кГс при плотностях тока, А/см²: 1 — 0,02; 2 — 0,04; 3 — 0,05

Литература

1. *Noninski C.* Concentration Changes in the Solution Layer Near the Electrode Connected With the Overvoltage in the Tafel Potential Region // 33 Réun. Soc. int. électrochim. Lyon, 6—10 sept. 1982. Res. dévelop. 2. S. l., s. a. P. 933—935.

2. *Нонински Хр.* Върху природата на електродното свръхнапрежение // Годишник на химико-технологическия институт. София. 1957. 4. С. 145—172.

3. *Noninski C., Noninski V., Terzyiski V.* Copper Deposition and Dissolution Overvoltage in Magnetic Field in the Tafel Potential Region // 33 Réun. Soc. int. électrochim. Lyon, 6—10 sept., 1982. Res. dévelop. 2. S. l. s. a. P. 939—941.

Поступила 24.XII 1984